CARBON CYCLING AND STABLE ISOTOPE EVOLUTION IN NEUTRAL MINE DRAINAGE

By

HENDRATTA N. ALI

Master of Science in Geology
University of Yaoundé I
Yaoundé, Cameroon
2003

Bachelor of Science in Earth Sciences
University of Yaoundé I
Yaoundé, Cameroon
1998

Submitted to the Faculty of the
Graduate College of the
Oklahoma State University
in partial fulfillment of
the requirements for
the Degree of
DOCTOR OF PHILOSOPHY
May, 2010

CARBON CYCLING AND STABLE ISOTOPE

EVOLUTION IN NEUTRAL MINE DRAINAGE

Dissertation Approved:

Dr. Eliot Atekwana

Dissertation Adviser

Dr Anna Cruse

Dr Todd Halihan

Dr. Tracy Quan

Dr. Bill Henley

Dr. A. Gordon Emslie

Dean of the Graduate College.

ACKNOWLEDGMENTS

I would like to thank everyone whose contribution, support, encouragements, love and teachings have kept me going during this process of pursuing higher education.

First I want to gratefully and sincerely acknowledge my advisor, Dr. Eliot Atekwana. His patience and interest in the work that I have done, made it possible for me to keep it up. The late nights and early mornings are a true sign of dedication and support for the success of the project. I would also like to thank all the members of my committees who worked with me and helped guide me in this process. I acknowledge Dr. Anna Cruse, for her support and commitment to “make things happen” when I least expected. Dr Todd Halihan for the memorable field trips and all the learning and fun times that came with it, Dr Tracy Quan for accepting to be on my committee on short notice and Dr Bill Henley for positive comments and motivation. A single remark from you gave me a lot of confidence in myself. Thank you! I thank my committee for feedback on my projects and research papers.

I have a special thank you to Dr Jay M. Gregg for, encouraging and advising me. The mentoring I was fortunate to receive from Dr Gregg will forever be valuable in my future pursuits.

I would also like to acknowledge and thank all the faculty members I was fortunate to meet, who never closed their doors to me whenever I needed advice, explanation or guidance on classes and various issues.

To the Boone Pickens School of Geology, graduate fellowship and scholarship committee, thank you for providing me with the means so that I could stay focused on the research. I am also very grateful for the friendships I made here at OSU and in Stillwater, OK. To all my friends, current and former graduate students at Oklahoma State University, the Graduate and Professional Student Government Association (GPSGA) for the wonderful leadership experience, I say thank you. I want to thank all the mentors and friends I met at meetings and conferences especially at the National Association of Black Geologist and Geophysicists (NABGG) for their unending support.

With my family and friends away in Cameroon, I found strong spiritual and moral support, a caring mentor and positive reinforcement in Dr Estella Atekwana. Thank You. Finally, and most importantly, I thank my family and friends in Cameroon for laying the right foundations during my early life. I would now like to remember my late father, Samuel Susung Ali, for his blessings and pride in me. My mother, Charity Mengla Ali, who is my inspiration, my rock , my role model and best friend. I thank you for always praying to God for my salvation, happiness, safety and success. Your support, encouragement, quiet patience, and unwavering love has kept me going all these years. My uncle Simon and aunt Lucy, whose unending support, and experience encouraged me and made it possible for me to pursue a doctorate. I am also very thankful to my sister, Anne for always checking, joggling between time zones to make sure I am alright. Thanks to all my siblings, family and friends for their continued love and prayers.

TABLE OF CONTENTS

II. THE EFFECT OF SULFURIC ACID NEUTRALIZATION ON CARBONATE EVOLUTION OF SHALLOW GROUNDWATER

III. DISSOLVED INORGANIC CARBON EVOLUTION IN NEUTRAL DISCHARGE FROM MINE TAILINGS PILES

IV. CONCLUSION

LIST OF TABLES

TABLE **PAGE**

III. DISSOLVED INORGANIC CARBON EVOLUTION IN NEUTRAL DISCHARGE FROM MINE TAILINGS PILES

IV. APPENDICES

Tables:

LIST OF FIGURES

FIGURE **PAGE**

I. EFFECT OF PROGRESSIVE ACIDIFICATION ON STABLE CARBON ISOTOPE OF DISSOLVED INORGANIC CARBON IN SURFACE WATERS

II. THE EFFECT OF SULFURIC ACID NEUTRALIZATION ON CARBONATE EVOLUTION OF SHALLOW GROUNDWATER

III. DISSOLVED INORGANIC CARBON EVOLUTION IN NEUTRAL DISCHARGE FROM MINE TAILINGS PILES

GENERAL INTRODUCTION

1. Motivation

Identification of the effects of acidification on the evolution of carbon in our environment is necessary to determine the impact of natural and anthropogenic forcing on the carbon cycle (Falkowski et al., 2000; Schimel, 2001; House et al., 2003; Takahashi, 2004). The US Carbon Cycle Research Program (www.carboncyclescience.gov) identifies several areas where gaps exist in our knowledge and understanding of carbon sources and fluxes from terrestrial reservoir to the atmosphere For example, carbon in bedrocks and freshwater systems is an important part of the carbon cycle and represent important links in the conversion of terrestrial carbon and its transfer to the atmospheric or ocean reservoirs. The carbon that is lost as CO_2 from terrestrial reservoirs to the atmosphere is generated either from organic carbon respiration or from weathering of watershed rocks such as limestone and dolomite (Wicks and Groves, 1993; Webb and Sasowsky, 1994; Affek et al., 1998; Telmer and Veizer, 1999; Karim and Veizer, 2000; Andrews and Schlesinger, 2001).

.

Natural weathering of carbonates provide the bulk of DIC in groundwater and surface water in terrestrial watersheds (Karim and Veizer, 2000). In several watersheds with a history of mining activities, the oxidation of sulfide minerals (e.g., PbS, FeS_2, and ZnS) generates sulfuric acid. The acid reacts with carbonate minerals to neutralize H^+ and release DIC. Despite the potential to generate significant DIC from carbonate mineral dissolution, few studies (e.g. Fonyuy and Atekwana 2008a&b) have examined carbon cycling and transfer in watersheds impacted by acidification. The carbon that is transformed, exchanged, or lost from the system imparts shifts on the isotopic ratio of DIC ($\delta^{13}C_{DIC}$) through isotopic fractionation. Fractionation may lead to distinct changes in the $\delta^{13}C_{DIC}$ that may be diagnostic of the acidification process. So far, little is known about the anthropogenic effects of acidification and subsequent neutralization processes on the cycling of carbon in groundwater and surface waters contaminated by anthropogenic effects e.g., mine drainage.

2. Research hypothesis and objectives

The goal of this research was to investigate the effect of acidification on carbon cycling in surface and groundwater using C isotopes. We hypothesize that ***DIC and isotope ratios can be diagnostic of the extent of acidification / neutralization in contaminated groundwater and surface waters.*** Our plan is to conduct field and laboratory experiments in order to investigate 1) DIC production and fate in groundwater, soil water, and lake water affected by acidification and neutralization in mine tailings, 2) the impact of drainage from mine tailings on surface water DIC cycling, and 3) the isotope fractionation of carbon during progressive acidification in surface waters. In order

to solve these issues, we need to determine: 1) information on DIC partitioning and $\delta^{13}C_{DIC}$ and $\delta^{13}C_{CO2}$ fractionation in groundwater, soil water, and surface water in a tailings environment, 2) Spatial evolution of DIC and the kinetic fractionation of $\delta^{13}C_{DIC}$ of drainage from mine tailings, and 3) a model of $\delta^{13}C_{DIC}$ and $\delta^{13}C_{CO2}$ evolution of surface waters due to acidification.

3. Significance of study

The results of this study contribute to our understanding of the role of anthropogenic acidification and subsequent neutralization on inorganic carbon cycling and evolution in contaminated surface and groundwater. Given that the conversion, transformation and transfer of DIC to the atmospheric reservoir will continue, the role of anthropogenic DIC sources needs to be factored in the terrestrial carbon budget. In this study, the impact of continuous acidification and neutralization on DIC generation and loss as CO_2 to the atmosphere is presented in three different investigations. This research met goals and objectives of the National Science Foundation (NSF) program (www.nsf.gov/pubs/2006/nsf06514/nsf06514.htm, March, 2007) on integrated carbon cycle and water in the earth system and the US Carbon Cycle Research (www.carboncyclescience.gov, March, 2007). Given that natural resource exploitation by mining and surface disposal of mine waste is likely to continue, this study sheds more light and understanding on how such activities impact carbon cycling. The results of this study also highlight the use of stable carbon isotope fractionation in addition to water chemistry analysis as a tool to study carbon evolution in mining environments

CHAPTER I

EFFECT OF PROGRESSIVE ACIDIFICATION ON STABLE CARBON ISOTOPE OF DISSOLVED INORGANIC CARBON IN SURFACE WATERS

Hendratta N. Ali and Eliot Atekwana
Chemical Geology Volume 260, Issues 1-2, 15 March 2009, Pages 102-111
Boone Pickens School of Geology, 105 Noble Research Center, Oklahoma State University, Stillwater, OK 74078, USA

Abstract

Acidification of surface waters by acid mine drainage (AMD) contamination or atmospheric deposition perturbs the carbonate equilibrium, with unknown effects to the isotope ratio of dissolved inorganic carbon (DIC). Here, we aimed to determine shifts in the $\delta^{13}C_{DIC}$ and to model carbon isotope fractionation during progressive acidification. We progressively acidified samples of $NaHCO_3$, stream water, groundwater, and spring water contaminated by AMD (AMD spring) to a pH <3 using H_2SO_4 under open conditions (exposed to the atmosphere) and closed conditions (isolated from the atmosphere). Duplicate sets of samples were left unacidified and allowed to chemically evolve under ambient conditions in the laboratory. The $\delta^{13}C_{DIC}$ of the acidified samples were enriched by 0.7‰ to 5.0‰ during the HCO_3^- dehydration phase and depleted by 0.6‰ to 2.3‰ during the phase when HCO_3^- was exhausted. The $\delta^{13}C$ of the initial CO_2 ($\delta^{13}C_{CO2}$) captured during closed acidification of $NaHCO_3$ (7.4‰,) stream water (7.9‰),

groundwater (8.3‰), and AMD spring (1.9‰) samples were more depleted than their respective $\delta^{13}C_{DIC}$. The $\delta^{13}C_{CO2}$ showed enrichment and depletion trends that were similar to those of the DIC. In addition, the $\delta^{13}C_{CO2}$ were of similar magnitude to the $\delta^{13}C_{DIC}$ after the HCO_3^- in the samples was exhausted. The positive enrichment in $\delta^{13}C_{DIC}$ during the HCO_3^- dehydration phase was driven by 1) kinetic fractionation of CO_2 during diffusion, or 2) a combination of fractionation accompanying HCO_3^- dehydration to $CO_{2(aq)}$ followed by isotopic exchange of carbon between $CO_{2(aq)}$ and HCO_3^-. The enrichment of ^{13}C was defined by slopes for close or open acidification of 7.3‰ or 3.4‰ for $NaHCO_3$, 7.7‰ or 4.8‰ for stream water, 6.8‰ or 2.9‰ for groundwater, and 4.8‰ or 2.5‰ for the AMD spring. The negative trend in $\delta^{13}C_{DIC}$ after HCO_3^- was exhausted was entirely due to kinetic fractionation associated with CO_2 loss by diffusion. The depletion of ^{13}C was defined by slopes for closed and open acidification of 6.8‰ or 2.2‰ for $NaHCO_3$, 7.4‰ or 3.9‰ for stream water, 6.9‰ or 4.8‰ for groundwater, and 7.9‰ or 6.3‰ for the AMD spring. The unacidified samples showed fluctuations in DIC concentrations of 8% for $NaHCO_3$, and decreases in DIC concentrations of 21% for stream water, 26% for groundwater, and 99% for AMD spring. The $\delta^{13}C_{DIC}$ of the unacidified samples were enriched by <1.0‰ for $NaHCO_3$, 7.0‰ for stream water, 3.3‰ for groundwater, and 2.7‰ for AMD spring. The enrichment of $\delta^{13}C_{DIC}$ of 1.0 to 7.0‰ for the unacidified $NaHCO_3$, stream water, and groundwater samples was due to exchange of carbon between HCO_3^- and atmospheric CO_2. Protons produced during hydrolysis of Fe^{3+} in the unacidified AMD spring caused this sample to behave isotopically similar to the acidified AMD spring. We conclude that carbon isotope values

in conjunction with concentrations of DIC species ($CO_{2(aq)}$, HCO_3^-, and CO_3^{2-}) can be used to provide evidence for the effects of acidification on DIC in surface waters.

Keywords: Acidification; Dissolved inorganic carbon; Stable carbon isotopes; Surface waters.

1. Introduction

The acidification of surface waters perturbs the carbonate equilibrium (e.g., Berelson et al., 1994; Heron et al., 1997; Lohse et al., 2000; Feely et al., 2004; Orr et al., 2005; Zachos et al., 2005). Acidification may result from acid mine drainage (AMD) contamination (e.g., Baker et al., 1991; Herlihy et al., 1991; Wicks and Groves, 1993; Webb and Sasowsky, 1994; Benson, 1998; Mayo et al., 2000; Espana et al., 2005; Lee and Chon, 2006; Fonyuy and Atekwana, 2008a), atmospheric deposition (e.g., Baker et al., 1991; Stoddard et al., 1999; Larssen and Carmichael, 2000; Wright et al., 2001), or organic anions from watersheds (e.g., Baker et al., 1991; Kaufmann et al., 1991; Kaufmann et al., 1992). Acidification lowers water pH and drives the carbonate equilibrium to produce $CO_{2(aq)}$ which may be lost to the atmosphere or facilitate exchange of carbon between dissolved inorganic carbon (DIC) and atmospheric CO_2. The carbon that is transformed, exchanged, or lost imparts shifts to the isotope ratio of DIC ($\delta^{13}C_{DIC}$) because of isotope fractionation accompanying each process. If the carbon isotope fractionation leads to distinct shifts in the $\delta^{13}C_{DIC}$ of acidified waters, this may be diagnostic of acidification. Therefore, given initial constraints, models based on DIC concentrations, DIC speciation, and the $\delta^{13}C_{DIC}$ may be an effective way of evaluating the extent of acidification in surface waters.

The extent to which acidification affects the $\delta^{13}C_{DIC}$ of surface waters is currently not well understood as this problem has not been intensively investigated. However, a few studies (e.g., Fonyuy and Atekwana, 2008 a&b) show large decreases in DIC (>98%) and variable shifts in $\delta^{13}C_{DIC}$ in AMD-contaminated samples in field and laboratory studies. Furthermore, Fonyuy and Atekwana (2008 a&b) suggest that the enrichment in $\delta^{13}C_{DIC}$ that is due to acidification alone may be in the range of ~1.0‰ to 3.0‰. A variety of competing reactions and processes (such as dissolution of streambed carbonates, CO_2 exchange with the atmosphere, photo-oxidation of organic matter, aquatic photosynthesis/respiration, and variable influx of DIC from groundwater and tributaries) may occur during acidification. These competing processes especially in field settings, make it difficult to sort out the effects of acidification from the measured DIC concentration and $\delta^{13}C_{DIC}$ (Fonyuy and Atekwana, 2008a).

There is a need to conduct detailed and controlled studies on acidification to determine carbon loss from which the effects of the isotopic fractionation of carbon on the $\delta^{13}C$ can be assessed. In this study we progressively acidified samples of $NaHCO_3$, stream water, groundwater, and a spring contaminated by AMD to pH of <3.0 by adding H_2SO_4. We measured DIC, alkalinity, cations and anions, the $\delta^{13}C$ of DIC, and the $\delta^{13}C$ of $CO_{2(g)}$ released during acidification. Our objective was to determine shifts in $\delta^{13}C_{DIC}$ and carbon isotope fractionation during DIC transformation and to model carbon isotope evolution during progressive acidification.

2. Method

2.1. Sample collection and preparation

A solution of $NaHCO_3$, and samples of stream water, groundwater, and spring water contaminated by AMD (AMD spring) were used for this experiment. The $NaHCO_3$ solution was made by dissolving 7.0 to 8.0 g of 99% laboratory grade $NaHCO_3$ (EMD Chemicals, Inc.) in 20 L of de-ionized (18.2 Ωm) water. The $NaHCO_3$ solution was used as a control because protons from acidification would only affect bicarbonate. In addition, we also wanted to minimize the effects from processes that could occur in natural samples (e.g., biological transformation of organic carbon, protons produced by metal precipitation, etc.) that may affect pH, DIC, and carbon isotope evolution. Natural samples were collected from Missouri, USA; AMD spring in Huntsville (39°26'22"N, 92°32'38"W), uncontaminated stream water from Little Piney Branch in Rolla (37°57'05"N, 91°46'16"W), and groundwater from the Federal Tailings Pile in Park Hills (37°49'16"N, 90°30'49"W). The AMD spring and stream water were collected by the grab technique and groundwater was pumped to the surface using a submersible pump. Samples for the laboratory experiment were collected in 20 L Fort-Paks® plastic containers (reactors), closed tight and transported to the laboratory. The $NaHCO_3$ solution was prepared and the natural samples were collected in triplicates.

2.2. Experimental procedure

In the laboratory, a set of reactor samples from each source was opened, left unacidified and allowed to evolve under ambient laboratory conditions and in contact with the atmosphere for up to 43 days. The other two reactor samples from each source

were progressively acidified with sulfuric acid to pH <3. One reactor from each set was acidified open to the atmosphere (open acidification) which allowed the reactor sample to lose or exchange CO_2 freely with atmosphere. The other reactor sample was acidified without contact with atmosphere (closed acidification) so as to collect the $CO_{2(g)}$ during acidification for isotope analysis. Acidification of the reactors was done by adding 0.2 to 0.75 mL 1.6 N of H_2SO_4 that was mixed with the sample by mechanical shaking of the reactor for about 5 minutes.

Modifications made to the closed acidification reactors are shown in Figure 1. The air-tight lid of the reactor was fitted with a septum through which H_2SO_4 was injected into the sample using a 1 mL glass syringe. An outlet was created and fitted with 6 mm OD plastic tubing and connected to a multipurpose vacuum line to 1) collect $CO_{2(g)}$ from the reactor headspace without contamination by atmospheric $CO_{2(g)}$ and 2) to remove all $CO_{2(g)}$ from the reactor before the next acidification. A 6 mm OD plastic tubing was fitted with a plastic syringe valve that provided access to the water sample which was withdrawn using a 60 mL plastic syringe. Because of the vacuum created in the reactor during removal of $CO_{2(g)}$ in the headspace, 99.99% helium was released into the reactor to restore pressure to atmospheric, followed by water sampling.

2.3. Analysis

Measurements of physical, chemical and isotopic parameters were done after each acidification and every 2-4 days for the unacidified samples. The temperature and pH were measured using a YSI multi-parameter probe after calibration to manufacturers specifications. All samples were filtered through a 0.45 µm syringe filter after collection. Alkalinity was determined immediately after filtration by acid titration (Hach, 1992).

Samples for anions were collected unacidified and samples for cations were acidified to a pH <2. All samples were stored at 4^{o}C until analysis. Anions were analyzed by ion chromatography and cations by either ion chromatography or inductively coupled plasma optical emission spectrometry.

Water samples for DIC were collected and the CO_2 extracted as described by Atekwana and Krishnamurthy (1998) with modifications as in Fonyuy and Atekwana (2008b). The DIC concentrations were calculated from the CO_2 measured by a pressure transducer. The CO_2 was collected and sealed in Pyrex tubes. The CO_2 in the reactor headspace was purified in the vacuum line and an aliquot was sealed in Pyrex tubes. Carbon isotope ratios of the CO_2 in the sealed Pyrex tubes were measured by isotope ratio mass spectrometry at Western Michigan University, Kalamazoo, Michigan. The carbon isotope ratios are reported in the delta notation relative to Vienna Pee Dee Belemnite (VPDB) carbon standard.

$$\delta^{13}C = \left(\frac{R}{R_{std}} - 1 \right) \times 1000 \ \%$$

3. Results

3.1. pH, HCO_3^-, and DIC

The pH, HCO_3^-, and DIC concentrations of samples from the open and closed acidification and of unacidified samples are presented in Table 1. With progressive addition of H_2SO_4, HCO_3^- concentrations decreased to below detection levels. DIC concentrations for samples in the open acidification decreased by 67% for $NaHCO_3$, 81%

in stream water, 72% for groundwater, and 96% for AMD spring. In the closed acidification, DIC decreased by 93% for $NaHCO_3$, 96% for stream water, 97% for groundwater, and 97% for the AMD spring. The trend of decreasing HCO_3^- concentrations with progressive acidification is similar for open and closed acidification (Fig. I-2a-d). However, the trend of decreasing DIC concentrations for open and closed acidification is different for $NaHCO_3$, stream water, and groundwater (Fig. I-2e-g), and similar for AMD spring (Fig. I-2h). The trends of decreasing DIC concentrations for open acidification are lower than for closed acidification (Fig. I-2e-g). This difference between the DIC concentrations for open and closed acidification is due to greater removal of $CO_{2(aq)}$ by applying vacuum to the closed acidification reactors. Despite this fact, the AMD spring samples also subjected to open and closed acidification show similar trends of decreasing DIC concentrations (Fig. I-2h).

Unacidified samples showed fluctuations in HCO_3^- concentrations of 7% in $NaHCO_3$, and decreased by 21% in stream water and 18% in groundwater (Fig. I-2a-d). The samples also showed fluctuations in DIC concentration of 8% in $NaHCO_3$, and decreases of 21% in stream water, and 26% in groundwater (Fig. I-2e-g). The pH increased by 0.2 in $NaHCO_3$, 0.7 in stream water, and 0.6 in groundwater. In contrast, the pH of the AMD spring sample decrease progressively from 5.9 to 3.1, while HCO_3^- concentrations decreased to below detection level and DIC concentrations decreased by 98%.

3.2. $\delta^{13}C$ of DIC and $\delta^{13}C$ of CO_2

The $\delta^{13}C_{DIC}$ and $\delta^{13}C_{CO2}$ of samples from the acidified and unacidified reactors are presented in Table 1. In the open and closed acidifications, the trend of $\delta^{13}C_{DIC}$ enrichment reversed at lower DIC concentrations to depletion which continued to the end

of the acidification (Fig. I-3a-d). The DIC concentrations were less than 2 mM C/L in closed acidification and 3 mM C/L in open acidification when the trends in $\delta^{13}C_{DIC}$ reversed from enrichment to depletion. The magnitude of the enrichment and depletion in the $\delta^{13}C_{DIC}$ was greater for the closed acidification than for the open acidification (Fig. I-3a-d).

The $\delta^{13}C$ of the CO_2 captured during closed acidification was progressively enriched before reversing to become progressively depleted at low DIC concentrations of <1.0 mM C/L (Fig. I-3e-h). The trend in the $\delta^{13}C_{CO2}$ mimics that observed for $\delta^{13}C_{DIC}$ of the closed acidification (Fig. I-3a-d). However, the $\delta^{13}C_{CO2}$ that was initially more depleted relative to $\delta^{13}C_{DIC}$ was progressively enriched to values nearly identical to those of $\delta^{13}C_{DIC}$ before the trend of enrichment reversed to depletion at low DIC (Table 1). Also, after reversal from ^{13}C enrichment to depletion, the values of $\delta^{13}C_{CO2}$ are similar to or slightly enriched than the $\delta^{13}C_{DIC}$.

The $\delta^{13}C_{DIC}$ of unacidified $NaHCO_3$, stream water, and groundwater samples showed enrichments of 0.6‰, 7.0‰, and 3.3‰, respectively (Fig. I-3a-c). The $\delta^{13}C_{DIC}$ of the AMD spring was enriched by 2.7‰, which reversed to depletion at low DIC (<2 mM C/L) and decreased to a minimum $\delta^{13}C_{DIC}$ of -18.8‰ (Table 1; Fig. I-3d).

4. Discussion

4.1. Effects of acidification on HCO_3^-, $CO_{2(aq)}$, and DIC

In the acidified reactors, protons from H_2SO_4 dissociation react with HCO_3^- to produce H_2CO_3 (reaction 1) reducing HCO_3^- concentrations. Decreases in DIC concentrations occur by loss of $CO_{2(g)}$ from solution (reaction 2):

$$H^+ + HCO_3^- \rightarrow H_2CO_3 \quad (1)$$

$$H_2CO_3 \rightarrow CO_{2(aq)} + H_2O \rightarrow CO_{2(g)} + H_2O \quad (2)$$

The decreasing trend of HCO_3^- concentration is similar for both open and closed acidification (Fig. I-2a-d). However, the trends of DIC concentration decreases are markedly different between open and closed acidifications (Fig. I-2e-g), except for the AMD spring sample (Fig. I-2h), because DIC loss from the samples is not directly controlled by acidification. For example, in sample sets (excluding AMD spring), a single pH value corresponds to different DIC concentrations in the open and closed acidification because of different amounts of CO_2 lost from solution (Fig. I-2e-g).

DIC loss from solution depends on 1) the partial pressure of CO_2 (pCO_2) in the reactor samples relative to that of the atmosphere, 2) the method of CO_2 removal from solution (e.g. vacuum assisted for closed acidification vs. diffusion controlled for open acidification), and 3) the effectiveness of each method in removing CO_2. The extent to which CO_2 is removed also depends on how much time is allowed for removal to occur. One way to evaluate how CO_2 is produced and lost as DIC decreases during acidification is to examine the relationship between the normalized DIC concentration which is the

ratio of DIC at any time (C_t) to the DIC concentration prior to acidification (C_0) and the pCO_2 in the samples. A plot of the C_t/C_0 vs. pCO_2 of samples from open and close acidification shows initial increase in the pCO_2 for $NaHCO_3$, stream water, and groundwater to peak values (Fig. I-4a-c). This was followed by pCO_2 decreases as acidification progressed to the end of the experiment. The trend of increasing followed by decreasing pCO_2 is more pronounced for the open acidification than for the closed acidification (Fig. I-4a-c). Enhanced CO_2 removal by applying vacuum to the reactor headspace is responsible for the lower pCO_2 magnitudes observed for closed acidification samples. At C_t/C_0 of about 0.2 and lower, the decrease in the pCO_2 for both open and closed acidifications show similar trends and magnitudes. The overall trend of pCO_2 for the acidified AMD spring is different from that of $NaHCO_3$, stream water, and groundwater (Fig. I-4d vs. 4a-c). The pCO_2 of the AMD spring decreased with decrease in DIC in both open and closed acidification. In addition, the trends of pCO_2 are similar and almost identical in magnitude at $C_t/C_0 \leq 0.2$ despite vacuum assisted CO_2 removal during closed acidification.

The pCO_2 trend in the acidified AMD spring which continuously declined from the start of experiment, suggest that HCO_3^- dehydration does not necessary lead to CO_2 accumulation (increased pCO_2 before decline). Considering that the initial pH of AMD spring was ~5.9 (compared to 8.1, 7.7, and 7.4 for $NaHCO_3$, stream water, and groundwater, respectively), we infer that the sample had already undergone some degree of DIC speciation due to acidification. The acidification occurred from protons produced during the generation of AMD underground and before discharging as the spring (Blodau, 2006). We note that at a pH below ~6.0, the pCO_2 of $NaHCO_3$, stream water,

and groundwater reverses from increasing trends to decreasing trends. Thus, at the moment of sampling the AMD spring for the laboratory experiment, we captured ongoing AMD related acidification process at the stage of decreasing pCO_2.

The initial pCO_2 of $NaHCO_3$ ($2.3x10^{-4}$ to $3.7x10^{-4}$ atm.), stream water ($7.5x10^{-4}$ to $1.5x10^{-3}$), and groundwater ($1.2x10^{-3}$ to $1.6x10^{-3}$ atm.) suggest that $CO_{2(aq)}$ initially comprised a much smaller fraction (<1%) of the DIC. This is in contrast to the AMD spring sample ($5.0x10^{-2}$ to $3.7x10^{-2}$ atm.) in which the initial $CO_{2(aq)}$ comprised 65% to 81% of the DIC. The trends in pCO_2 during acidification therefore suggest that despite overall DIC concentration decreases, accumulation of $CO_{2(aq)}$ in the reactors or lack thereof is related to the ratio of $CO_{2(aq)}$ to HCO_3^- at the start of the laboratory acidification (Table 1). We reiterate that the behavior of CO_2 (pCO_2) in AMD spring samples during open and closed acidification was similar to that of other acidified samples (Fig. I-4a-c vs. 4h) although only the declining trend of $pCO_{2(aq)}$ was captured during the laboratory acidification. Thus, it appears that the initial ratio of CO_2:DIC and HCO_3^-:DIC is important in predicting the behavior of the pCO_2 of the samples during HCO_3^- dehydration by protons.

The pCO_2 of unacidified $NaHCO_3$ ($1.2x10^{-4}$ to $2.7x10^{-4}$ atm.), stream water ($2.9x10^{-4}$ to $1.5x10^{-3}$ atm.), and groundwater ($3.5x10^{-4}$ to $1.6x10^{-3}$ atm.) did not change significantly during the experiment (Fig 4e-g). In contrast, the unacidified AMD spring samples showed a decreasing trend in pCO_2 similar to the acidified AMD spring sample due to acid production in the sample (Fig. I-4h vs. 4d). Fe^{2+} in the AMD spring sample was oxidized to Fe^{3+}, followed by hydrolysis to produce precipitates and H^+ (e.g., Espana et al., 2005; Lee and Chon, 2006). The H^+ ions are responsible for HCO_3^- dehydration

that caused this sample to behave chemically like the acidified samples (Fonyuy and Atekwana, 2008b).

4.2. Effect of acidification on carbon isotopes of DIC

4.2.1. Carbon isotope fractionation

Carbon isotope fractionation occurs during HCO_3^- dehydration: $\varepsilon_{HCO3\text{-}CO2(aq)}$ (Mills and Urey, 1940; Clark and Lauriol, 1992; Halas et al., 1997) and loss of CO_2 from solution: $\varepsilon_{CO2(aq)\text{-}CO2(g)}$ (Vogel et al., 1970; Zhang et al., 1995; Szaran, 1998). In $NaHCO_3$, stream water, and groundwater, the carbon lost as $CO_{2(g)}$ is less than the $CO_{2(aq)}$ produced during HCO_3^- dehydration as evidenced by increased pCO_2 despite decrease in DIC (Fig. I-4a-c). It is not possible to determine the fractional contribution to the overall isotopic fractionation by HCO_3^- dehydration or CO_2 loss in the measured $\delta^{13}C_{DIC}$ values. However, we can gain insights into the behavior of $\delta^{13}C_{DIC}$ by evaluating DIC speciation to HCO_3^- and $CO_{2(aq)}$ during acidification and comparing variations in the concentrations of HCO_3^- and $CO_{2(aq)}$ to the $\delta^{13}C_{DIC}$ (Fig. I-5). For both open and closed acidifications involving $NaHCO_3$, stream water, and groundwater, the trends in $\delta^{13}C_{DIC}$ are similar to those of $CO_{2(aq)}$ (Fig. I-5a-c), albeit subdued for closed acidification (Fig. I-5e-g). For these samples, the positive trends in $\delta^{13}C_{DIC}$ correspond to decreasing concentrations of HCO_3^- and increasing concentrations of $CO_{2(aq)}$, while the negative trends in $\delta^{13}C_{DIC}$ corresponds to decreasing concentrations of $CO_{2(aq)}$ after HCO_3^- was exhausted.

We first examine the negative trends in $\delta^{13}C_{DIC}$ and its causal mechanism, as this will lay the foundation for exploring the mechanism responsible for the positive trends in $\delta^{13}C_{DIC}$ during HCO_3^- dehydration (Fig. I-5). The negative trends in the $\delta^{13}C_{DIC}$ for all

acidified samples (Fig. I-5a-h) is due only to $CO_{2(g)}$ loss from solutions, because during this phase of acidification HCO_3^- was exhausted. There is experimental evidence that shows that during the dissolution of $CO_{2(g)}$ in water, $^{12}CO_2$ is slightly more soluble than $^{13}CO_2$, causing the $\delta^{13}C_{DIC}$ of the solution to become depleted (Vogel et al., 1970; Usdowski and Hoefs, 1990). The depletion in $\delta^{13}C_{DIC}$ should continue over time and the final $\delta^{13}C_{DIC}$ of the solution for a system in which $CO_{2(g)}$ equilibrates with $CO_{2(aq)}$ will be determined by the equilibrium fractionation factor at the given temperature and the $\delta^{13}C$ of $CO_{2(g)}$ (Mook et al., 1974; Usdowski and Hoefs, 1990). In this experiment, the pCO_2 of the reactor samples were higher than atmospheric during the negative $\delta^{13}C_{DIC}$ excursion, thus CO_2 loss was controlled by diffusion. Models of isotopic fractionation based on the differences in the diffusivities of $^{12}CO_2$ and $^{13}CO_2$ from solution should lead to enrichment of $\delta^{13}C_{DIC}$ (e.g., Usdowski and Hoefs, 1990). However, Usdowski and Hoefs (1990) provide experimental evidence which suggest that pH increase during CO_2 loss from solution produces a fractionation effect counteracted by greater reaction of $^{12}CO_2$, effectively negating the diffusive fractionation effect. In the acidified reactors the pH was decreasing, thus we can not invoke a similar mechanism. The isotopic fractionation that leads to negative $\delta^{13}C_{DIC}$ in the reactor solution can be explained if as $CO_{2(aq)}$ is desorbed from solution, $^{12}CO_2$ which is more reactive is retained in solution relative to $^{13}CO_2$ (Vogel et al., 1970). In addition, because the CO_2 removed from solution was unable to equilibrate with CO_2 in the aqueous phase, this led to continuous depletion in the $^{13}C_{DIC}$ as the DIC continued to decrease (Fig. I-5a-h).

The positive trends in the $\delta^{13}C_{DIC}$ during the HCO_3^- dehydration (Fig. I-5) must then be due to preferential loss of $^{12}CO_2$ vs. $^{13}CO_2$ from the reactor samples. This is in contrast

with the observations that $^{12}CO_2$ which is more reactive with water (Vogel et al., 1970; Usdowski and Hoefs, 1990) is retained in solution causing negative trends in the $\delta^{13}C_{DIC}$. We invoke a CO_2 loss mechanism mostly controlled by HCO_3^- dehydration. As HCO_3^- dehydration proceeds, ^{12}C is preferentially incorporated into $CO_{2(aq)}$, leaving HCO_3^- enriched in ^{13}C. Although $^{13}CO_2$ is preferentially incorporated into gas phase during CO_2 loss, more ^{12}C is lost as $CO_{2(g)}$ relative to the HCO_3^- that is enriched in ^{13}C. The overall effect of this is to make the solution more enriched in ^{13}C with progressive HCO_3^- dehydration, and thus the positive trend in $\delta^{13}C_{DIC}$. We suggest that HCO_3^- dehydration and physical loss of CO_2 together control the observed ^{13}C isotopic enrichment.

The $\delta^{13}C$ of $CO_{2(g)}$ captured during closed acidification can be used to make an even stronger case for the HCO_3^- dehydration effects on the isotope fractionation that causes ^{13}C enrichment along the positive trend of $\delta^{13}C_{DIC}$ (Fig. I-6e-g). During acidification, the $\delta^{13}C$ of $CO_{2(g)}$ produced after the first acid application was 7.4 to 8.3‰ more negative than the $\delta^{13}C_{DIC}$ of $NaHCO_3$, stream water, and groundwater, and 1.9‰ more negative than the $\delta^{13}C_{DIC}$ of the AMD spring (Table 1). The variations in the magnitudes of depletion are due to differences in the initial HCO_3^-:DIC ratios since the enrichment between HCO_3^--$CO_{2(aq)}$ ($\alpha_{HCO3\text{-}CO2(aq)}$ = -9.2‰ at 23^{o}C) is much greater than between $CO_{2(aq)}$-$CO_{2(g)}$ ($\alpha_{CO2(aq)\text{-}CO2(g)}$ = 1.1‰ at 23^{o}C) (Mook et al., 1974).

For a carbon reservoir that 1) is continuously decreasing due to DIC loss and governed by first order kinetics and 2) has a constant isotopic fractionation during HCO_3^- dehydration, the $\delta^{13}C_{DIC}$ and $\delta^{13}C_{CO2}$ can be described by a Rayleigh function (e.g., Monson and Hayes, 1980; Mariotti et al, 1981; Galimov, 2006; Fonyuy and Atekwana, 2008b):

$$\delta^{13}C_t = \varepsilon\ (C_t/C_0) + \delta^{13}C_0 \qquad (3)$$

where $\delta^{13}C_t$ is the carbon isotope ratio to be predicted, $\delta^{13}C_0$ is the initial carbon isotope ratio of the reactor sample, ε is the isotopic enrichment factor (given as: $[(\delta_{product}/\delta_{reactant})-1] \times 10^3$), C_t is the DIC concentration measured at any time t and C_0 is the DIC concentration at the beginning of the experiment. The relationship between C_t/C_0 vs. $\delta^{13}C$ of DIC or CO_2 (Fig. I-6a-d) can be used to determine the ^{13}C enrichment (slope of the regression of the data points) and whether the fractionation associated with the process can be described as occurring in an "equilibrium open" or "equilibrium closed" system (e.g., Gat and Gonfiantini, 1981; Kendall and Caldwell, 1998). The $\delta^{13}C$ of DIC and CO_2 from the closed acidification are positively correlated with DIC decrease (C_t/C_0) during the HCO_3^- dehydration phase (C_t/C_0 >~0.2) and negatively correlated during the phase (C_t/C_0 <~0.2) after HCO_3^- was exhausted in the samples (Fig. I-6a-d). The least squares regression equations defining enrichment and depletion trends in $\delta^{13}C_{DIC}$ and $\delta^{13}C_{CO2}$ are presented in Table 2. The correlation coefficients for the regression of the data points range from 0.77 to 0.99. The fact that the ^{13}C enrichments and depletions can be defined by linear equations suggests that the overall effects of isotopic fractionation on DIC during acidification occur in an "equilibrium closed" system (Fonyuy and Atekwana, 2008b). We note that the data for some of the regressions are few (n=3). However, the increasing and decreasing trends in $\delta^{13}C$ exhibited by all the different samples are similar, thus validating those trends defined by fewer points.

4.2.2. Carbon isotope enrichment during close acidification

The $\delta^{13}C_{DIC}$ and $\delta^{13}C_{CO2}$ were progressively enriched during the HCO_3^- dehydration phase (Fig. I-6a-d). However, the enrichments occur at different rates for CO_2 and DIC, i.e., the slopes of the trends in the isotopic enrichment are steeper for CO_2 (14.3, 20.3, 17.7, and 10.4) compared to DIC (5.9, 7.7, 6.3, and 4.7) (Table 2). The $\delta^{13}C_{CO2}$ from closed acidification supports a reaction mechanism in which the carbon in $CO_{2(aq)}$ equilibrates with carbon in HCO_3^- (Fonyuy and Atekwana., 2008b). Isotopic exchange of carbon in $CO_{2(aq)}$ with carbon in HCO_3^- during progressive acidification caused enrichment in $^{13}C_{CO2(g)}$ to occur at a higher rate compared to the enrichment of $^{13}C_{DIC}$. The enrichment in the $^{13}C_{CO2}$ occurs until it is equal to that of DIC near the point where HCO_3^- is exhausted (Fig. I-6a-d). This concept of carbon equilibration between HCO_3^- and $CO_{2(aq)}$ allows us to explain the rather small initial $\delta^{13}C_{CO2}$ depletion compared to $\delta^{13}C_{DIC}$ of the acidified AMD spring. As previously stated, the AMD spring had already undergone some degree of acidification in the field. During the laboratory acidification of AMD, equilibration of carbon between HCO_3^- and $CO_{2(aq)}$ is responsible for the smaller negative enrichment of the $\delta^{13}C_{CO2}$.

The magnitude of the negative shift in $\delta^{13}C_{DIC}$ and the rate of depletion (slopes of the trend lines) vary for $NaHCO_3$, stream water, groundwater, and the AMD spring. Least squares regression equations fitted to the data for the negative $\delta^{13}C_{DIC}$ trends have slopes between 7.4 and 14.6 for closed acidifications (Table 2). The differences in the slopes are due to the relative difference in the initial DIC concentrations and DIC speciation during acidification.

4.2.3. Carbon isotope enrichment during open acidification

The samples acidified under open conditions show the same general trends in $\delta^{13}C_{DIC}$ as exhibited by samples acidified under close conditions with two main differences. During HCO_3^- dehydration in the open acidification, the rates of $CO_{2(aq)}$ accumulation are higher (overall higher concentration of $CO_{2(aq)}$) and the $\delta^{13}C_{DIC}$ enrichment is of lower magnitude (Fig. I-5a-d). The trends in $\delta^{13}C_{DIC}$ enrichment followed by trends in the depletion of $\delta^{13}C_{DIC}$ indicate that the mechanism(s) causing isotopic fractionation during open acidification are the same as in the closed acidification. However, the greater accumulation of $CO_{2(aq)}$ in the solution during the open acidification facilitated the exchange of carbon between $CO_{2(aq)}$ and HCO_3^- to a much greater extent. This resulted in overall lower ^{13}C enrichment during the HCO_3^- dehydration phase and ^{13}C depletion after all HCO_3^- was exhausted.

4.2.4. Carbon isotope enrichment in unacidified samples

The $\delta^{13}C_{DIC}$ was enriched by 0.6‰ in $NaHCO_3$, 5.0‰ in stream water, and 3.4‰ in groundwater. The $\delta^{13}C_{DIC}$ of the AMD spring was initially enriched and reversed to depletion late in the experiment (Fig. I-3a-d). The ^{13}C enrichment was 2.7‰ and the depletion was 9.8‰ in the AMD spring. The temporal $\delta^{13}C_{DIC}$ for the unacidified samples are positively correlated with time except for the AMD spring (Fig. I-7a-c). The lack of a positive correlation for the enrichment in $\delta^{13}C_{DIC}$ vs. time for the AMD spring (Fig. I-7d) is due to the differences in the mechanisms causing isotope fractionation and enrichment in the samples. The isotope fractionation of carbon in $NaHCO_3$, stream water, and groundwater is due to equilibrium exchange of carbon between HCO_3^- and atmospheric CO_2 (e.g., Fonyuy and Atekwana, 2008b). For these samples, least squares

regression equations of time vs. $\delta^{13}C_{DIC}$ shows that stream water has the highest enrichment rate given by a slope of 0.007, while $NaHCO_3$ has the lowest slope of 0.0006. At equilibrium, the $\delta^{13}C$ enrichment should approach values for equilibrium exchange of carbon (~8.02‰ at 23^{o}C) between HCO_3^- and $CO_{2(g)}$ (Lesniak and Zawidzki, 2006; Mook et al., 1974). The differences in the rate at which these samples are exchanging carbon with atmospheric CO_2 varies with the initial $CO_{2(aq)}$:HCO_3^- ratio. Carbon equilibration between HCO_3^- in the samples and atmospheric CO_2 is facilitated by increasing concentration of $CO_{2(aq)}$. The higher the $CO_{2(aq)}$:HCO_3^- the faster the rate of equilibration (slope of the regression line) and the greater the enrichment rate.

The AMD spring sample lost more than 99% of its original DIC accompanied by a decrease in pH from 5.7 to 3.2. The DIC loss was concomitant with a $\delta^{13}C$ enrichment of 2.7‰ followed by depletion. We observed depletion of $\delta^{13}C$ of -18.8‰ at DIC concentration of 0.23 mM C/L. Although we are unable to explain this depletion, such depleted $\delta^{13}C$ in AMD contaminated samples have been reported by Fonyuy and Atekwana (2008a). We attribute the enrichment and the depletion trends of the unacidified AMD spring sample to the same processes that cause fractionation in the acidified samples (section 4.2.2 and 4.2.3.) Oxidation of Fe^{2+} to Fe^{3+} and followed by hydrolysis of Fe^{3+} to form Fe-precipitates and protons. The dehydrated of HCO_3^- by protons causes this sample to behave similar to samples from the open acidification.

5. Summary and implications

We progressively acidified natural and artificial water samples to study the effects of acidification on carbon isotope fractionation. Another set of water samples used as controls were allowed to evolve unacidfied and in contact with ambient laboratory air for 7 to 43 days. During acidification, HCO_3^- dehydration was concomitant with increase in the pCO_2 in the samples. The pCO_2 increased with progressive acidification to maximum values near the point when HCO_3^- in the samples was exhausted, after which the pCO_2 values decline continuously to the end of the experiment. The $\delta^{13}C_{DIC}$ was enriched during the HCO_3^- dehydration phase and was depleted after HCO_3^- was exhausted. The trends in enrichment and depletion of the $\delta^{13}C_{DIC}$ mimicked those of the pCO_2. However, the rate of isotopic enrichment and depletion in each acidified sample was different and depended on the initial HCO_3^-:$CO_{2(aq)}$ ratio. The concentration of $CO_{2(aq)}$ in each sample controlled the extent of isotopic exchange of carbon between the un-dehydrated HCO_3^- and the $CO_{2(aq)}$. The $\delta^{13}C$ of CO_2 captured from the acidified samples showed a steep enrichment trend with progressive acidification consistent with such a carbon exchange. The $\delta^{13}C_{CO2}$ evolved was identical to the $\delta^{13}C_{DIC}$ of samples at the point where all HCO_3^- was exhausted. Thus, higher concentrations of $CO_{2(aq)}$ resulted in greater exchange of carbon between HCO_3^- and $CO_{2(aq)}$ which minimized the enrichment in $\delta^{13}C_{DIC}$ from HCO_3^--$CO_{2(g)}$ fractionation during progressive acidification. The depletion of the $\delta^{13}C_{DIC}$ after HCO_3^- was exhausted in the samples was governed by isotopic fractionation controlled by the solubilities of ^{13}C vs. ^{12}C during water-gas exchange. The slightly more soluble and reactive ^{12}C is retained in solution causing the observed ^{13}C depletion.

The unacidified samples also showed isotopic enrichment which we attribute to exchange of carbon between HCO_3^- and atmospheric CO_2. The rate and extent of exchange was facilitated by the $CO_{2(aq)}$ concentration. Samples with higher initial $CO_{2(aq)}$ relative to HCO_3^- had higher rates of carbon exchange, and the higher rates caused the ^{13}C enrichment in the samples to approach values expected for equilibrium isotopic exchange between HCO_3^- and atmospheric CO_2.

From the results of our laboratory experiments, the $\delta^{13}C_{DIC}$ measured for samples undergoing acidification show variable enrichment or depletion. Whether enrichments or depletion in the $\delta^{13}C_{DIC}$ are measured for field samples will depend on the extent to which the acidification process occurred before sampling. If samples are collected during the HCO_3^- dehydration phase, enrichment in the $\delta^{13}C_{DIC}$ will be observed, the magnitude of which will depend on the extent of HCO_3^- dehydration. Alternatively, if samples are collected after all HCO_3^- is dehydrated, a depletion in the $\delta^{13}C_{DIC}$ will be measured, the magnitude of which will also dependent on the progress of acidification. Thus, measured enrichment followed by depletion in $\delta^{13}C_{DIC}$ of samples in the downstream direction in an AMD contaminated stream and over time in laboratory studies (e.g., Fonyuy and Atekwana, 2008 a&b) can be explained by the process of acidification. We conclude that in order to adequately assess the effects of acidification on the stable carbon isotopes of DIC in surface waters, time series measurements may be necessary to capture the progressive changes. When spatial and time series measurements are made, DIC species and the $\delta^{13}C_{DIC}$ should be measured along with routine physical and chemical parameters, as this would provide adequate input to model the process of acidification and its effect on stable carbon isotopes.

Acknowledgements

This work was funded by the US National Science Foundation Award EAR-0510954. We thank F. Ekollo, J. Magers, and S. Drueckhammer for their laboratory assistance. Comments and suggestions from two anonymous reviewers helped improve this manuscript.

References

Atekwana, E.A. and Krishnamurthy, R.V., 1998. Seasonal variations of dissolved inorganic carbon and $d^{13}C$ of surface waters: application of a modified gas evolution technique. Journal of Hydrology 205, 265-278.

Baker, L.A., Herlihy, A.T., Kaufmann, P.R. and Eilers, J.M., 1991. Acidic lakes and streams in the United-States - the role of acidic deposition. Science 252, 1151-1154.

Benson, A.K., 1998. Detecting the presence of acid mine drainage using hydrogeological, geochemical, and geophysical data; applications to contrasting conditions at mine sites in Little Cottonwood and American Fork canyons, Utah. In: C.L. Addams (Editor), Environmental Geosciences. Blackwell Science: Cambridge, MA, United States, pp. 17.

Berelson, W.M., Hammond, D.E., McManus, J. and Kilgore, T.E., 1994. Dissolution kinetics of calcium-carbonate in Equatorial Pacific sediments. Global Biogeochemical Cycles 8, 219-235.

Blodau, C., 2006. A review of acidity generation and consumption in acidic coal mine lakes and their watersheds. Science of the Total Environment 369, 307-332.

Clark, I.D., and Lauriol, B., 1992. Kinetic enrichment of stable isotopes in cryogenic calcites. Chemical Geology 102, 217–228.

Espana, J.S., Pamo, E.L., Santofimia, E., Aduvire, O., Reyes, J. and Barettino, D., 2005. Acid mine drainage in the Iberian Pyrite Belt (Odiel river watershed, Huelva, SW Spain): Geochemistry, mineralogy and environmental implications. Applied Geochemistry 20, 1320-1356.

Feely, R.A., Sabine, C.L., Lee K, et al., 2004. Impact of anthropogenic CO_2 on the $CaCO_3$ system in the oceans. Science 305, 362-366.

Fonyuy, E.W. and Atekwana, E.A., 2008a. Effects of acid mine drainage on dissolved inorganic carbon and stable carbon isotopes in receiving streams. Applied Geochemistry 23, 743-764.

Fonyuy, E.W. and Atekwana, A.E., 2008b. Dissolved inorganic carbon evolution and stable carbon isotope fractionation in acid mine drainage impacted streams: insights from a laboratory study. Journal of Applied Geochemistry 23, 2634-2648.

Galimov, E.M., 2006. Isotope organic geochemistry. Organic Geochemistry 37, 1200-1262.

Gat, J.R. and Gonfiantini, R., 1981. Stable isotope hydrology: Deuterium and oxygen-18 in the water cycle. IAEA Technical Report Series No. 210, IAEA Vienna, 337 p.

Hach Company, 1992. Water analysis handbook, Hach Company, Loveland, Co.

Halas, S., Szaran, J. and Niezgoda, H., 1997. Experimental determination of carbon isotope equilibrium fractionation between dissolved carbonate and carbon dioxide. Geochimica et Cosmochimica Acta 61, 2691-2695.

Herlihy, A.T., Kaufmann, P.R. and Mitch, M.E., 1991. Stream chemistry in the Eastern United-States. Part 2. Current sources of acidity in acidic and low acid-neutralizing capacity streams. Water Resources Research 27, 629-642.

Heron, G., Barcelona, M.J., Andersen, M.L. and Christensen, T.H., 1997. Determination of nonvolatile organic carbon in aquifer solids after carbonate removal by sulfurous acid. Ground Water 35, 6-11.

Kaufmann, P.R., Herlihy, A.T., Mitch, M.E., Messer, J.J., and Overton,W.S., 1991. Stream chemistry in the eastern United States, 1. Synoptic survey design, acid-base status, and regional patterns. Water Resource. Research 27, 611- 627.

Kaufmann, P.R., Herlihy, A.T., and Baker L.A., 1992. Sources of acidity in lakes and streams of the United-States. Environmental Pollution77, 115-122.

Kendall, C. and Caldwell, E.A., 1998. Fundamentals of isotope geochemistry In: C. Kendall and J.J. McDonnell (Editors), Isotope Tracers in Catchment Hydrology. Elsevier Science B.V., Amsterdam.

Larssen, T. and Carmichael, G.R., 2000. Acid rain and acidification in China: the importance of base cation deposition. Environmental Pollution 110, 89-102.

Lee, J.S. and Chon, H.T., 2006. Hydrogeochemical characteristics of acid mine drainage in the vicinity of an abandoned mine, Daduk Creek, Korea. Journal of Geochemical Exploration 88, 37-40.

Lesniak, P.M. and Zawidzki, P., 2006. Determination of carbon fractionation factor between aqueous carbonate and CO_2(g) in two-direction isotope equilibration. Chemical Geology 231, 203-213.

Lohse, L., Kloosterhuis, R.T., de Stigter, H.C., et al., 2000. Carbonate removal by acidification causes loss of nitrogenous compounds in continental margin sediments. Marine Chemistry 69, 193-201.

Mariotti A., Germon J.C., Hubert P., et al., 1981. Experimental determination of nitrogen kinetic isotope fractionation: Some principles; illustration for the denitrification and nitrification processes. Plant and Soil 62, 413.

Mayo, A.L., Petersen, E.C. and Kravits, C., 2000. Chemical evolution of coal mine drainage in a non-acid producing environment, Wasatch Plateau, Utah, USA. Journal of Hydrology 236, 1-16.

Mills, A., and Urey, H.C., 1940. The kinetics of isotope exchange between carbon dioxide, bicarbonate ion, carbonate ion, and water. Journal of American Chemistry Society 62, 1019.

Monson, K.D. and Hayes, J.M., 1980. Biosynthetic control of the natural abundance of carbon-13 at specific positions within fatty acids in *Escherichia coli*. Evidence regarding the coupling of fatty acid and phospholipid synthesis. Journal of Biological Chemistry 255, 11435-11441.

Mook, W.G., Bommerson, J.C. and Staverman, W.H., 1974. Carbon isotope fractionation between dissolved bicarbonate and gaseous carbon dioxide. Earth and Planetary Science Letters 22, 169-176.

Orr, J.C., Fabry, V.J., Aumont, O., et al., 2005. Anthropogenic ocean acidification over the twenty-first century and its impact on calcifying organisms. Nature 437, 681-686.

Stoddard, J.L., Jeffries, D.S., Lukewille, A., et al., 1999. Regional trends in aquatic recovery from acidification in North America and Europe. Nature 401, 575-578.

Szaran, J., 1998. Carbon isotope fractionation between dissolved and gaseous carbon dioxide. Chemical Geology 150, 331-337.

Usdowski, E. and Hoefs, J., 1990. Kinetic $^{13}C/^{12}C$ and $^{18}O/^{16}O$ effects upon dissolution and outgassing of CO_2 in the system CO_2-H_2O. Chemical Geology: Isotope Geoscience section 80, 109-118.

Vogel, J.C., Grootes, P.M. and Mook, W.G., 1970. Isotopic fractionation between gaseous and dissolved carbon dioxide. Zeitschrift fur Physik A (Atoms and Nuclei) 230, 225-238.

Webb, J.A. and Sasowsky, I.D., 1994. The interaction of acid mine drainage with a carbonate terrane: evidence from the Obey River, north-central Tennessee. Journal of Hydrology 161, 327-346.

Wicks, C.M. and Groves, C.G., 1993. Acidic mine drainage in carbonate terrains: geochemical processes and rates of calcite dissolution. Journal of Hydrology 146, 13-27.

Wright, R.F., Alewell, C., Cullen, J.M., et al., 2001. Trends in nitrogen deposition and leaching in acid-sensitive streams in Europe. Hydrology and Earth System Sciences 5, 299-310.

Zachos, J.C., Rohl, U., Schellenberg, S.A., et al., 2005. Rapid acidification of the ocean during the Paleocene-Eocene thermal maximum. Science 308, 1611-1615.

Zhang, J., Quay, P.D., and Wilbur, D.O., 1995. Carbon isotope fractionation during gas-water exchange and dissolution of CO_2. Geochimica et Cosmochimica Acta 59, 107–114.

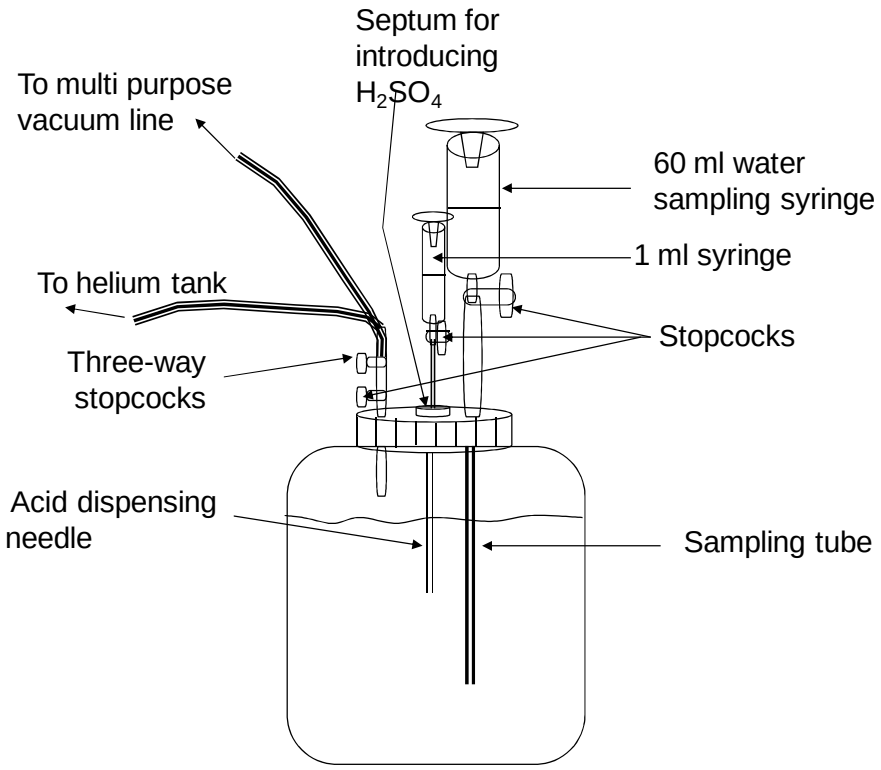

Figure I-1: Reactor modification for closed acidification

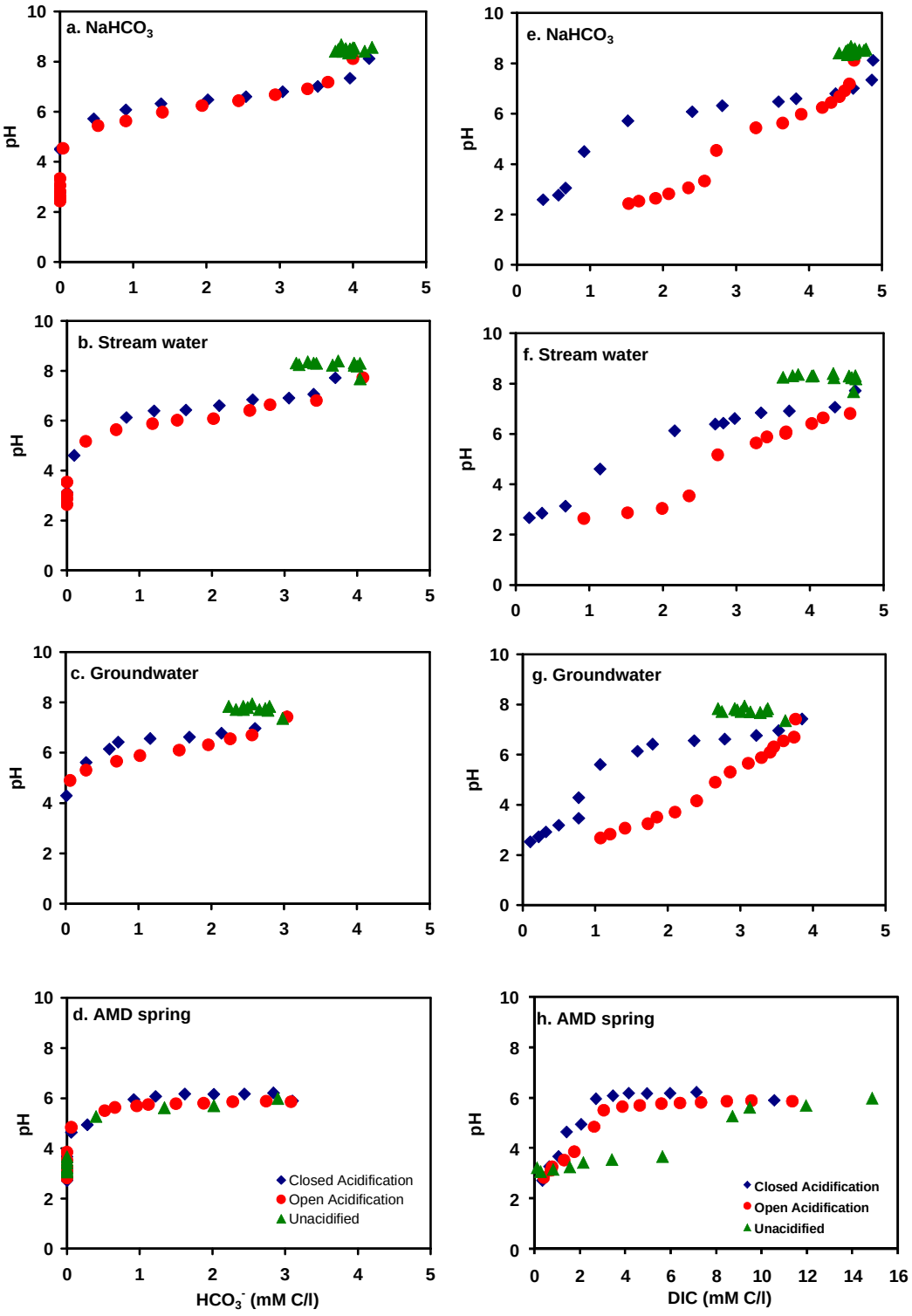

Figure I-2: Cross plots of pH vs. HCO_3^- (a–d) and pH vs. DIC (e–h) for closed acidification, open acidification, and for unacidified samples of $NaHCO_3$, stream water, groundwater, and spring water (AMD spring) contaminated by acid mine drainage.

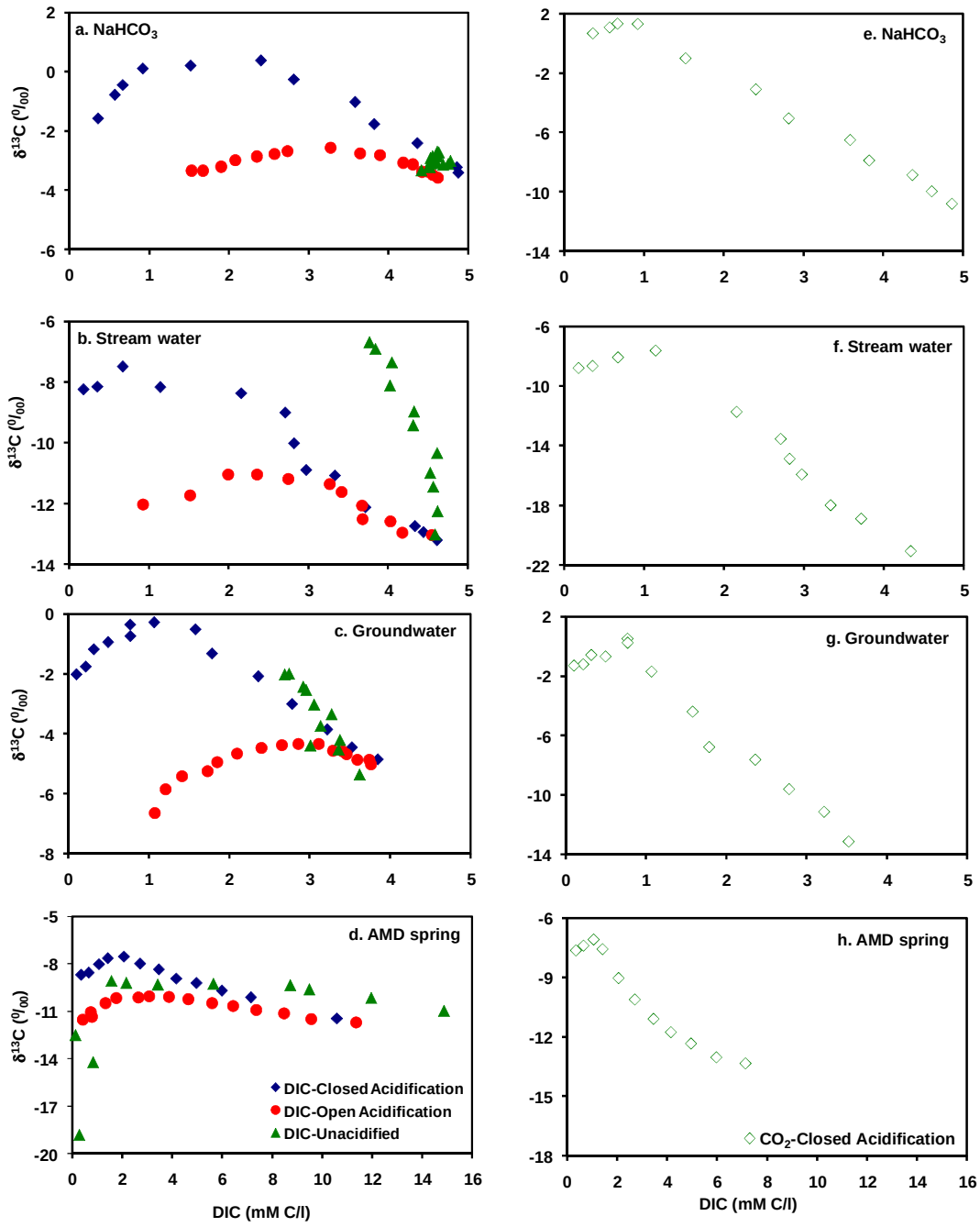

Figure I-3: Cross plots of $\delta^{13}C_{DIC}$ vs. DIC for closed acidification, open acidification, and unacidified samples (a–d) and the $\delta^{13}C_{CO2}$ vs. DIC for closed acidification (e–h) of $NaHCO_3$, stream water, groundwater, and spring water (AMD spring) contaminated by acid mine drainage.

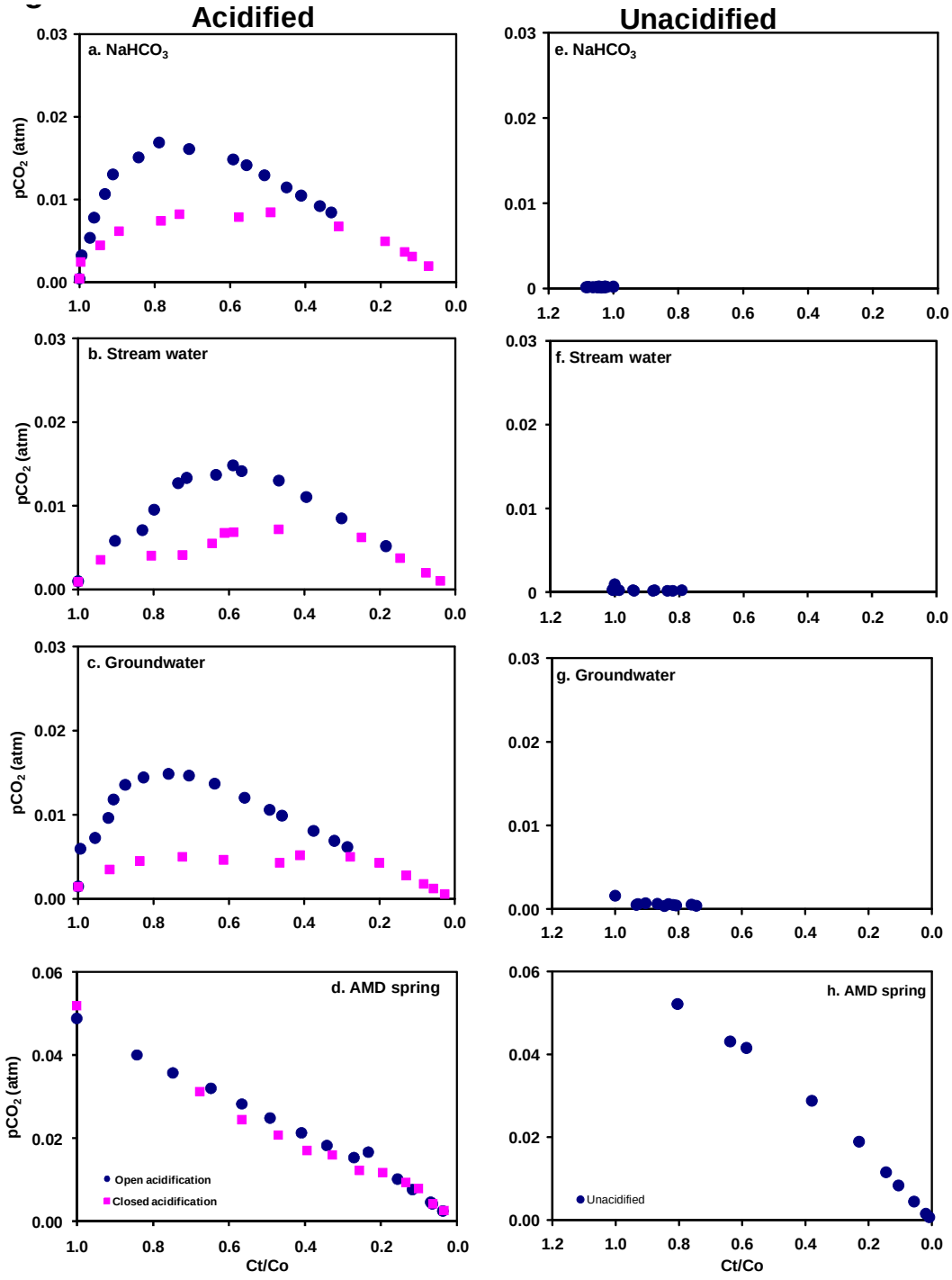

Figure I-4: Cross plots of the calculated partial pressure of CO_2 (pCO_2) vs. fraction of DIC at any time to that at the beginning (C_t/C_0) for closed acidification and open acidification, (a–d) and unacidified samples (e–h) of $NaHCO_3$, stream water, groundwater, and spring water (AMD spring) contaminated by acid mine drainage.

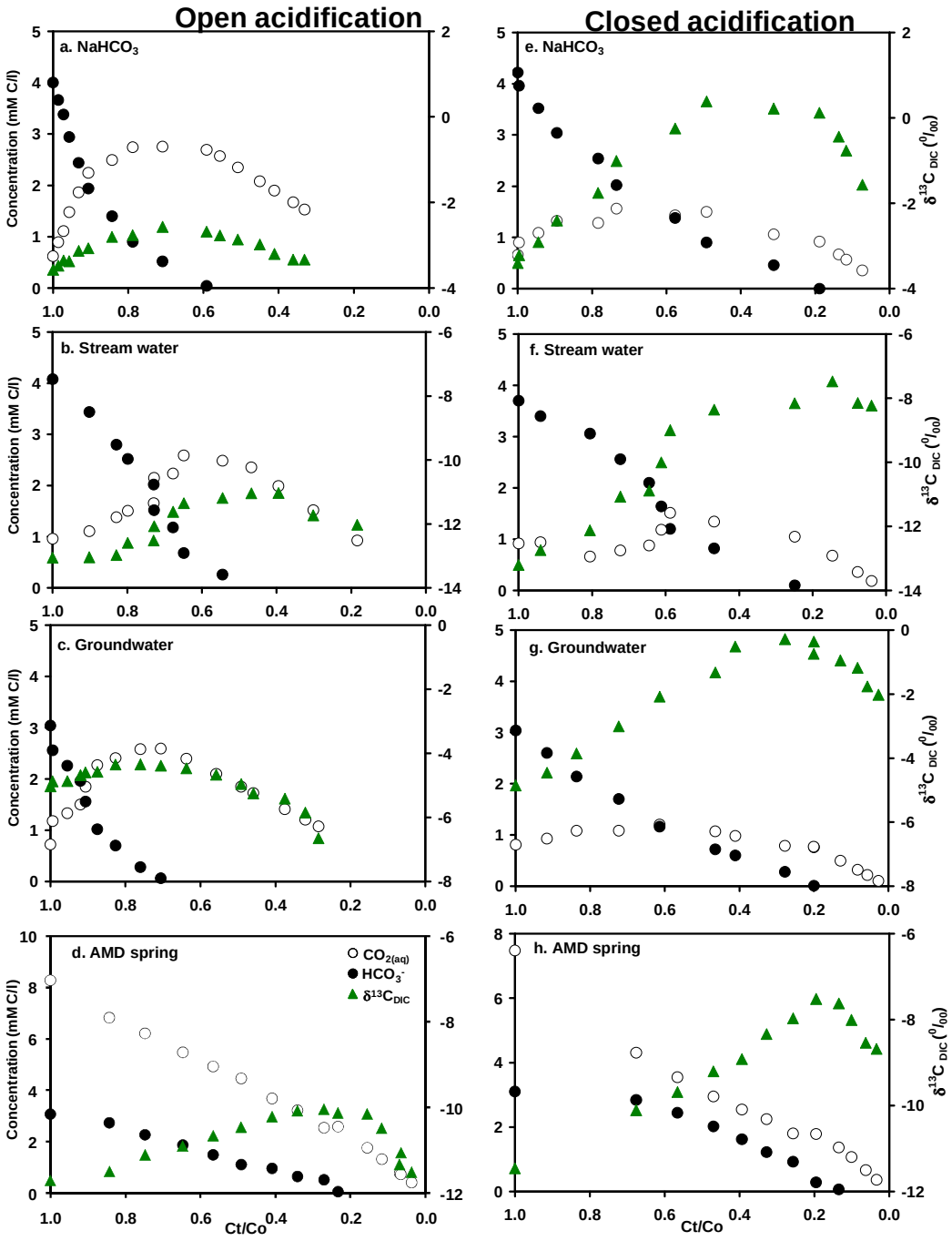

Figure I-5: Cross plots of concentration of HCO_3^- and H_2CO_3 primary axis and $\delta^{13}C$ of DIC (secondary axis) vs. fraction of DIC at any time to that at the beginning (C_t/C_0) for closed acidification and open acidification of samples of $NaHCO_3$, stream water, groundwater, and spring water (AMD spring) contaminated by acid mine drainage. of $NaHCO_3$, stream water, groundwater, and spring water contaminated by acid mine drainage (AMD spring).

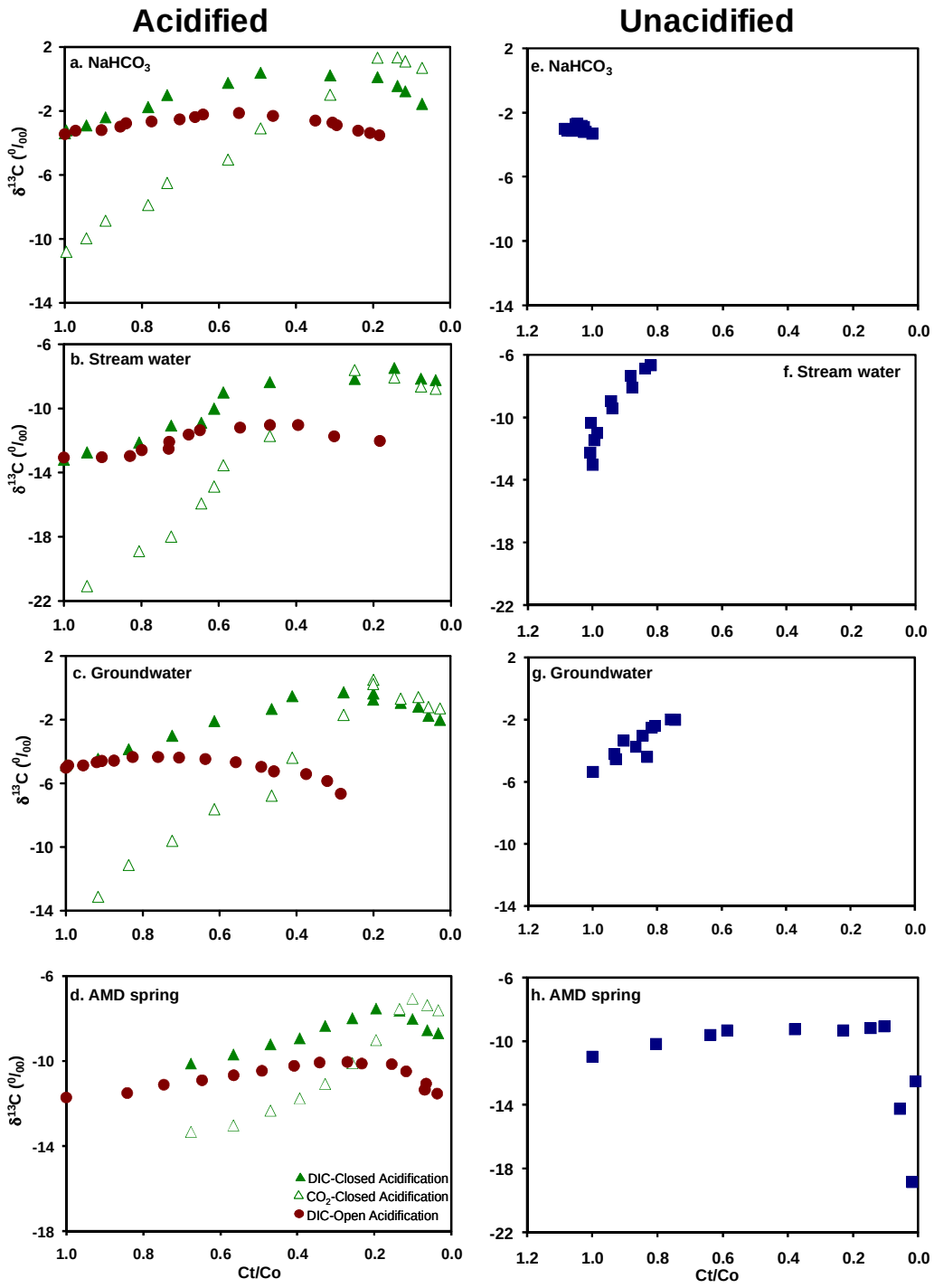

Figure I-6: Cross plots of fraction of DIC at anytime to that at the beginning (C_t/C_0) vs. $\delta^{13}C_{DIC}$ and $\delta^{13}C_{CO2}$ for closed acidification and open acidification (a-d), and unacidified samples (e-h) of $NaHCO_3$, stream water, groundwater, and spring water (AMD spring) contaminated by acid mine drainage.

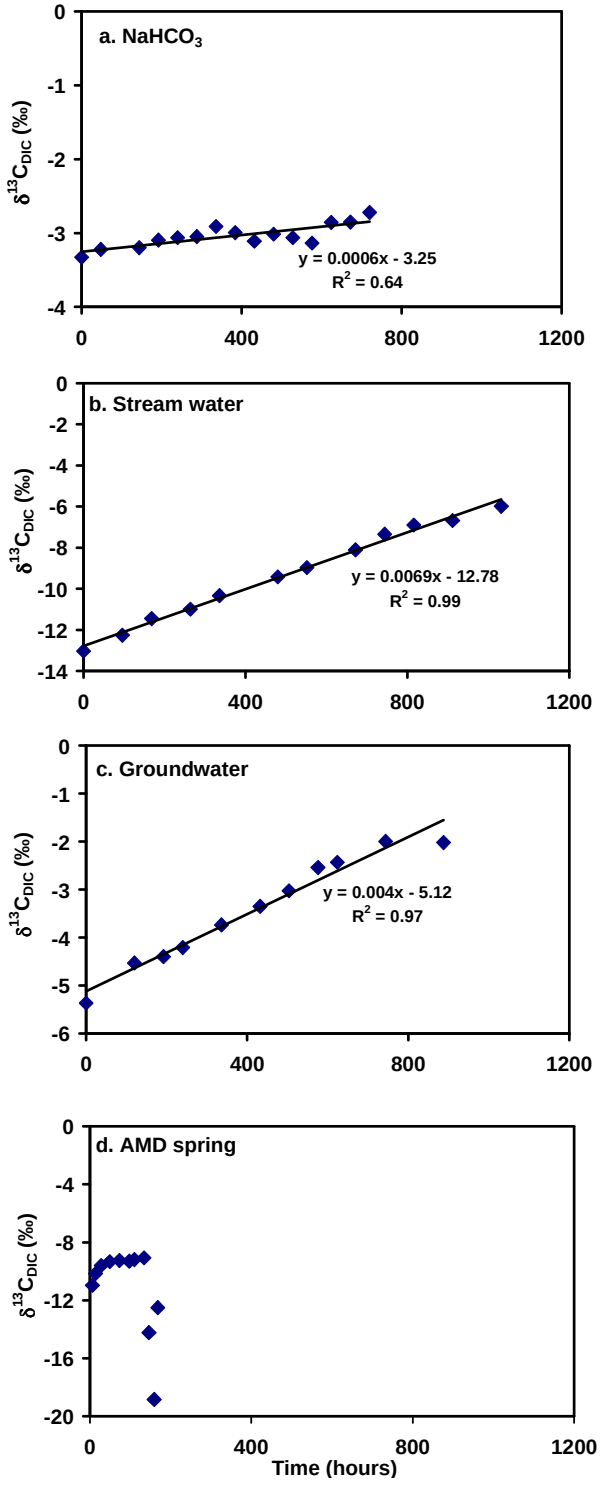

Figure I-7: Time series plots of $\delta^{13}C_{CO2}$of unacidified samples of $NaHCO_3$, stream water, groundwater, and spring water (AMD spring) contaminated by acid mine drainage.

Table I-1: Results of physical, chemical, and isotopic analyses of closed and open acidification and for unacidified samples of $NaHCO_3$, stream water, groundwater and AMD contaminated spring (AMD spring).
.

Sample ID	Cum. Time (hours)	Temp (°C)	pH	DIC (mM C/l)	H_2CO_3 (mM C/l)	HCO_3^- (mM C/l)	Ct/Co	$\delta^{13}C_{DIC}$ (‰)	$\delta^{13}C_{CO2(g)}$ (‰)	pCO_2 (atm)	Fe^{2+} (mM/l)
$NaHCO_3$: Closed acidification											
AC1-1	_	23.12	8.12	4.88	0.66	4.22	1.000	-3.4	-	4.46E-04	_
AC1-2	_	23.42	7.34	4.86	0.90	3.96	0.996	-3.22	-10.81	2.50E-03	_
AC1-3	_	23.26	7.01	4.61	1.09	3.52	0.944	-2.91	-9.97	4.57E-03	_
AC1-4	_	23.46	6.8	4.36	1.32	3.04	0.895	-2.4	-8.87	6.34E-03	_
AC1-5	_	23.27	6.6	3.82	1.28	2.54	0.784	-1.76	-7.89	7.62E-03	_
AC1-6	_	23.32	6.48	3.58	1.56	2.02	0.735	-1.01	-6.5	8.46E-03	_
AC1-7	_	23.4	6.32	2.81	1.43	1.38	0.577	-0.25	-5.05	8.09E-03	_
AC1-8	_	23.13	6.08	2.40	1.50	0.90	0.492	0.39	-3.09	8.62E-03	_
AC1-9	_	23.33	5.72	1.52	1.06	0.46	0.311	0.22	-0.99	6.82E-03	_
AC1-10	_	22.87	4.5	0.92	0.92	_	0.189	0.12	1.33	4.94E-03	_
AC1-11	_	23.17	3.05	0.67	0.67	_	0.137	-0.44	1.35	3.66E-03	_
AC1-12	_	22.81	2.77	0.57	0.57	_	0.116	-0.77	1.1	3.09E-03	_
AC1-13	_	23.28	2.59	0.36	0.36	_	0.073	-1.57	0.7	1.97E-03	_
$NaHCO_3$: Open acidification											
AC2-1	_	23.19	8.12	4.62	0.62	4.00	1.000	-3.57	_	4.23E-04	_
AC2-2	_	23.2	7.18	4.55	0.89	3.66	0.986	-3.48	_	3.24E-03	_
AC2-3	_	23.19	6.91	4.49	1.11	3.38	0.972	-3.36	_	5.35E-03	_
AC2-4	_	23.23	6.68	4.42	1.48	2.94	0.957	-3.37	_	7.79E-03	_
AC2-5	_	23.24	6.44	4.30	1.86	2.44	0.932	-3.13	_	1.07E-02	_
AC2-6	_	23.26	6.24	4.18	2.24	1.94	0.906	-3.07	_	1.30E-02	_
AC2-7	_	23.27	5.98	3.89	2.49	1.40	0.843	-2.81	_	1.51E-02	_
AC2-8	_	23.27	5.63	3.64	2.74	0.90	0.788	-2.77	_	1.69E-02	_
AC2-9	_	23.29	5.44	3.27	2.75	0.52	0.709	-2.57	_	1.61E-02	_
AC2-10	_	23.3	4.54	2.73	2.69	0.04	0.592	-2.68	_	1.48E-02	_
AC2-11	_	23.3	3.33	2.57	2.57	_	0.556	-2.77	_	1.42E-02	_

Sample ID	Cum. Time (hours)	Temp (°C)	pH	DIC (mM C/l)	H_2CO_3 (mM C/l)	HCO_3^- (mM C/l)	Ct/Co	$d^{13}C_{DIC}$ (‰)	$d^{13}C_{CO2(g)}$ (‰)	pCO_2 (atm)	Fe^{2+} (mM/l)
AC2-12	_	23.3	3.06	2.35	2.35	_	0.509	-2.86	_	1.29E-02	_
AC2-13	_	23.3	2.82	2.08	2.08	_	0.450	-2.98	_	1.15E-02	_
AC2-14	_	23.31	2.64	1.90	1.90	_	0.411	-3.2	_	1.05E-02	_
AC2-15	_	23.32	2.53	1.67	1.67	_	0.362	-3.34	_	9.21E-03	_
AC2-16	_	23.32	2.43	1.53	1.53	_	0.331	-3.34	_	8.44E-03	_
$NaHCO_3$: Unacidified											
UC1-1	0	23.66	8.41	4.41	0.65	3.76	1.000	-3.33	_	2.09E-04	_
UC1-2	48	23.73	8.41	4.52	0.66	3.86	1.025	-3.22	_	2.14E-04	_
UC1-3	144	22.7	8.48	4.50	0.70	3.80	1.021	-3.20	_	1.79E-04	_
UC1-4	192	22.56	8.54	4.53	0.51	4.02	1.027	-3.10	_	1.56E-04	_
UC1-5	240	22.74	8.55	4.56	0.56	4.00	1.034	-3.06	_	1.54E-04	_
UC1-6	288	22.93	8.37	4.60	0.64	3.96	1.043	-3.05	_	2.37E-04	_
UC1-7	336	23.09	8.35	4.53	0.59	3.94	1.026	-2.91	_	2.44E-04	_
UC1-8	384	23.04	8.51	4.53	0.63	3.90	1.028	-3.00	_	1.69E-04	_
UC1-9	432	22.97	8.51	4.75	0.79	3.96	1.077	-3.11	_	1.77E-04	_
UC1-10	480	23.08	8.57	4.78	0.52	4.26	1.083	-3.01	_	1.55E-04	_
UC1-11	528	22.89	8.67	4.57	0.74	3.84	1.037	-3.06	_	1.17E-04	_
UC1-12	576	23.42	8.52	4.69	0.79	3.90	1.063	-3.14	_	1.71E-04	_
UC1-13	624	23.49	8.58	4.63	0.79	3.84	1.048	-2.86	_	1.47E-04	_
UC1-14	672	23.11	8.48	4.55	0.66	3.90	1.032	-2.85	_	1.82E-04	_
UC1-15	720	23.23	8.45	4.63	0.65	3.98	1.050	-2.72	_	1.99E-04	_
UC1-16	768	23.2	8.41	4.61	0.46	4.16	1.046	-2.70	_	2.17E-04	_
Stream water: Closed acidification											
ALP1-1	_	19.34	7.72	4.61	0.91	3.70	1.000	-13.2	_	9.82E-04	_
ALP1-2	_	21.4	7.06	4.34	0.94	3.40	0.940	-12.74	-21.08	3.80E-03	_
ALP1-3	_	21.44	6.91	3.72	0.66	3.06	0.806	-12.12	-18.9	4.31E-03	_
ALP1-4	_	21.69	6.84	3.34	0.78	2.56	0.723	-11.07	-17.99	4.40E-03	_
ALP1-5	_	23.1	6.61	2.98	0.88	2.10	0.645	-10.89	-15.92	5.83E-03	_
ALP1-6	_	23.26	6.43	2.82	1.18	1.64	0.612	-10.01	-14.87	7.11E-03	_
ALP1-7	_	23.25	6.39	2.71	1.51	1.20	0.588	-9	-13.54	7.17E-03	_

ALP1-8	_	23.28	6.13	2.16	1.34	0.82	0.468	-8.36	-11.72	7.47E-03	_

Sample ID	Cum. Time (hours)	Temp (°C)	pH	DIC (mM C/l)	H_2CO_3 (mM C/l)	HCO_3^- (mM C/l)	Ct/Co	$\delta^{13}C_{DIC}$ (‰)	$\delta^{13}C_{CO2(g)}$ (‰)	pCO_2 (atm)	Fe^{2+} (mM/l)
ALP1-9	_	23.31	4.61	1.15	1.05	0.10	0.249	-8.16	-7.6	6.22E-03	_
ALP1-10	_	23.49	3.13	0.68	0.68	_	0.146	-7.48	-8.06	3.74E-03	_
ALP1-11	_	23.56	2.85	0.36	0.36	_	0.077	-8.14	-8.63	1.98E-03	_
ALP1-12	_	23.45	2.67	0.18	0.18	_	0.040	-8.23	-8.77	1.01E-03	_
Stream water: Open acidification											
ALP2-1	_	19.83	7.73	5.04	0.96	4.08	1.000	-13.06	_	1.06E-03	_
ALP2-2	_	20.51	6.81	4.55	1.11	3.44	0.902	-13.04	_	6.16E-03	_
ALP2-3	_	20.95	6.64	4.18	1.38	2.80	0.829	-12.97	_	7.50E-03	_
ALP2-4	_	21.49	6.41	4.02	1.51	2.52	0.799	-12.6	_	1.00E-02	_
ALP2-5	_	22.83	6.08	3.67	1.66	2.02	0.729	-12.52	_	1.31E-02	_
ALP2-6	_	22.92	6.02	3.67	2.15	1.52	0.728	-12.07	_	1.37E-02	_
ALP2-7	_	23.02	5.88	3.41	2.23	1.18	0.677	-11.62	_	1.40E-02	_
ALP2-8	_	23.11	5.64	3.27	2.59	0.68	0.649	-11.35	_	1.50E-02	_
ALP2-9	_	23.22	5.17	2.75	2.49	0.26	0.545	-11.19	_	1.42E-02	_
ALP2-10	_	23.33	3.54	2.36	2.36	_	0.468	-11.04	_	1.30E-02	_
ALP2-11	_	23.47	3.04	1.99	1.99	_	0.395	-11.04	_	1.10E-02	_
ALP2-12	_	23.66	2.87	1.52	1.52	_	0.302	-11.73	_	8.46E-03	_
ALP2-13	_	23.66	2.64	0.93	0.93	_	0.184	-12.02	_	5.16E-03	_
Stream water: Unacidified											
LP1-1	0	19.25	7.68	4.59	0.55	4.04	1.000	-13.02	_	1.07E-03	_
LP1-2	96	24.28	8.19	4.62	0.62	4.00	1.007	-12.25	_	3.66E-04	_
LP1-3	168	23.91	8.23	4.57	0.61	3.96	0.995	-11.45	_	3.29E-04	_
LP1-4	264	23.27	8.3	4.53	0.49	4.04	0.987	-10.99	_	2.75E-04	_
LP1-5	336	22.49	8.31	4.62	0.66	3.96	1.006	-10.33	_	2.71E-04	_
LP1-6	480	22.97	8.4	4.32	0.58	3.74	0.940	-9.42	_	2.07E-04	_
LP1-7	552	24.91	8.23	4.33	0.67	3.66	0.942	-8.96	_	3.16E-04	_
LP1-8	672	24.6	8.3	4.02	0.59	3.44	0.877	-8.1	_	2.49E-04	_
LP1-9	744	24.03	8.31	4.05	0.65	3.40	0.882	-7.34	_	2.43E-04	_
LP1-10	816	25.1	8.36	3.84	0.52	3.32	0.837	-6.9	_	2.09E-04	_

LP1-11	912	22.7	8.31	3.76	0.60	3.16	0.820	-6.68	_	2.22E-04	_
Sample ID	**Cum. Time (hours)**	**Temp (^{o}C)**	**pH**	**DIC (mM C/l)**	**H_2CO_3 (mM C/l)**	**HCO_3^- (mM C/l)**	**Ct/Co**	**$\delta^{13}C_{DIC}$ (‰)**	**$\delta^{13}C_{CO2(g)}$ (‰)**	**pCO_2 (atm)**	**Fe^{2+} (mM/l)**
LP1-12	1032	29.1	8.25	3.63	0.43	3.20	0.792	-5.98	_	2.70E-04	_
Groundwater: Closed acidification											
ATP1-1	_	23.22	7.43	3.85	0.81	3.04	1.000	-4.85	_	1.63E-03	_
ATP1-2	_	23.83	6.96	3.53	0.93	2.60	0.916	-4.45	-13.14	3.89E-03	_
ATP1-3	_	23.99	6.77	3.22	1.08	2.14	0.837	-3.85	-11.14	4.98E-03	_
ATP1-4	_	23.89	6.62	2.78	1.08	1.70	0.723	-3.01	-9.61	5.46E-03	_
ATP1-5	_	23.86	6.56	2.36	1.20	1.16	0.614	-2.08	-7.63	5.06E-03	_
ATP1-6	_	24.01	6.42	1.79	1.07	0.72	0.465	-1.33	-6.78	4.64E-03	_
ATP1-7	_	23.64	6.14	1.58	0.98	0.60	0.411	-0.52	-4.39	5.47E-03	_
ATP1-8	_	23.93	5.61	1.07	0.79	0.28	0.278	-0.28	-1.7	5.08E-03	_
ATP1-9	_	23.72	4.29	0.77	0.76	0.01	0.200	-0.36	0.52	4.26E-03	_
ATP1-10	_	23.63	3.47	0.77	0.77	_	0.201	-0.74	0.24	4.29E-03	_
ATP1-11	_	23.69	3.19	0.50	0.50	_	0.129	-0.95	-0.68	2.77E-03	_
ATP1-12	_	23.45	2.92	0.32	0.32	_	0.083	-1.18	-0.58	1.77E-03	_
ATP1-13	_	23.34	2.73	0.22	0.22	_	0.057	-1.76	-1.21	1.21E-03	_
ATP1-14	_	23.41	2.53	0.10	0.10	_	0.027	-2.02	-1.29	5.70E-04	_
Groundwater: Open acidification											
ATP2-1	_	24.54	7.42	3.76	0.72	3.04	1.000	-5.03	_	1.66E-03	_
ATP2-2	_	24.47	6.7	3.74	1.18	2.56	0.994	-4.87	_	6.54E-03	_
ATP2-3	_	24.49	6.55	3.59	1.33	2.26	0.955	-4.87	_	7.89E-03	_
ATP2-4	_	24.5	6.31	3.46	1.50	1.96	0.920	-4.68	_	1.03E-02	_
ATP2-5	_	24.55	6.1	3.41	1.85	1.56	0.906	-4.6	_	1.24E-02	_
ATP2-6	_	24.6	5.88	3.29	2.27	1.02	0.875	-4.58	_	1.40E-02	_
ATP2-7	_	24.62	5.66	3.11	2.41	0.70	0.826	-4.35	_	1.48E-02	_
ATP2-8	_	24.62	5.31	2.86	2.58	0.28	0.760	-4.34	_	1.50E-02	_
ATP2-9	_	24.64	4.9	2.65	2.59	0.06	0.706	-4.39	_	1.47E-02	_
ATP2-10	_	24.62	4.16	2.40	2.40	_	0.637	-4.47	_	1.36E-02	_
ATP2-11	_	24.62	3.71	2.10	2.10	_	0.558	-4.67	_	1.20E-02	_
ATP2-12	_	24.53	3.51	1.85	1.85	_	0.492	-4.96	_	1.05E-02	_
ATP2-13	_	24.5	3.25	1.73	1.73	_	0.459	-5.25	_	9.83E-03	_

ATP2-14	_	24.54	3.07	1.41	1.41	_	0.375	-5.41	_	8.04E-03	_
Sample ID	**Cum. Time (hours)**	**Temp (^{o}C)**	**pH**	**DIC (mM C/l)**	**H_2CO_3 (mM C/l)**	**HCO_3^- (mM C/l)**	**Ct/Co**	**$d^{13}C_{DIC}$ (‰)**	**$d^{13}C_{CO2(g)}$ (‰)**	**pCO_2 (atm)**	**Fe^{2+} (mM/l)**
ATP2-15	_	24.47	2.83	1.20	1.20	_	0.320	-5.85	_	6.85E-03	_
ATP2-16	_	24.52	2.68	1.07	1.07	_	0.285	-6.65	_	6.12E-03	_
Groundwater: Unacidified											
TP1-1	0	23.81	7.36	3.62	0.64	2.98	1.000	-5.37	_	1.80E-03	_
TP1-2	120	22.31	7.75	3.36	0.62	2.74	0.928	-4.53	_	7.00E-04	_
TP1-3	192	22.16	7.72	3.01	0.57	2.44	0.832	-4.4	_	6.70E-04	_
TP1-4	240	22.08	7.84	3.38	0.58	2.80	0.933	-4.21	_	5.74E-04	_
TP1-5	336	22	7.71	3.14	0.48	2.66	0.867	-3.74	_	7.12E-04	_
TP1-6	432	22.06	7.68	3.27	0.49	2.78	0.904	-3.35	_	7.94E-04	_
TP1-7	504	22.32	7.94	3.06	0.50	2.56	0.845	-3.03	_	4.17E-04	_
TP1-8	576	21.94	7.79	2.96	0.46	2.50	0.817	-2.54	_	5.62E-04	_
TP1-9	624	22.22	7.84	2.92	0.48	2.44	0.807	-2.43	_	4.98E-04	_
TP1-10	744	21.88	7.72	2.75	0.41	2.34	0.759	-2	_	6.09E-04	_
TP1-11	888	21.89	7.84	2.69	0.45	2.24	0.744	-2.02	_	4.58E-04	_
AMD Spring: Closed acidification											
AMS1-1	_	26.08	5.89	10.58	7.48	3.10	1.000	-11.47	-	4.64E-02	_
AMS1-2	_	25.33	6.21	7.15	4.31	2.84	0.676	-10.11	-13.34	2.40E-02	_
AMS1-3	_	25.69	6.17	5.98	3.54	2.44	0.566	-9.68	-13.04	2.10E-02	_
AMS1-4	_	24.22	6.16	4.97	2.95	2.02	0.469	-9.2	-12.34	1.71E-02	_
AMS1-5	_	24.08	6.17	4.16	2.54	1.62	0.393	-8.92	-11.76	1.41E-02	_
AMS1-6	_	24.36	6.07	3.47	2.25	1.22	0.328	-8.33	-11.09	1.29E-02	_
AMS1-7	_	24.32	5.95	2.72	1.80	0.92	0.257	-7.97	-10.11	1.10E-02	_
AMS1-8	_	24.94	4.94	2.06	1.78	0.28	0.195	-7.52	-9.02	1.15E-02	_
AMS1-9	_	24.47	4.64	1.42	1.36	0.06	0.135	-7.62	-7.56	7.95E-03	_
AMS1-10	_	24.65	3.67	1.07	1.07	_	0.101	-8.01	-7.07	6.10E-03	_
AMS1-11	_	24.22	3.27	0.66	0.66	_	0.062	-8.54	-7.38	3.73E-03	_
AMS1-12	_	24.18	2.72	0.36	0.36	_	0.034	-8.68	-7.62	2.02E-03	_
AMD Spring: Open acidification											
AMS2-1	_	27.12	5.86	11.35	8.27	3.08	1.000	-11.71	_	5.19E-02	_
AMS2-2	_	26.67	5.88	9.56	6.82	2.74	0.842	-11.5	_	4.28E-02	_

AMS2-3	_	26.43	5.86	8.48	6.20	2.28	0.747	-11.11	_	3.82E-02	_

Sample ID	Cum. Time (hours)	Temp (^{o}C)	pH	DIC (mM C/l)	H_2CO_3 (mM C/l)	HCO_3^- (mM C/l)	Ct/Co	$\delta^{13}C_{DIC}$ (‰)	$\delta^{13}C_{CO2(g)}$ (‰)	pCO_2 (atm)	Fe^{2+} (mM/l)
AMS2-4	_	26.38	5.8	7.35	5.47	1.88	0.647	-10.9	_	3.42E-02	_
AMS2-5	_	26.42	5.78	6.42	4.92	1.50	0.566	-10.66	_	3.02E-02	_
AMS2-6	_	26.46	5.75	5.58	4.46	1.12	0.491	-10.46	_	2.66E-02	_
AMS2-7	_	26.46	5.69	4.64	3.68	0.96	0.408	-10.22	_	2.28E-02	_
AMS2-8	_	26.48	5.63	3.87	3.21	0.66	0.341	-10.08	_	1.95E-02	_
AMS2-9	_	26.52	5.5	3.07	2.55	0.52	0.270	-10.04	_	1.61E-02	_
AMS2-10	_	26.52	4.84	2.64	2.58	0.06	0.233	-10.13	_	1.54E-02	_
AMS2-11	_	26.11	3.85	1.76	1.76	_	0.155	-10.15	_	1.04E-02	_
AMS2-12	_	25.94	3.52	1.32	1.32	_	0.116	-10.49	_	7.81E-03	_
AMS2-13	_	25.79	3.26	0.78	0.78	_	0.069	-11.34	_	4.60E-03	_
AMS2-14	_	25.37	3.1	0.73	0.73	_	0.065	-11.06	_	4.27E-03	_
AMS2-15	_	25.6	2.82	0.41	0.41	_	0.036	-11.52	_	2.42E-03	_
AMD Spring: Unacidified											
AMS1-1	6.2	29.41	5.99	14.88	11.98	2.90	1.000	-10.97	_	6.57E-02	2.42
AMS1-2	14.2	23.2	5.7	11.97	9.95	2.02	0.804	-10.15	_	5.39E-02	1.41
AMS1-3	28.2	23.37	5.62	9.49	8.15	1.34	0.638	-9.6	_	4.43E-02	1.36
AMS1-4	49.2	21.03	5.27	8.73	8.33	0.40	0.586	-9.33	_	4.18E-02	1.08
AMS1-5	73.4	21.61	3.66	5.65	5.65	_	0.379	-9.25	_	2.96E-02	0.67
AMS1-6	97.4	21.75	3.54	3.42	3.42	_	0.230	-9.3	_	1.80E-02	0.38
AMS1-7	110.4	21.72	3.42	2.16	2.16	_	0.145	-9.18	_	1.14E-02	0.36
AMS1-8	134.4	21.69	3.24	1.57	1.57	_	0.105	-9.07	_	8.25E-03	0.09
AMS1-9	146.4	21.64	3.14	0.83	0.83	_	0.056	-14.22	_	4.39E-03	0.03
AMS1-10	159.4	21.83	3.06	0.28	0.28	_	0.019	-18.84	_	1.47E-03	0.00
AMS1-11	168.4	21.89	3.21	0.12	0.12	_	0.008	-12.51	_	6.55E-04	0.00

- = Not applicable
bdl =below detection level

Table I-2: Least squares regression equations defining the enrichment and depletion in ^{13}C in open and closed acidification of samples of $NaHCO_3$, stream water, groundwater and AMD contaminated spring water (AMD spring). .

Sample Identification	**$\delta^{13}C_{DIC}$ enrichment trend**	**R^2**	**n**	**$\delta^{13}C_{DIC}$ depletion trend**	**R^2**	**n**	**$\delta^{13}C_{CO2}$ enrichment trend**	**R^2**	**n**	**$\delta^{13}C_{CO2}$ depletion trend**	**R^2**	**n**
$NaHCO_3$: Closed acidification	y = -5.9x + 2.8	0.92	9	y = 14.6x – 2.5	0.97	4	y = -14.6x + 3.6	0.99	9	y = 15.5x +4.0	0.99	4
Stream water: Closed acidification	y = -7.7x - 5.5	0.91	9	y = 7.4x - 8.6	0.94	3	y = -20.3x - 2.5	0.98	8	y = 6.9x - 9.1	0.97	3
Groundwater: Closed acidification	y = -6.3x + 1.4	0.97	9	y = 7.4x - 2.1	0.86	5	y = -17.7x + 3.1	0.97	7	y = 8.6x - 1.6	0.92	5
AMD Spring: Closed acidification	y = -4.7x - 6.8	0.98	9	y = 10.2x – 9.1	0.94	3	y = -10.4x – 7.1	0.91	8	y = 8.2x - 7.9	0.99	3
$NaHCO_3$: Open acidification	y = -2.4x – 1.0	0.81	10	y = 2.8x - 4.3	0.96	6	–	–	–	–	–	–
Stream water: Open acidification	y = -4.9x - 8.5	0.84	9	y = 3.9x- 12.8	0.91	4	–	–	–	–	–	–
Groundwater: Open acidification	y = -2.2x - 2.7	0.83	9	y = 5.5x - 7.8	0.89	7	–	–	–	–	–	–
AMD Spring: Open acidification	y = -2.3x - 9.3	0.97	10	y = 11.9x – 12.0	0.95	5	–	–	–	–	–	–

CHAPTER II

THE EFFECT OF SULFURIC ACID NEUTRALIZATION ON CARBONATE EVOLUTION OF SHALLOW GROUNDWATER

Submitted for review (Chemical Geology)
Authors: Hendratta N. Ali and Eliot Atekwana
Boone Pickens School of Geology, 105 Noble Research Center, Oklahoma State University, Stillwater, OK 74078, USA

Abstract

Carbonate neutralization of sulfuric acid has been observed in natural groundwater impacted by anthropogenic activities such as mine waste disposal. Our aim in this study is to provide greater insights as to how dissolved inorganic carbon (DIC) generation and $CO_{2(g)}$ production from acidification and neutralization reactions affect the carbonate evolution of groundwater. We measured the concentrations of DIC and major ions and the stable carbon isotope ratio of DIC ($\delta^{13}C_{DIC}$) in water samples from a metal sulfide- and carbonate-rich mine tailings pile considered an analogue to natural environments where acid generation and neutralization occur. In addition, we measured the concentrations of $CO_{2(g)}$ and the $\delta^{13}C$ of $CO_{2(g)}$ in the vadose zone and at a background soil zone. Our aim was to gain greater insights as to how DIC generation and $CO_{2(g)}$ production from acidification and neutralization reactions affect the carbonate evolution of groundwater. Near neutral pH and high concentrations of SO_4, Ca, and Mg

and the positive correlation between Ca+Mg and SO_4+HCO_3 is evidence that acid produced by metal sulfide oxidation neutralizes carbonates. Soil water and perched groundwater (saturated zone above the water table) had significantly higher DIC concentrations compared to groundwater which suggest that DIC production from acid neutralization occurs primarily in the vadose zone where metal sulfide oxidation generates acidity. The concentration of $CO_{2(g)}$ in the vadose zone was high compared to atmospheric and the $\delta^{13}C_{CO2}$ was enriched compared to background soil $CO_{2(g)}$, consistent with $CO_{2(g)}$ production from HCO_3 neutralization of acid and from DIC loss as $CO_{2(g)}$ due to high pCO_2 in the water samples. The range in $\delta^{13}C_{DIC}$ of soil water and perched groundwater is also consistent with the dissolution of carbonates with heavy $\delta^{13}C$ and the loss of $CO_{2(g)}$ from solution to the vadose zone by acid dehydration of HCO_3. Geochemical and isotopic modeling suggest that the DIC concentrations and the $\delta^{13}C_{DIC}$ of shallow groundwater is due to: (1) mixing of the DIC in leachate formed by carbonate dissolution in the vadose zone with infiltration from precipitation and/or lake recharge and (2) "open system" groundwater DIC interaction with $CO_{2(g)}$ in the vadose zone produced from HCO_3 dehydration. This study suggests that in natural and anthropogenic settings where sulfuric acid production by metal sulfides and neutralization by carbonates occur, the carbonate evolution of shallow groundwater is not described by the classical model ascribed to soil zone $CO_{2(g)}$.

Keywords: Acidification; neutralization; dissolved inorganic carbon; stable carbon isotopes; carbonate-rich tailings pile; soil water; groundwater; soil $CO_{2(g)}$

1. Introduction

The major weathering agent that generates dissolved inorganic carbon (DIC) and controls carbonate evolution of shallow groundwater is acidity produced from organic acids (e.g., Chin and Mills, 1991; Douglas, 2006) or carbonic acid (formed from the dissolution of $CO_{2(g)}$) generated in the soil zone by microbial degradation of organic matter (e.g., Andrews and Schlesinger, 2001; Macpherson et al., 2008). However, there are natural environments (e.g., Yoshimura et al., 2001; Li et al., 2008) and anthropogenic settings such as waste material from mineral exploitation (e.g., Al et al., 1997; Espana et al., 2005) which contain sulfide minerals (e.g., pyrite) that can be oxidized to generate H_2SO_4 that is subsequently neutralized by carbonates to produce DIC (Fonyuy and Atekwana, 2008a; Atekwana and Fonyuy, 2009).

A conceptual model of how acid production and neutralization affects carbonate evolution in a shallow groundwater system is presented in Figure II-1. In the conceptual model, 4 main processes are identified: (1) acid generation and neutralization by carbonates that produces leachate, (2) HCO_3 dehydration by neutralization of acidity to produce $CO_{2(g)}$ released to the vadose zone, (3) mixing of leachate with infiltration and groundwater, and (4) interaction of groundwater with the $CO_{2(g)}$ in the vadose zone. As an example, pyrite oxidation and subsequent neutralization of the acid by dolomite dissolution is shown in Equations 1 and 2:

$$FeS_2 + 7/2O_2 + H_2O \rightarrow Fe^{2+} + H_2SO_4 \quad (1)$$

$$H_2SO_4 + MgCa(CO_3)_2 \rightarrow SO_4^{2-} + Mg^{2+} + Ca^{2+} + 2HCO_3^- \quad (2)$$

These reactions together will release Fe, SO_4, Mg, Ca, and HCO_3 into solution and good correlation between these variables have been used as evidence of acidification and neutralization in groundwater (e.g., Yoshimura et al., 2001; Li et al., 2008). In addition, the neutralization reaction is significant due to the potential for uncommonly high DIC production. The HCO_3 produced from carbonate dissolution may neutralize additional protons from H_2SO_4 dissociation to produce H_2CO_3 (Equation 3) which is dehydrated to $CO_{2(g)}$ (Equation 4):

$$HCO_3^- + H^+ \leftrightarrow H_2CO_3 \quad (3)$$

$$H_2CO_3 \leftrightarrow H_2O + CO_{2(aq)} \leftrightarrow CO_{2(g)} \quad (4)$$

High concentrations of $CO_{2(g)}$ in the vadose zone have been reported in mine waste disposal sites (e.g., Jaynes et al., 1983; Nitzsche et al., 2002; Laughrey and Baldassare, 2003).

The conceptual model (Fig. II-1) suggests that carbonate evolution in groundwater is unlikely to be controlled by $CO_{2(g)}$ from the soil zone as described in classical models of groundwater carbonate evolution (e.g., Clark and Fritz, 1997). We predict that if the processes of natural and anthropogenic acidification and neutralization are significant in carbonate evolution, then the conceptual model can be tested by evaluating DIC concentrations, the stable isotope composition of DIC ($\delta^{13}C_{DIC}$), the concentration of vadose zone $CO_{2(g)}$ and the stable isotopic composition ($\delta^{13}C_{CO2}$) of vadose zone $CO_{2(g)}$. During acid neutralization by carbonate and subsequent HCO_3 dehydration, the transformation of DIC species ($CO_{2(aq)}$, H_2CO_3, HCO_3) impart shifts to the stable carbon isotope composition of DIC and $CO_{2(g)}$ due to isotopic fractionation (e.g., Ali and

Atekwana, 2009). Also, because the source of carbon in the groundwater is predicted to be predominantly derived from carbonate host rock/mineral, the groundwater $\delta^{13}C_{DIC}$ and vadose zone $\delta^{13}C_{CO2}$ can constrain models that will provide insights for understanding DIC evolution in the groundwater system.

Production of H_2SO_4 in natural environments provides a unique situation in which carbonate evolution in groundwater systems is not primarily influenced by organic acids or soil zone $CO_{2(g)}$. Studies by Yoshimura et al. (2001), Dietzel and Kirchhoff (2002), and Li et al. (2008) have been instrumental in advancing our knowledge on acidification and neutralization in groundwater systems. However, the systems investigated had additional factors that affected the groundwater carbonate evolution including deep source $CO_{2(g)}$ (Yoshimura et al., 2001), magmatic $CO_{2(g)}$ (Dietzel and Kirchhoff, 2002), and a mixture of soil zone $CO_{2(g)}$ and DIC from carbonate neutralization of sulfuric acid (Yoshimura et al., 2001; Li et al., 2008). Ideally, the effect of sulfuric acid is best investigated in a system in which sulfuric acid neutralization is most dominant. Mine wastes disposal sites rich in metal sulfides and carbonates can be considered analogues for natural environments where acid production and neutralization occur, and are suitable settings to investigate the extent to which these processes affect the chemical and isotopic evolution of groundwater.

In this study, we measured the concentrations of DIC and major ions and the $\delta^{13}C_{DIC}$ in soil water, perched groundwater (lenses of water saturation above the water table), groundwater, and lake water samples in a metal sulfide-rich and carbonate-rich mine tailings pile. In addition, we measured the concentrations and the $\delta^{13}C_{CO2}$ of $CO_{2(g)}$ in the

vadose zone and soil zone at a background location. We aimed to investigate how acid production and neutralization affects DIC generation and $CO_{2(g)}$ production in the vadose zone and how these reactions affect the carbonate evolution of groundwater. Information on the generation and evolution of DIC in carbonate-rich environments is important in our understanding of perturbations of carbon cycling in groundwater settings by acidification reactions. Particularly, acid generation and neutralization can result in high $CO_{2(aq)}$ concentrations in groundwater systems (Dietzel and Kirchhoff, 2002) and lead to enhanced carbonate weathering in some watersheds (Li et al., 2008).

2. Study site

This study was conducted at the Federal Tailings Pile (FTP) in the St. Joe State Park (37°49'16"N, 90°30'49"W) in southeastern Missouri, USA (Fig. II-2). The study site is located in the "Old Lead Belt" where several large piles of tailings material estimated at more than 250 million tons generated during more than 100 years of mining (Kramer, 1976) are disposed directly on the land surface. The region has a temperate climate with mean annual precipitation and temperature for 1971-2006 of 1,086 mm and 12.7 °C, respectively (Midwest Regional Climate Center, 2008). The geology of the area surrounding the study site is mainly carbonate rocks that host major ore deposits of lead and economic quantities of zinc, copper, silver, and cadmium, with minor quantities of other metals such as cobalt and nickel. The Bonneterre Formation which consists of medium to fine-grained dolostone is the host rock for the lead ore deposits. The Bonneterre dolostone overlie sandstones with occasional siltstone that lie directly on granites and volcanic rocks of the Ozark Uplands (Koenig, 1961). The Bonneterre

Formation is overlain by carbonate rocks including limestone of the Davis Formation and additional overlying stratigraphic units that are predominantly dolomitic (e.g., Gregg et al., 1993).

The FTP covers a surface area of about 3.24 km^2 and the tailings range in thickness from less than 1 m in the southern portion to about 30.4 m in the northern portion. The soil in the tailings pile area is silty-loam to silty-clay-loam, with the loam sometimes underlain at varying depths by clay-silt or clay. The mineralogical composition of the tailings material consist of (1) carbonates including dolomite ($MgCa(CO_3)_2$), calcite ($CaCO_3$), ankerite $Ca(Fe\ Mg)(CO_3)_2$), and Zn-rich carbonates (e.g., smithsonite), (2) sulfides consisting of pyrite (FeS_2), galena (PbS), sphalerite (ZnS), chalcopyrite ($CuFeS_4$), and borite ($CuFeS_4$), and (3) silicates consisting of mainly quartz and K-feldspar. Dolomite constitutes about 75 wt% of the tailings material (Smith and Schumacher, 1993).

The FTP site is bounded to the west, south, and east by densely forested area and to the north by an earthen dam built to retain the tailings (Fig. II-2). The surface elevations at the site decrease from the south (279.3 m asl) towards the earthen dam to the north (269.9 m asl). There is no integrated surface drainage within the tailings pile area, and periodically, excess precipitation ponds on the surface and eventually infiltrates or is evaporated. The FTP site is drained by the intermittent Shaw Branch that begins at the Dam area and flows into the Flat River to the North. In the southern portion of the tailings pile, four artificial lakes (Monsanto Lake, Pim Lake, Jo Lee lake, and Apollo Lake) are open to the public for recreational fishing and swimming. The bedrock below the tailings pile varies from less than 1 m near the valley walls to about 30 m in the

middle of the valley. Considering the south-to-north slopping topography and that the fact that the tailings were disposed in a v-shaped valley (Buccellato, 2006), groundwater flows northwards towards the earthen dam. Depths to water table vary from <0.5 m below ground surface (bgs) near the lakes and increase northwards to about 10.0 m bgs near the earthen dam. Within the tailings pile, there is perched groundwater between 1.5 to 3.0 m bgs

3. Methods

3.1. Sample collection

Lake water, soil water, perched groundwater, and groundwater samples were collected from the FTP in June 2006 and June 2007. The lake samples were collected from Pim, Jo Lee, and Monsanto Lakes by the grab technique. Perched groundwater and groundwater was pumped from piezometers and monitoring wells using either a peristaltic pump or inertia pump. The monitoring wells were installed by the United State Geological Survey (USGS) in 2005. Eight groups of groundwater sampling stations (MW01 to MW08) were installed in the tailings material, each with 1 to 3 monitoring wells. The monitoring well depths vary between 3.4 to 30.7 m bgs. The perched groundwater (PGW) samples were collected from 0.64 cm diameter plastic tubing screened over a 10 cm interval and installed at depths between 0.5 to 3.0 m bgs at sampling stations MW01, MW03, and MW06. Soil water was sampled by suction lysimeters installed at 0.5 m bgs near MW01, MW03, and MW06. A vacuum pump was used to induce suction of soil water into the lysimeter and the water was pumped to the

surface into a clean glass vessel for measurements and sampling. The lysimeter at MW03 did not yield water.

All water samples were filtered through a 0.45 µm syringe filter during collection. The samples were collected in HDPE bottles that were unacidified for anions and acidified to a pH <2 with high purity HNO_3 for cations. The samples were cooled on ice in the field and transported to the laboratory where they were stored at 4^{o}C until analyses. Samples for DIC analysis were collected as described by Atekwana and Krishnamurthy (1998). Samples for stable oxygen and hydrogen isotope analysis were collected in 25 ml scintillation vials with inverted cone closures and stored at room temperature until analysis.

Gas was collected from the vadose zone from gas samplers consisting of plastic tubing perforated over a 10 cm length and installed between 0.25 and 3.00 m bgs near sampling stations MW01, MW03, and MW06 (Fig.2). A vacuum pump was used to purge gas from the samplers and gas was collected into custom made pre-evacuated 1.0 liter glass vessels. Background gas was collected in the soil zone at 25 and 50 cm bgs in a forested area west of tailings pile (Fig. II-2).

Sediment samples were collected from the tailings pile at a depth of 50 cm bgs near stations MW01 and MW03 and stored in plastic bags for carbon isotope analysis of carbonates.

3.2. Sample analyses

Prior to collecting water samples, water levels in monitoring wells were measured using an electronic water level tape. Temperature, pH, dissolve oxygen (DO), oxidation

reduction potential (ORP), and specific conductance (SPC) were measured using a Yellow Spring Instrument (YSI) multi-parameter probe calibrated to manufacturers specifications. Alkalinity was measured by acid titration (Hach, 1992) immediately after sampling. Anions were analyzed by ion chromatography and cations were analyzed by a PerkinElmer Optima 2100DV inductively coupled plasma optical emission spectrometer (ICP-OES).

Water samples for DIC were extracted for $CO_{2(g)}$ as described by Atekwana and Krishnamurthy (1998). DIC concentration was calculated from $CO_{2(g)}$ yields measured by a pressure transducer. Gas from the vadose and soil zones was purified in a vacuum line and the $CO_{2(g)}$ concentrations determined by a pressure transducer. The $CO_{2(g)}$ samples were sealed in Pyrex tubes for stable isotope analysis. The extraction of $CO_{2(g)}$ for carbon isotope analysis from sediments was performed following the technique of Krishnamurthy et al. (1997). The $CO_{2(g)}$ from sediments was sealed in Pyrex tubes for stable isotope analysis. The stable carbon isotope ratio of $CO_{2(g)}$ was measured by isotope ratio mass spectrometry at Western Michigan University, Kalamazoo Michigan. Measurements of stable isotopes of hydrogen and oxygen were made by high temperature conversion elemental analyzer (TC/EA) coupled to a Finnigan Delta plus XL isotope ratio mass spectrometer at Oklahoma State University, Stillwater Oklahoma. The isotope ratios are reported in the delta notation in per mil:

$$\delta\ (‰) = ((R_{sample} / R_{standard}) - 1) \times 10^3 \qquad (5)$$

Where R is $^{13}C/^{12}C$, D/H, or $^{18}O/^{16}O$.

The δ values are reported relative to VPDB standard for C and VSMOW for H and O isotopes. Routine δ measurements have an overall precision of better than 0.1‰ for $\delta^{13}C$ and $\delta^{18}O$ and 1.0‰ for δD.

4. Results

4.1. SO_4, Ca, and Mg in the water samples

The SO_4, Ca, and Mg concentrations in the water samples are presented in Table 1. The SO_4 concentrations range from 3.1 to 12.4 mM/L in soil water, 2.4 to 13.4 mM/L in perched groundwater and 0.9 to 16.8 mM/L in groundwater. The Ca concentrations range from 3.0 to 11.1 mM/L in soil water, 4.6 to 13.2 mM/L in perched groundwater, and 1.0 to 5.0 mM/L in groundwater, while the Mg concentrations range from 2.1 to 4.8 mM/L in soil water, 1.8 to 5.8 mM/L in perched groundwater, and 1.9 to 13.4 mM/L in groundwater. The range in the concentrations of SO_4 was similar for soil water, perched groundwater and groundwater. In contrast, Ca concentrations were generally higher in soil and perched groundwater compared to higher Mg concentrations in groundwater compared to soil and perched groundwater. The lowest concentration of SO_4 of 0.1 to 0.5 mM/L, Ca of 0.6 to 0.8 mM/L, and Mg of 0.5 to 0.8 mM/L were measured in lake samples.

4.2. pH, HCO_3, and DIC in the water samples

The results of pH and HCO_3 and DIC concentrations for the water samples are presented in Table 3. Lake samples have the highest pH of 8.6 to 7.7 and the lowest HCO_3 concentration of 1.7 to 2.5 mM/L. Meanwhile, soil water and perched groundwater have the highest HCO_3 concentrations that range between 3.1 and 10.3 mM/L and lower

pH values between 6.4 and 7.1. The HCO_3 concentrations in groundwater vary between 1.1 mM/L and 6.0 mM/L. The DIC concentrations in the soil water and perched groundwater samples range between 4.6 and 22.8 mM C/L, whereas, the DIC concentrations in groundwater has a narrower range between 1.1 and 7.2 mM C/L. The DIC and HCO_3 concentrations were generally higher in the soil water and perched groundwater than for groundwater samples. Lake samples have lowest DIC concentrations which range from 1.6 to 2.2 mM C/L.

4.3. $\delta^{13}C_{DIC}$, δD, and $\delta^{18}O$ in the water samples

The $\delta^{13}C_{DIC}$, δD, and $\delta^{18}O$ for the water samples are presented in Table 3. The $\delta^{13}C_{DIC}$ of soil water and perched groundwater samples range from -6.8 to -4.1‰ and -12.9‰ and -2.9‰ for groundwater samples. The $\delta^{13}C_{DIC}$ for lake water samples is between -7.7‰ and -9.3‰. Soil water and perched groundwater samples have relatively heavy $\delta^{13}C_{DIC}$ compared to the groundwater samples. Lake samples have $\delta^{13}C_{DIC}$ that are generally more depleted than for groundwater samples with the exception of groundwater from MW06-94 with the most depleted $\delta^{13}C_{DIC}$ of -12.9‰.

The δD for soil water and perched groundwater samples ranged from 1.0 to -6.3‰ and -9.0 to -40.1‰, respectively, and $\delta^{18}O$ ranged from 1.1 to -7.5‰ and -7.7 to -42.5‰, respectively for groundwater samples, and from 0 to -2.0‰ and -8.6 to -20.2‰, respectively for lake samples. In general, lake samples are more enriched than the bulk of soil water, perched groundwater, and groundwater samples.

4.4. CO_2 concentrations and $\delta^{13}C$ of CO_2 in the vadose zone and soil zone gas

The partial pressure of $CO_{2(g)}$ ($logpCO_2$) in the vadose zone between -3.1 and -1.3 atm (Table 4) is higher than atmospheric (~ -3.5 atm). The $\delta^{13}C$ of the $CO_{2(g)}$ in the vadose zone range between -16.4 and -11.4‰. The $logpCO_2$ in the soil zone from the forested background area is between -2.1 to -1.7 atm and the $\delta^{13}C$ of the CO_2 averages -22.2 ±0.1‰ (n=2).

5. Discussion

5.1. Acid neutralization and water chemistry in the tailings pile

The conceptual model presented in Figure II-1 suggests that leachate produced from acidification and neutralization in metal sulfide-rich and carbonate-rich environments produces high concentrations of SO_4, Ca, Mg, and DIC. High SO_4 concentrations in the water samples at the tailings pile are due to sulfide mineral oxidation (Smith and Schumaker, 1991; 1993). For the water samples, SO_4+HCO_3 is positively correlated to Ca+Mg concentrations (Fig. II-3), described by the least squares equation: $(Ca+Mg) = 0.97(SO_4 + HCO_3) – 1.96$; ($R^2 = 0.94$). The sum of $(HCO_3/2)/(Ca+Mg)$ and $(SO_4/Ca+Mg)$ is close to 1.0. The relationships between SO_4+HCO_3 and Ca+Mg concentrations suggests that acid production from sulfide mineral oxidation and neutralization by dolomite are the dominant processes governing the production and fate of SO_4, Ca, Mg, HCO_3, and DIC in the samples (Yoshimura et al., 2001; Li et al., 2008), and are therefore the important drivers of water chemistry in the tailings pile. Lake water is Ca-Mg-HCO_3 type, whereas soil water and perched groundwater are exclusively Ca-Mg-SO_4-HCO_3 types, and groundwater shows a range of

water types including Mg-SO_4, Mg-Ca-SO_4-HCO_3, or Ca-Mg-SO_4-HCO_3 types. The variations in water types reflect differences in the magnitude and extent of acid neutralization that produces leachate (soil water and perched groundwater), and the interaction of the leachate with infiltration and recharge from lakes

5.2. DIC production and evolution during acid neutralization by carbonates

The higher DIC concentrations in the leachate than in groundwater indicates greater amount of carbonate dissolution above the water table. This observation is similar to other studies that showed that sulfide mineral oxidation and subsequent acid neutralization occurs mainly in a "reaction zone" in the shallow vadose zone of tailings (e.g., Jaynes et al., 1983; Bain et al., 2000). We explore the production and evolution of DIC by examining the relationship between DIC and HCO_3 (Fig. II-4). The water samples show a positive correlation between DIC and HCO_3 expressed by the least squares equation: DIC = 2.8HCO_3 - 6.3 (R^2 = 0.96; n=11) for soil water and perched groundwater and by DIC = 1.1HCO_3 - 0.1 (R^2 = 0.94; n=31) for groundwater and lake water samples (Fig. II-4). Groundwater samples lie near the DIC = HCO_3 trend line and based on the pH of the samples, the DIC occurs mostly as HCO_3 species (e.g., Clark and Fritz, 1997). Leachate samples lie above the DIC = HCO_3 line along a trend line with a slope of 2.8, suggesting that greater amounts of DIC occur as $CO_{2(aq)}$ species (H_2CO_3 and dissolved $CO_{2(aq)}$). The relationship between DIC and HCO_3 for the samples indicates that there are two different mechanisms of DIC production and/or evolution in the tailings pile. The predominance of $CO_{2(aq)}$ in the leachate samples suggest that DIC evolution is not occurring under equilibrium conditions, while groundwater where DIC is

represented mostly by HCO_3 suggest an equilibrium process (e.g., Svensson and Dreybrodt, 1992; Dreybrodt et al., 1996).

In a groundwater system where DIC species are conserved (i.e., there is no loss of $CO_{2(g)}$ or precipitation of carbonates) during carbonate evolution initiated by H_2SO_4 neutralization by dolomite, the relationship between SO_4 vs. DIC or Ca+Mg vs. DIC should be positively correlated. The lack of a positive correlation for SO_4 vs. DIC and for Ca+Mg vs. DIC (Fig. II-5a and b) for the water samples suggest carbonate evolution under "open system" conditions accompanied by addition, loss, or exchange of carbon in the DIC pool (e.g., Fonyuy and Atekwana, 2008b). The water samples can thus be grouped into 3 clusters that indicate the dominance of different processes during the carbonate evolution. Cluster 1 (Fig. II-5a) includes mostly leachate samples, where an increase in DIC concentrations is accompanied by an increase in SO_4 and in Ca+Mg concentrations (Fig. II-5b). The overall positive relationship shown by samples in Cluster 1 suggests that DIC production occurs from the addition of carbon during neutralization of H_2SO_4 by carbonates (Equation 1 and 2) (e.g., Moral et al., 2008). Cluster 2 shows a trend of decreasing DIC concentrations concomitant with increasing SO_4 concentrations (Fig. II-5a). Samples in Cluster 2 are consistent with carbonate evolution dominated by the dehydration of HCO_3 (Fonyuy and Atekwana, 2008b; Atekwana and Fonyuy, 2009; Ali and Atekwana, 2009), and where DIC concentration decrease is balanced by an increase in SO_4 concentration (Equation 3 and 4). On the other hand, groundwater samples in Cluster 3 that show low DIC, high SO_4, and significantly higher Ca+Mg concentrations suggest a DIC evolution that is due to both carbonate dissolution and HCO_3 dehydration. For the samples in Cluster 3, higher Mg compared to Ca

concentrations (Table 3) suggests that these samples may have undergone incongruent dissolution of carbonate (Busenberg and Plummer, 1982). Alternatively, lower Ca concentrations may result from precipitation of Ca in solid mineral phases notably Ca-montmorillonite, as these samples are supersaturated with respect to this mineral phase (Table 5). In addition, the groundwater samples in Cluster 3 have relatively high Cl concentrations (Table 3) that may have come from salt used to deice the roads in the park and leached into groundwater during spring snow melt. Because the recharge occurs along the southern edge of the FTP site (Fig. II-2), the groundwater flow pathway causes the recharged water to flow deeper within the tailings pile. Thus, because of the longer residence time, samples in Cluster 3 have undergone a chemical evolution not entirely driven by the acidification and neutralization processes.

To further evaluate carbonate evolution due to acid neutralization, we examine the relationship between pH and pCO_2 for the water samples. The plot of pH vs. $\log pCO_2$ (Fig. II-6) shows a negative correlation ($\log pCO_2 = -1.4pH + 7.8$; $R^2=0.93$). The lower pH and high pCO_2 for soil water and perched groundwater is due to $CO_{2(aq)}$ generation from carbonate dissolution in the reaction zone (e.g., Jaynes et al., 1983). Lower pCO_2 in the groundwater samples and the relatively higher pH values compared to soil water and perched groundwater samples is either due to lower DIC production or to loss of $CO_{2(g)}$ from the samples. In fact, all the water samples from the tailings pile have pCO_2 values that are higher than atmospheric ($\log pCO_{2(atm)} = -3.5$). Thus, the negative relationship between pH and $\log pCO_2$ and the spatial position of perched groundwater and soil water samples relative to groundwater samples in Figure II-6 support a carbonate evolution whereby $CO_{2(g)}$ is lost from the water samples to the vadose zone, causing the sample pH

to increase (e.g., Choi et al., 1998). In addition, because the $CO_{2(g)}$ concentrations in the vadose zone are high, $CO_{2(g)}$ in the soil zone or atmosphere has little impact on the carbonate evolution of groundwater.

5.3. DIC-$\delta^{13}C_{DIC}$ evolution during acid neutralization in a carbonate-rich setting

Water samples from the FTP show an overall positive relationship for DIC vs. $\delta^{13}C_{DIC}$ (Fig. II-7), although the correlation (R^2=0.51) is rather poor. This is due to different mechanisms of DIC evolution for different sample types (e.g., different clusters in Fig. II-5a) accompanied by different carbon isotopic fractionation effects (Deines, 2004). During carbonate evolution (e.g., $CaMg(CO_3)_{2(s)} \Leftrightarrow CO_3^{2-} \Leftrightarrow HCO_3^- \Leftrightarrow H_2CO_3 \Leftrightarrow CO_{2(g)}$), the isotopic effect depends on the addition or removal of carbon from the DIC pool. Since all water samples are either undersaturated or near saturation with respect to carbonates, the enrichment in ^{13}C in the samples is mainly controlled by the formation of HCO_3 and $CO_{2(aq)}$ from carbonate or loss of $CO_{2(g)}$ and the depletion in ^{13}C in the samples is controlled by the dissolution of isotopically light $CO_{2(g)}$. The positive relationship suggests an evolution that is best described by the addition of heavy carbon (^{13}C) from carbonate dissolution ($\delta^{13}C_{Carbonate}$ = -1.5‰). The higher pCO_2 in the water samples compared to atmospheric does not however preclude the addition of carbon as dissolved $CO_{2(g)}$ from the vadose zone into the groundwater, particularly if the vadose zone pCO_2 concentrations are higher than for groundwater. Thus, the scatter in the data in Figure II-7 could be due to the addition of variable amounts of isotopically lighter $CO_{2(g)}$ to the water samples.

5.3.1. Carbon isotope evidence of DIC production and evolution in soil water and perched groundwater

In the leachate, DIC production is dominated by carbonate dissolution. Thus, given the $\delta^{13}C$ composition of carbonates in the tailings of -1.5‰, dissolution would introduce relatively heavy ^{13}C that will cause enrichment of the samples in the reaction zone. For the pH range measured, the CO_3^{2-} ion concentration is negligible, implying that carbonate dissolution directly produces HCO_3 or $CO_{2(aq)}$ in solution. The enrichment of ^{13}C during carbonate dissolution to form HCO_3: $\varepsilon_{CaCO3–HCO3}$ ranges from -0.4‰ ± 0.2‰ to -3.4 ± 0.4‰ at 25 ^{0}C (e.g., Turner, 1982). Based on this ^{13}C enrichment factor, the resulting $\delta^{13}C_{DIC}$ of the water samples should be in the range -1.9‰ to -4.8‰ ±0.8‰. The leachate samples have $\delta^{13}C_{DIC}$ values between -3.1‰ and -6.8‰ and thus cannot be explained solely by the isotopic fractionation associated with carbonate dissolution and HCO_3 formation. Because these water samples have high pCO_2, $CO_{2(g)}$ is lost to the unsaturated zone. The loss of $CO_{2(g)}$ from solution is accompanied by an enrichment: $\varepsilon_{CO2(aq)-CO2(g)}$ of ~1.1‰ (e.g., Vogel et al., 1970; Mook et al., 1974). If the isotopic fractionation during $CO_{2(g)}$ loss from solution is taken into account, then the $\delta^{13}C_{DIC}$ of the residual DIC in the leachate should be in the range -2.1‰ and -5.8‰, which is within the range of the $\delta^{13}C_{DIC}$ values of the tailings leachate to within ±1‰.

5.3.2. Carbon isotope evidence of $CO_{2(g)}$ production and evolution in the vadose zone

The range in the $\delta^{13}C$ of $CO_{2(g)}$ in the vadose zone (Table 4) suggests isotopic depletion consistent with the production of $CO_{2(g)}$ from leachate in the reaction zone. The enrichment of ^{13}C for HCO_3 dehydration: $\varepsilon_{HCO3-CO2(aq)}$ in the temperature range of 14 to

27°C for the water samples is between -8.9 to -10.3‰ (e.g., Mills and Urey, 1940; Mook et al., 1974) and the ^{13}C enrichment for degassing of $CO_{2(g)}$ is about 1.1‰ (e.g., Fritz and Clark, 1977). A model where HCO_3 dehydration is followed by $CO_{2(g)}$ degassing from the water samples into the vadose zone should result in a $\delta^{13}C$ depletion for $CO_{2(g)}$ released to vadose zone in the range of -7.8‰ to -9.2‰ [(1.1‰ + -8.9‰) to (1.1‰ + -10.3‰)] relative to the $\delta^{13}C_{DIC}$ of the samples. By applying this ^{13}C depletion range to groundwater samples (-2.0‰ to -12.0‰), the $CO_{2(g)}$ that would be degassed into the vadose zone should have $\delta^{13}C$ in the range of -10.9‰ to -23.1‰ shown in Figure II-7 with dots. However, the range for measured $\delta^{13}C$ of the vadose zone $CO_{2(g)}$ of -16.2‰ to -11.4‰ closely compares to $\delta^{13}C_{CO2(g)}$ values of -17.0‰ to -10.9‰ estimated for vadose zone $CO_{2(g)}$ produced from leachate and represented by the hatched interval in Figure II-7. This suggests that the $CO_{2(g)}$ in the vadose zone is produced from HCO_3 dehydration and subsequent degassing of $CO_{2(g)}$ from leachate in the reaction zone. Incidentally, Nitzsche et al. (2002) and Laughrey and Balsassare (2003) report high concentrations of $CO_{2(g)}$ in the vadose zone at abandoned mine sites which they attribute to acid neutralization by carbonates. In addition, Nitzsche et al. (2002) report $\delta^{13}C_{CO2}$ values of -9.0‰ to -15.9‰. The $CO_{2(g)}$ concentrations and $\delta^{13}C_{CO2}$ (Fig. II-8; solid and dashed arrows) is in the range observed in this study.

5.3.4. Stable carbon isotope evidence of DIC production and evolution in groundwater

To account for the wide range in the DIC concentrations and the $\delta^{13}C_{DIC}$ observed for the groundwater, we modeled the carbon isotopic evolution of DIC (2007 data) using the computer program NETPATH (Plummer et al., 1991). The approach was based on

models described by Plummer and Back (1980) and Plummer et al. (1990). Assumptions used for the models are: (1) constraints and phases were limited to species that control acid generation and neutralization, (2) CO_2 could be lost or absorbed, models allowed for (3) dissolution or precipitation of calcite and dolomite, (4) evaporation or dilution of leachate, (5) redox processes including ion and proton exchange, and (6) Rayleigh calculations and fractionation (Mook et al., 1974).

The $\delta^{13}C$ of carbonates used is 1.5‰. The same leachate sample (PGW03-3) with $\delta^{13}C_{DIC}$ of -5.3‰ was used to model all groundwater samples. This sample was selected because its $\delta^{13}C_{DIC}$ value is close to the average value for leachate of -5.1.‰. The $\delta^{13}C$ for vadose zone $CO_{2(g)}$ used in models is the average value of -14.2‰. The saturation indices of the mineral phases (Table 4) for groundwater samples were considered in selecting the correct model output. Modeled results (Table 6) indicate dissolution of carbonates, dilution with recharge, and dissolution or loss of $CO_{2(g)}$ as the major controls on the $\delta^{13}C_{DIC}$ of groundwater. Following carbonate dissolution in the reaction zone, the leachate is diluted to varying degrees by uncontaminated or less contaminated groundwater, likely recharged from precipitation or lakes. The exception to the above evolutionary model is the groundwater sample from MW06-94 with the most depleted $\delta^{13}C_{DIC}$ value of -12.5‰ that failed the modeling exercise. The isotopic value of this sample suggests that DIC evolution along groundwater flow pathway to this location may occur under a “closed system” and may not be directly influenced by acid neutralization reactions in the tailings pile. A sensitivity analysis shows that using the most enriched reaction zone sample; PW-02 with a $\delta^{13}C_{DIC}$ of -3.1‰ or the most depleted sample;

PGW06-3 with a $\delta^{13}C_{DIC}$ of -5.8‰, the modeled results obtained agree to within 1.0 ±0.5‰ of the $\delta^{13}C_{DIC}$ values modeled for the $\delta^{13}C_{DIC}$ of the initial water PGW03-3.

Relationships for $\delta^{13}C_{DIC}$ vs. depth for leachate samples and $\delta^{13}C_{DIC}$ vs. depth for groundwater samples are shown in Figure II-9a and II-9b, respectively. The depth relationships are consistent with our model where the $\delta^{13}C_{DIC}$ of samples in the reaction zone is controlled mainly by dissolution of carbonates that adds heavy ^{13}C to the DIC. The narrow range in $\delta^{13}C_{DIC}$ between -9.0‰ and -6.0‰ for the bulk of the groundwater samples suggest an evolution whereby dissolution of $CO_{2(g)}$ from the vadose zone plays an important role in DIC and carbon isotope evolution. For samples with $\delta^{13}C_{DIC}$ values heavier than -5.3‰ (Fig. II-9b), our models indicate that the $\delta^{13}C_{DIC}$ is controlled mostly by dissolution of dolomite + calcite (Table 6).

The oxygen and hydrogen isotopic compositions of the different waters were used to evaluate recharge conditions for groundwater in the tailings pile. A plot of the δD and $\delta^{18}O$ of the water samples are presented in Figure II-10. Also shown in Figure II-10 is the global meteoric water line (GMWL) (Craig, 1961) and a local meteoric water line (LMWL) for reference. The LMWL was constructed using stream data from Coplen and Kendal (2000) for the Gasconade River located 120 km to the northwest of the study site. The δD and $\delta^{18}O$ of the water samples show a good positive relationship represented by the least squares equation: $\delta D = 3.99\delta^{18}O - 10.7$ ($R^2 = 0.93$). The bulk of the water samples deviate from and lies below the LMWL due to evaporative enrichment. We use this observation to argue that the groundwater in the tailings pile is mostly recharged from seasonal precipitation and lake water that has undergone some evaporative

enrichment. This is consistent with our carbon isotope model results which indicate that groundwater evolves from the leachate produced in the reaction zone that is diluted and mixed with local recharge.

6. Conclusions

In this study, we investigated the effects of acidification and neutralization on the carbonate evolution in shallow groundwater in a metal sulfide-rich and carbonate-rich tailings pile. Mine wastes disposal sites rich in metal sulfides and carbonates can be considered an analogue for natural environments where sulfuric acid production and neutralization occur. Sulfuric acid neutralization by carbonates in the shallow subsurface produces leachate (soil water and perched groundwater) above the water table that has relatively high concentrations of DIC, SO_4, and Ca+Mg. The DIC in leachate samples is characterized by high $CO_{2(aq)}$ relative to HCO_3 and has relatively enriched $\delta^{13}C_{DIC}$ from carbonate dissolution. Additional neutralization of protons from H_2SO_4 dissociation by HCO_3 in addition to degassing of $CO_{2(g)}$ from solution create high concentrations of $CO_{2(g)}$ into the vadose zone. The $\delta^{13}C$ of the $CO_{2(g)}$ in the vadose zone is isotopically heavier and clearly distinguishable from the isotopically lighter $CO_{2(g)}$ in a background soil zone. On the other hand, DIC in the groundwater is characterized by higher proportions of HCO_3 relative to $CO_{2(aq)}$ and the $\delta^{13}C_{DIC}$ is much lighter compared to leachate samples. The DIC concentration and $\delta^{13}C_{DIC}$ of the groundwater is controlled by two dominant processes; (1) mixing and dilution of leachate with infiltration from precipitation and/or lake water as well as lateral groundwater recharge and (2) groundwater interaction with the $CO_{2(g)}$ in the vadose zone. The high $CO_{2(g)}$

concentrations produced from the acid and neutralization reactions in the vadose can be a potential source of $CO_{2(g)}$ to the atmosphere. Most importantly, in natural and anthropogenic settings where sulfuric acid production by metal sulfides and neutralization by carbonates occur, the carbonate evolution of shallow groundwater is not described by the classical model ascribed to soil zone $CO_{2(g)}$.

Acknowledgements

This work was funded by the National Science Foundation Award EAR-0510954. The National Association of Black Geologist and Geophysicists provided financial support to H.A. We thank A. Mukherjee and E. Fonyuy for field help. Anna Cruse provided constructive comments on an earlier version of this manuscript.

References

Al, T.A., Martin, C.J. and Blowes, D.W., 2000. Carbonate-mineral/water interactions in sulfide-rich mine tailings. Geochim. Cosmochim. Acta 64, 3933-3948.

Ali, H.N. and Atekwana, E.A., 2009. Effect of progressive acidification on stable carbon isotopes of dissolved inorganic carbon in surface waters. Chem. Geol. 260, 102-111.

Atekwana, E.A. and Fonyuy, E.W., 2009. Dissolved inorganic carbon concentrations and stable carbon isotope ratios in streams polluted by variable amounts of acid mine drainage. J. Hydrol. 372, 136-148.

Andrews, J.A. and Schlesinger, W.H., 2001. Soil CO_2 dynamics, acidification, and chemical weathering in a temperate forest with experimental CO_2 enrichment. Global Biogeochem. Cycles 15, 149-162.

Atekwana, E.A. and Krishnamurthy, R.V., 1998. Seasonal variations of dissolved inorganic carbon and $\delta^{13}C$ of surface waters: application of a modified gas evolution technique. J. Hydrol. 205, 265-278.

Bain, J.G., Blowes, D.W., Robertson, W.D. and Frind, E.O., 2000. Modeling of sulfide oxidation with reactive transport at a mine drainage site. J. Cont. Hydrol. 41, 23-47.

Buccellato A.D., 2006. Geophysical investigation of lead and zinc mine tailings at Saint Joe State Park, Park Hills, Missouri. M.S. Thesis. University of Missouri Rolla 44p.

Chin, P.-K.F. and Mills, G.L., 1991. Kinetics and mechanisms of kaolinite dissolution: effects of organic ligands. Chem. Geol. 90, 307-317.

Choi, J., Hulseapple, S.M., Conklin, M.H. and Harvey, J.W., 1998. Modeling CO_2 degassing and pH in a stream-aquifer system. J. Hydrol. 209, 297-310.

Clark, I.D. and Fritz P., 1997. Environmental isotopes in hydrogeology. Lewis Publishers, Boca Raton, NY 1-328.

Coplen T.B. and Kendall C., 2000. Stable hydrogen and oxygen isotope ratios for selected sites of the U.S. Geological Survey's ASQAN and benchmark surface-water Networks U.S. Geol. Surv. Open File Rep. 00-160, 1-403.

Craig, H., 1961. Isotopic variations in meteoric waters. Science 133, 1702-1703.

Deines, P., 2004. Carbon isotope effects in carbonate systems. Geochim.Cosmochim. Acta 68, 2659-2679.

Dietzel, M. and Kirchhoff, T., 2002. Stable isotope ratios and the evolution of acidulous ground water. Aquat. Geochem. 8, 229-254.

Douglas, T.A., 2006. Seasonality of bedrock weathering chemistry and CO_2 consumption in a small watershed, the White River, Vermont. Chem. Geol. 231, 236-251.

Dreybrodt, W., Lauckner, J., Zaihua, L., Svensson, U. and Buhmann, D., 1996. The kinetics of the reaction $CO_2 + H_2O$ --> $H^+ + HCO_3^-$ as one of the rate limiting steps for the dissolution of calcite in the system H_2O-CO_2-$CaCO_3$. Geochim. Cosmochim. Acta 60, 3375-3381.

España J.S., Pamo E.L., Santofimia S., Aduvire O., Reyes J., Barrettino D., 2005. Acid mine drainage in the Iberian Pyrite Belt (Odiel river watershed, Huelva, SW Spain): Geochemistry, mineralogy and environmental implications. Appl. Geochem. 20, 1320-1356.

Fonyuy, E.W. and Atekwana E.A., 2008a. Effects of acid mine drainage on dissolved inorganic carbon and stable carbon isotopes in receiving streams. Appl. Geochem. 23, 743-764.

Fonyuy, E.W. and Atekwana, A.E., 2008b. Dissolved inorganic carbon evolution and stable carbon isotope fractionation in acid mine drainage impacted streams: insights from a laboratory study. Appl. Geochem. 23, 2634-2648.

Gehre M., Geilmann H., Richter J., Werner R.A. and Brand W.A., 2004. Continuous flow $^{2}H/^{1}H$ and $^{18}O/^{16}O$ analysis of water samples with dual inlet precision. Rapid Commun. Mass Sp. 18, 2650–2660

Gonfiantini, R. and Zuppi, G.M., 2003. Carbon isotope exchange rate of DIC in karst groundwater. Chem. Geol. 197, 319-336.

Gregg, J.M., Laudon, P.R., Woody, R.E. and Shelton, K.L., 1993. Porosity evolution of the Cambrian Bonneterre dolomite, south-eastern Missouri, USA. Sed. 40, 1153-1169.

Hach Company, 1992. Water Analysis Handbook. Hach Company, Loveland, Co.

Jaynes, D.B., Rogowski, A.S., Pionke, H.B. and Jacoby, E.L., 1983. Atmosphere and temperature-changes within a reclaimed coal strip mine. J. Soil Sci. 136, 164-177.

Koenig, J.W., 1961. The stratigraphic succession in Missouri. Missouri Div. Geol. Land Surv. Rolla, Vol. XL, 2d series, 1-185.

Kramer R.L., 1976. Effects of century old Missouri lead mining operation upon the water quality, sediments and biota of the Flat River Creek: M.S. Thesis, University of Missouri Rolla, 111p.

Krishnamurthy, R.V., Atekwana, E.A., and Guha H., 1997. A simple, inexpensive carbonate-phosphoric acid reaction method for the determination of the $\delta^{13}C$ and $\delta^{18}O$ of carbonates. Anal. Chem. 69, 4256, 4258.

Laughrey, C.D., Baldassare, F.J., 2003. Some applications of isotope geochemistry for determining sources of stray carbon dioxide gas. Environ. Geosci. 10, 107-122.

Li, S.-L., Calmels, D., Han, G., Gaillardet, J. and Liu, C.-Q., 2008. Sulfuric acid as an agent of carbonate weathering constrained by $\delta^{13}C_{DIC}$: Examples from Southwest China. Earth Planet. Sci. Lett. 270, 189-199.

Macpherson, G.L., Roberts J.A., Blair J.M., Townsend M.A., Fowle D.A. and Beisner K.R., 2008. Increasing shallow groundwater CO_2 and limestone weathering, Konza Prairie, USA. Geochim. Cosmochim. Acta 72, 5581-5599.

Midwest Climate Watch, 2008. http://mcc.sws.uiuc.edu/cliwatch/watch.htm.

Mills, G.A. and Urey, H.C., 1940. The kinetics of isotopic exchange between carbon dioxide, bicarbonate ion, carbonates ion and water. J. Am. Chem. Soc. 62, 1019-1026.

Mook, W.G., Bommerson, J.C. and Staverman, W.H., 1974. Carbon isotope fractionation between dissolved bicarbonate and gaseous carbon dioxide. Earth Planet. Sci. Lett. 22, 169-176.

Moral, F., Cruz-Sanjulián J., and Olias M., 2008. Geochemical evolution of groundwater in the carbonate aquifers of Sierra de Segura (Betic Cordillera, southern Spain). J. Hydrol. 360, 281-296.

Nitzsche, H.M., Glaber, W. and Harting, P., 2002. Gas forming processes within lignite mining dumps. Isot. Environ. Health Stud. 38, 207-214.

Parkhurst, D.L. and Appelo, C.A.J., 1999. User's guide to PHREEQC (Version 2)-A computer program for speciation, batch-reaction, one-dimensional transport, and inverse geochemical calculations. U.S. Geol. Surv. Water Resour. Investig. Rep. 99-4259.

Plummer, L.N. and Back W., 1980. The mass balance approach: application to interpreting the chemical evolution of hydrologic systems, Am. J. Sci. 280, 130-142.

Plummer, L.N., Busby J.F., Lee R.W. and Hanshaw B.B. 1990. Geochemical modeling of the Madison Aquifer in parts of Montana, Wyoming, and South Dakota. Water Resour. Res. 26, 1981-2014.

Plummer, L.N., Prestemon, E.C. and Parkhurst, D.L., 1991. NETPATH-An interactive code for modeling net geochemical reactions along a flow path. Water Resour. Investig. Rep. 91- 4078.

Schumacher, J.G. and Hockanson, E.A., 1996. Hydrogeology and water quality at the St. Francois county landfill and vicinity-Southeastern Missouri, 1990-94. U.S. Geol. Surv. Water Resour. Investig. Rep. 96-4022.

Sherlock, E.J., Lawrence, R.W. and Poulin, R., 1995. On the neutralization of acid rock drainage by carbonate and silicate minerals. Environ. Geol. 25, 43-54.

Smith, B.J. and Schumacher, J.G., 1991. Hydrochemical and sediment data for the old lead belt, Southeastern Missouri-1988-89. U.S. Geol. Surv. Open File Rep. 91-211, 1-98.

Smith, B.J. and Schumacher, J.G., 1993. Surface-water and sediment quality in the old lead belt, Southeastern Missouri-1988-89. U.S. Geol. Surv. Water Resour. Investig. Rep. 93-4012, 1-92.

Svensson, U. and Dreybrodt W., 1992. Dissolution kinetics of natural calcite minerals in CO_2-water systems approaching calcite equilibrium. Chem. Geol. 100, 129-145.

Turner, J.V., 1982. Kinetic fractionation of carbon-13 during calcium carbonate precipitation. Geochim. Cosmochim. Acta 46, 1183-1191.

Vogel, J.C., Grootes, P.M. and Mook, W.G., 1970. Isotopic fractionation between gaseous and dissolved carbon dioxide. Zeitschrift fur Physik A (Atoms and Nuclei) 230, 225-238.

Yoshimura, K., Nakao, S., Noto, M., Inokura, Y., Urata, K., Chen M. and Lin, P.-W., 2001. Geochemical and stable isotope studies on natural water in the Taroko Gorge karst area, Taiwan-chemical weathering of carbonate rocks by deep source CO_2 and sulfuric acid. Chem. Geol. 177, 415-430.

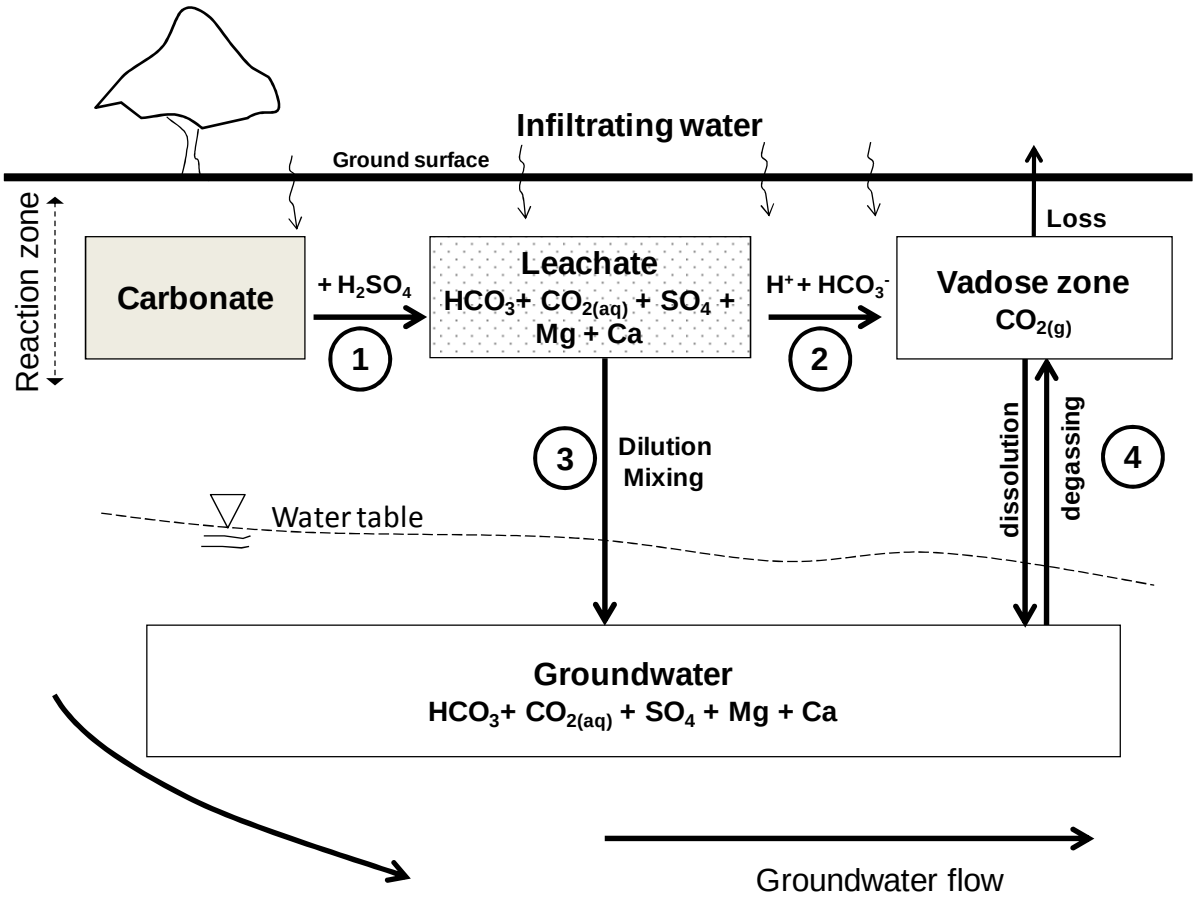

Figure II-1: Conceptual model of DIC production and carbonate evolution in a sulfide-rich and carbonate-rich shallow groundwater system.

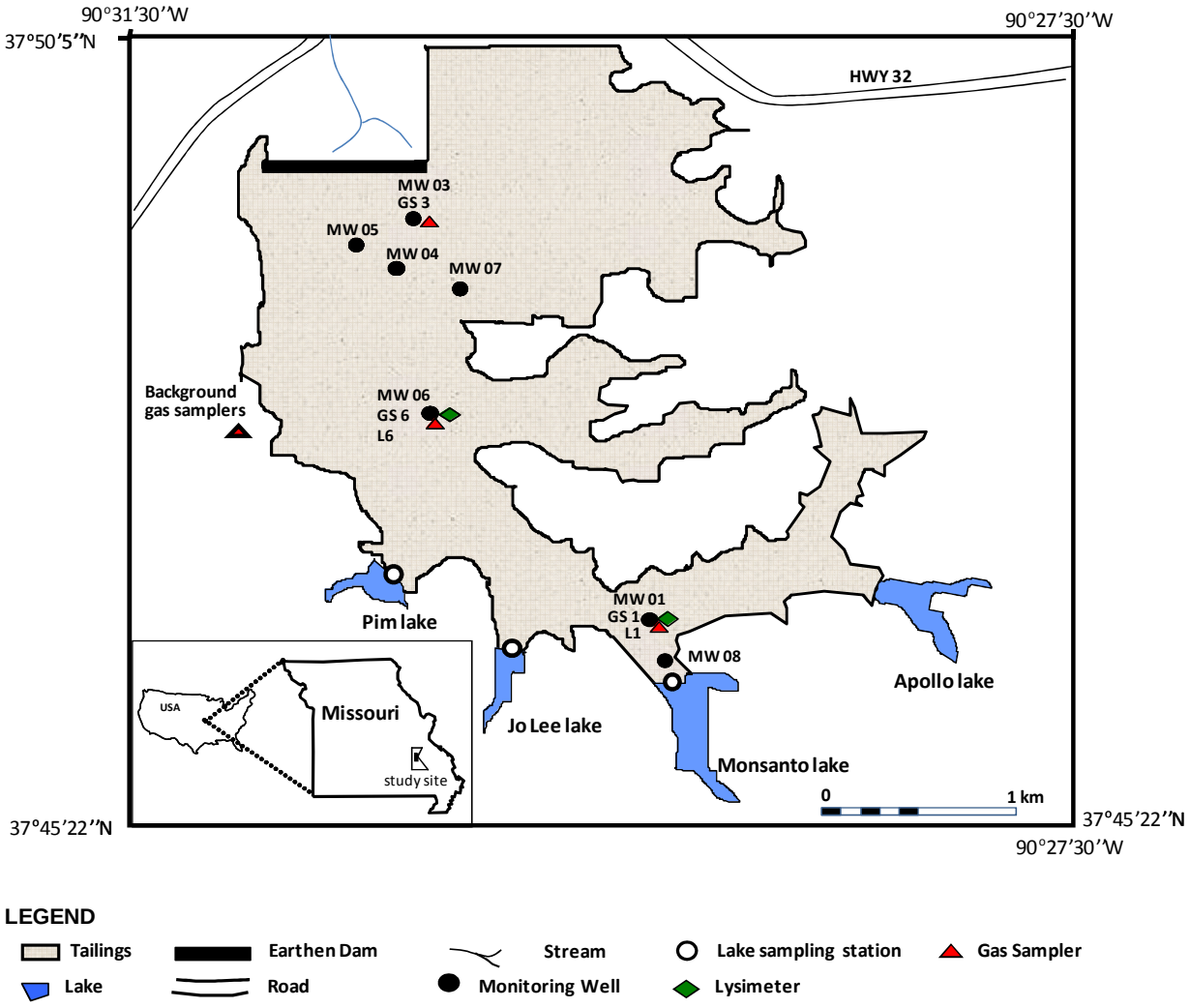

Figure II-2: Map of study site showing water sampling locations for lake water, soil water, perched groundwater and groundwater. Also shown are all locations for gas sampling from the vadose zone and the background station for soil gas sampling. Sample location codes are as follows: MW= monitoring well, L= lysimeter, GS = gas sampler, modified from Schumacher and Hockanson (1996) and from Google Earth (2008).

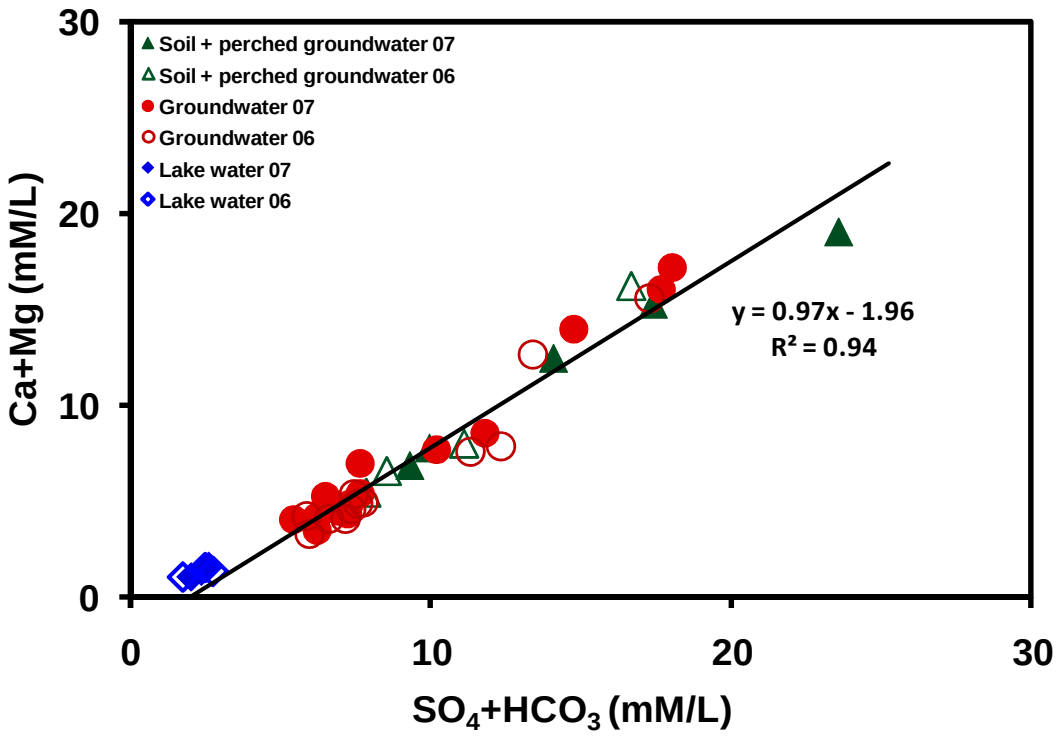

Figure II-3: Cross plot of SO_4+HCO_3 vs. Ca+Mg for lake water, soil water, perched groundwater, and groundwater from the Federal Tailings Pile, St Joe State Park, SE Missouri USA.

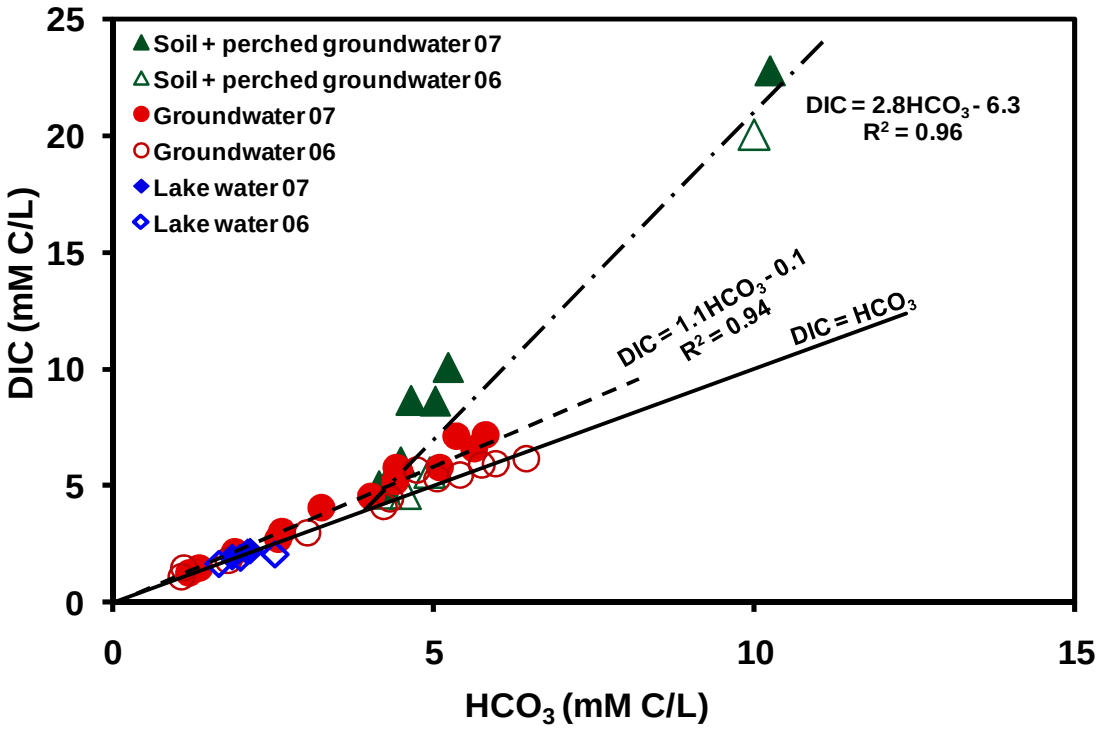

Figure II-4: Cross plots of DIC vs. HCO_3 of soil water, perched groundwater, groundwater, and lake water samples from the Federal Tailings Pile, St Joe State Park, SE Missouri USA.

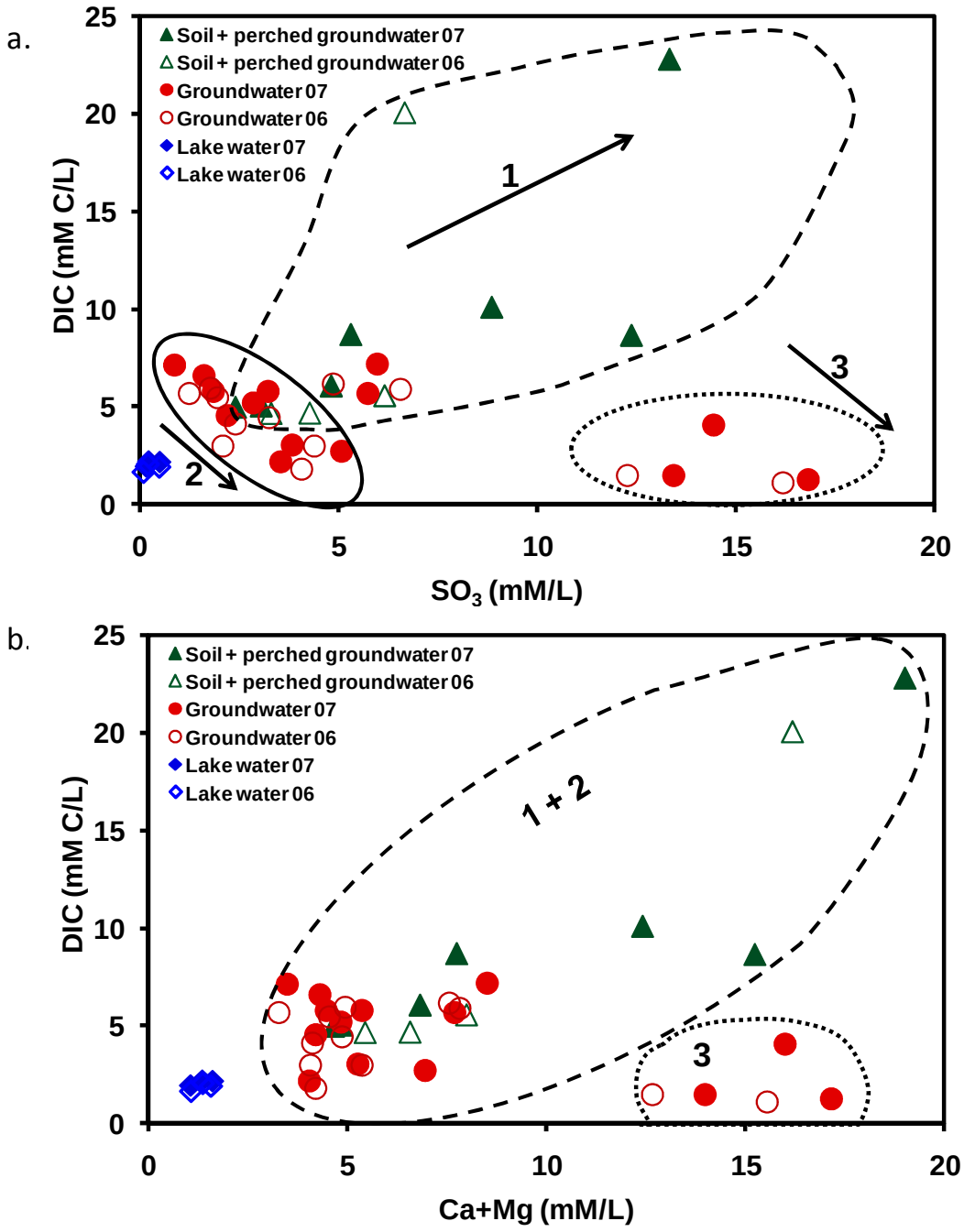

Figure II-5: Cross plots of (a) DIC vs. SO4 and (b) DIC vs. Ca+Mg for soil water, perched groundwater, groundwater, and lake water samples from the Federal Tailings Pile, St Joe State Park, SE Missouri USA. The ellipses represent sample clusters; dashed circle represents cluster 1 evolving by dissolution of carbonates, solid circle represents cluster 2 for samples evolving dominantly by HCO_3 dehydration, and dotted circle represents cluster 3 for samples evolving by dissolution, HCO_3 dehydration and degassing of CO_2.

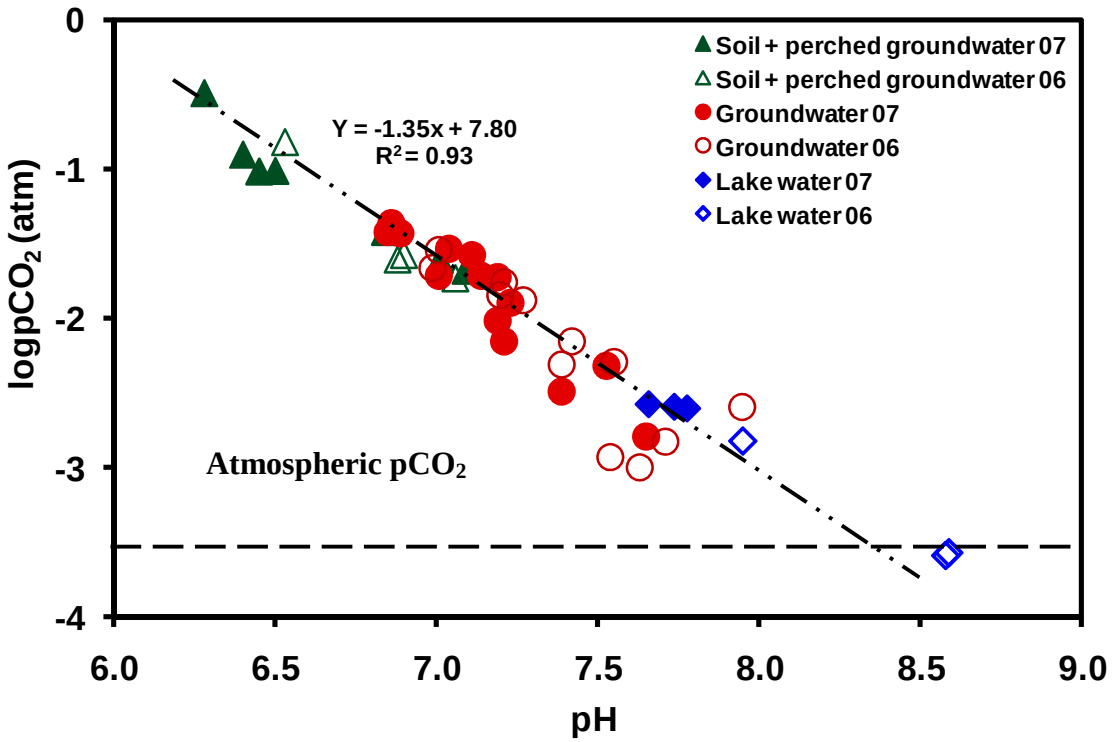

Figure II-**6**: Cross plot of pH vs. logpCO_2 for soil water, perched groundwater, groundwater, and lake water samples from the Federal Tailings Pile, St Joe State Park SE, Missouri USA. The dashed line represents average log$pCO_{2(g)}$ for atmosphere.

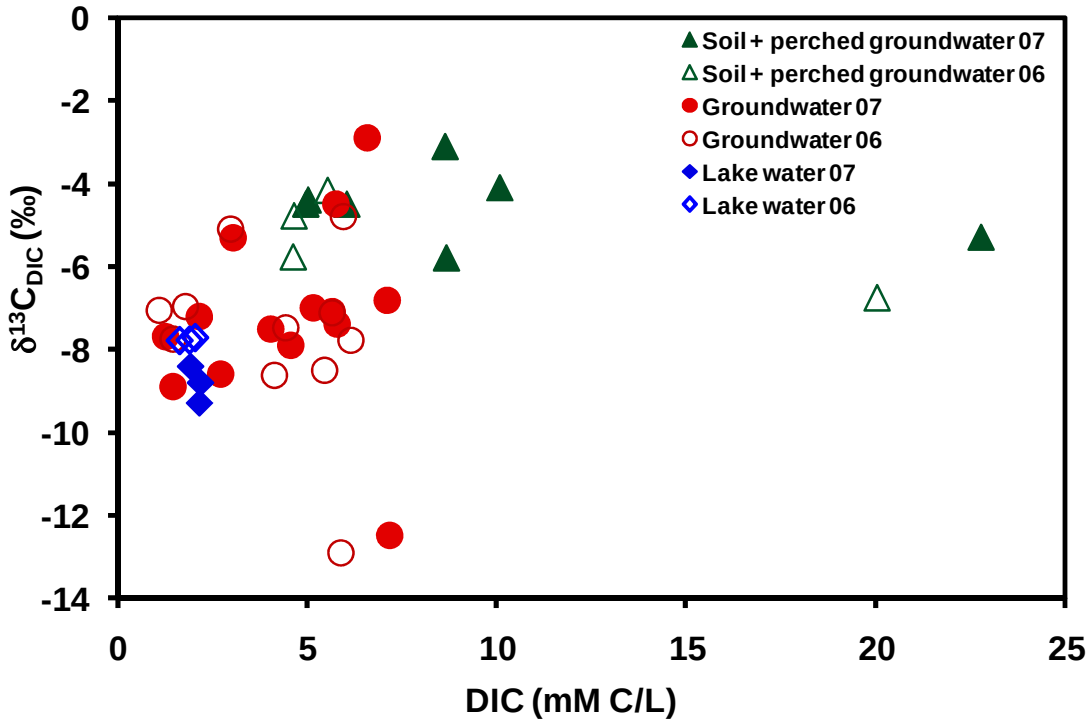

Figure II-7: Cross plot of $\delta^{13}C_{DIC}$ vs. DIC for soil water, perched groundwater, groundwater, and lake water from the Federal Tailings Pile, St Joe State Park, SE Missouri USA.

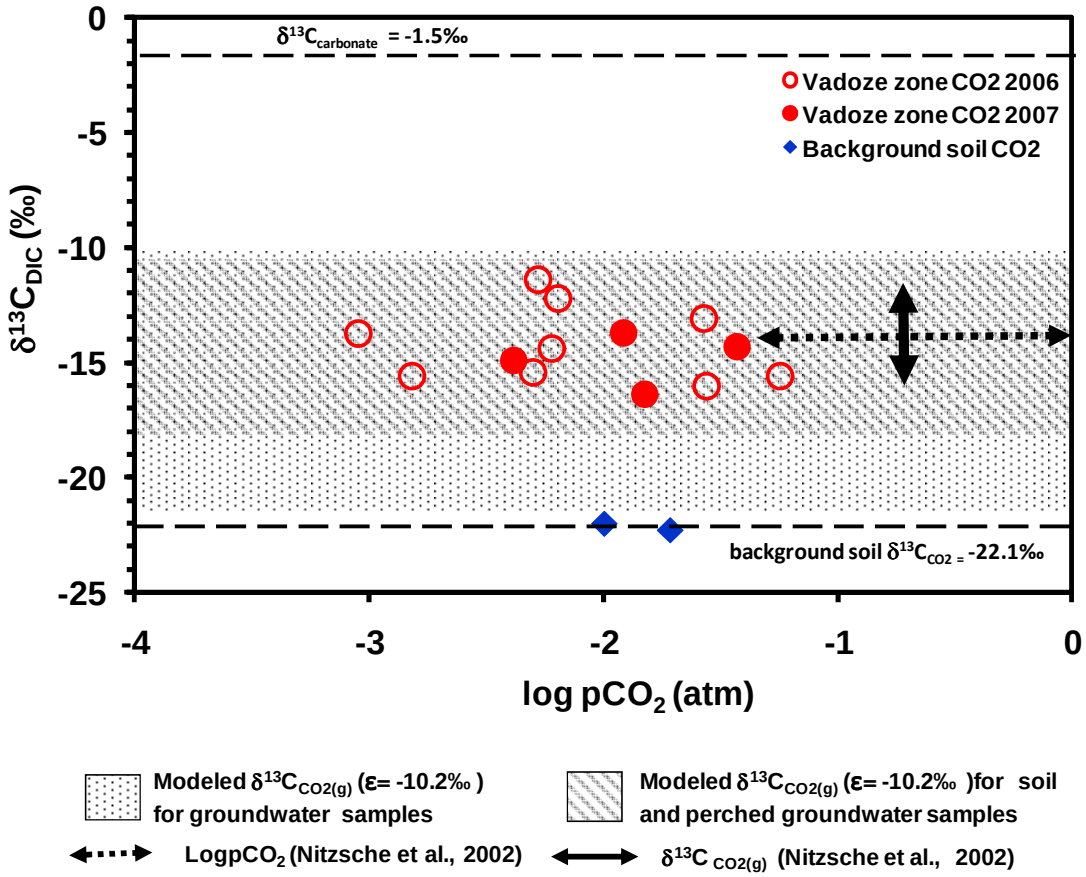

Figure II-8: Plot of $\delta^{13}C_{CO2}$ vs. logpCO_2 for vadose zone $CO_{2(g)}$ and background soil zone $CO_{2(g)}$ from the St Joe State Park SE, Missouri USA. The hatched interval represents the range of modeled $\delta^{13}C_{CO2}$ enrichment (-10.9‰ to -17.0‰) for CO_2 production from soil water and perched groundwater and the dotted interval represent the range for modeled $\delta^{13}C_{CO2}$ enrichment (-10.7‰ to -23.1) for CO_2 production from groundwater samples. Dashed and filled arrows represent the range for logpCO_2 and $\delta^{13}C_{CO2}$ respectively from Nitzsche et al. (2002). Dashed lines represent average $\delta^{13}C$ for carbonates (-1.5‰) in the tailings pile and average $\delta^{13}C_{CO2}$ of background soil gas (-22.1‰).

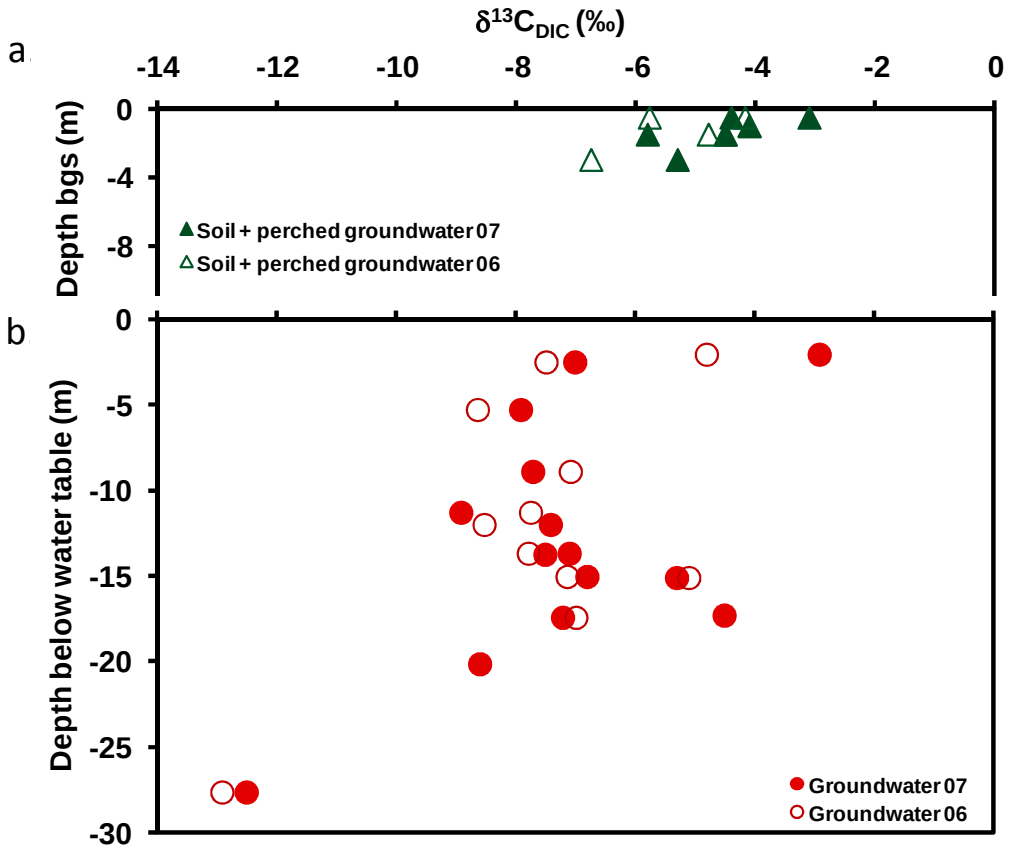

Figure II-9: Cross plot of $\delta^{13}C_{DIC}$ vs. depth below (a) ground surface for soil water and perched groundwater and (b) water table for groundwater samples from the Federal Tailings Pile, St Joe State Park, SE Missouri USA.

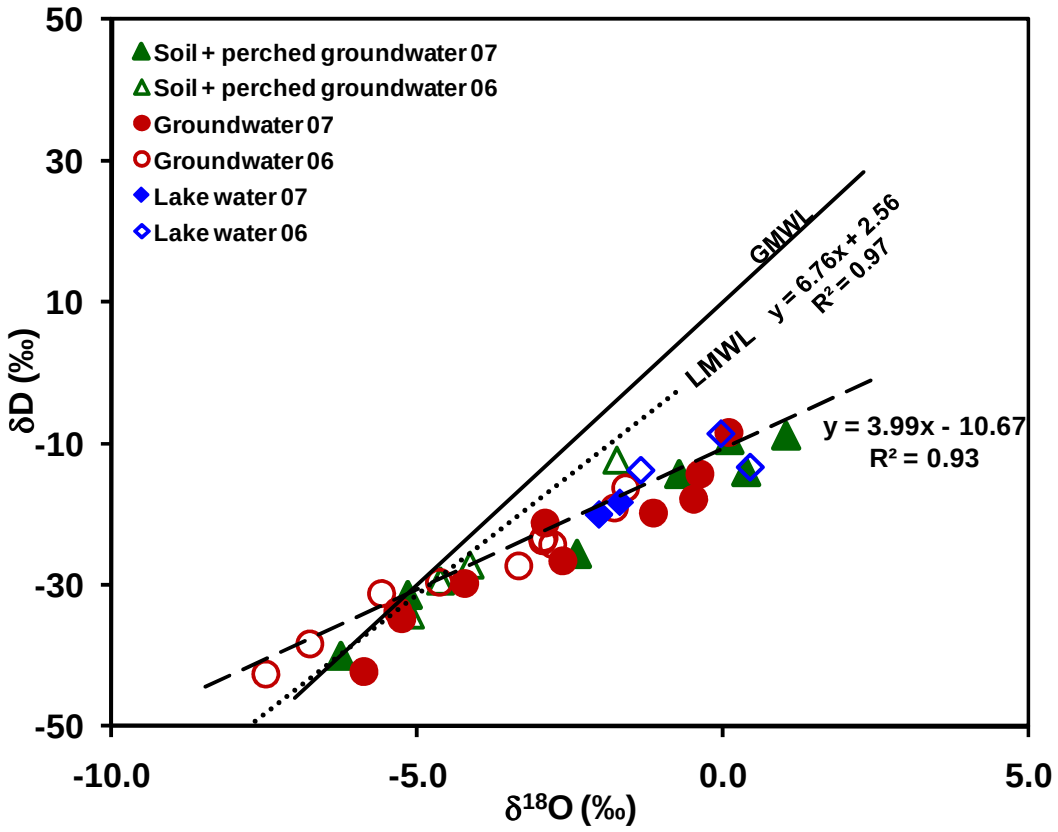

Figure II-10: Cross plot of $\delta^{18}O$ vs. δD for soil water and perched groundwater and groundwater samples from the Federal Tailings Pile, St Joe State Park, SE Missouri USA. Included is the Global Meteoric Water Line (GMWL) from Craig (1961) and a Local Meteoric Water Line (LMWL) adapted from Gasconade River data (Coplan and Kendal, 2000).

Table II-1: Results of the physical, chemical, and stable isotope analyses of lake water, soil water, perched groundwater and groundwater from the Federal Tailings Pile, St Joe State Park, SE Missouri, USA.

Sample ID	Water level bgs (m)	Temp. (^{o}C)	SPC (uS/cm)	pH	DIC (mM C/L)	$\delta^{13}C_{DIC}$ (‰)	δD (‰)	$\delta^{18}O$ (‰)	HCO_3^- (mM/l)	SO_4^{2-} (mM/L)	Cl (mM/L)	Ca (mM/L)	Mg (mM/L)	Na (mM/L)	K (mM/L)	Si (mM/L)	Log pCO_2 (atm)
2006																	
Lake water																	
Monsanto Lake	-	27.4	287	7.95	2.1	-7.7	-13.4	0.4	2.5	0.2	0.03	0.76	0.61	0.03	0.03	0.12	-2.82
Pim Lake	-	28.2	330	8.59	1.9	-7.8	-8.6	0.0	2.0	0.5	0.04	0.82	0.75	0.06	0.05	0.04	-3.57
Joe Lee Lake	-	29.2	221	8.58	1.6	-7.8	-13.8	-1.4	1.7	0.1	0.02	0.57	0.50	0.03	0.04	0.05	-3.59
Groundwater																	
MW 01_42	-1.2	18.9	718	7.27	5.5	-8.5	-38.3	-6.8	5.4	2.0	0.06	2.27	2.29	0.05	0.2	0.48	-1.88
MW 01_60	-1.9	20.0	872	7.71	1.8	-7.0	-42.5	-7.5	1.8	4.1	0.89	0.99	3.22	1.1	0.44	0.09	-2.83
MW 08_11	-1.0	19.9	844	7.42	4.4	-7.5	-23.4	-2.9	4.3	3.3	0.05	1.92	2.94	0.04	0.39	0.43	-2.15
MW 08_20	-0.9	17.7	694	7.55	4.1	-8.6	-23.7	-2.9	4.2	2.4	0.05	1.06	3.06	0.06	0.33	0.34	-2.29
MW 08_52	-1.4	20.3	925	6.99	5.7	-7.1	-19.1	-1.8	4.7	1.2	2.91	0.95	2.35	2.77	0.35	0.18	-1.66
MW 06_53	-1.3	14.9	801	7.39	3.0	-5.1	-29.6	-4.6	3.0	4.4	0.05	3.23	2.14	0.03	0.33	0.18	-2.31
MW 06_94	-1.5	19.6	1577	7.2	5.9	-12.9	-16.3	-1.6	5.8	6.6	2.78	2.13	5.71	2.99	0.4	0.33	-1.84
MW 07_20	-4.2	20.6	794	7.21	6.0	-4.8	-24.4	-2.8	6.0	1.8	0.02	2.76	2.18	0	0.08	0.35	-1.76
MW 07_70	-7.2	29.2	947	7.95	5.3	-	-27.3	-3.3	5.1	2.1	0.03	1.77	2.30	0.02	0.09	0.37	-2.60
MW 05_58	-5.2	30.9	2021	7.01	6.2	-7.8	-31.3	-5.6	6.5	4.9	0.28	4.04	3.51	0.21	0.24	0.35	-1.54
MW 04_101	-	-	-	-	-	-	-	-	-	-	-	-	-	-	-	-	-
MW 04_80	-	-	-	-	-	-	-	-	-	-	-	-	-	-	-	-	-
MW 03_62	-10.7	34.5	3687	7.54	1.1	-7.1	-37.6	-7.4	1.1	16.2	7.23	3.57	11.99	6.95	0.47	0.12	-2.93
MW 03_72	-13.0	28.7	2938	7.63	1.5	-7.7	-34.6	-6.8	1.1	12.3	7.74	3.10	9.57	6.21	0.45	0.14	-3.00

Sample ID	Water level bgs (m)	Temp. (^{o}C)	SPC (uS/cm)	pH	DIC (mM C/L)	$\delta^{13}C_{DIC}$ (‰)	δD (‰)	$\delta^{18}O$ (‰)	HCO_3^- (mM/l)	SO_4^{2-} (mM/L)	Cl (mM/L)	Ca (mM/L)	Mg (mM/L)	Na (mM/L)	K (mM/L)	Si (mM/L)	Log pCO_2 (atm)
Soil water																	
PW 01	-	24.2	942	7.06	4.6	-5.8	-12.4	-1.7	4.6	3.3	0.04	3.35	2.09	0.03	0.08	0.5	-1.73
PW 02	-	23.2	1318	6.9	5.5	-4.2	-27.2	-4.1	4.9	6.2	0.03	5.40	2.60	-0.01	0.03	0.28	-1.57
Perched groundwater																	
PGW 01-3	-1.5	-	-	-	-	-	-	-	-	-	-	-	-	-	-	-	-
PGW 03-3	-1.5	23.1	2265	6.53	22.0	-6.8	-34.2	-5.1	10.0	6.7	0.01	10.92	5.27	0	0.10	0.65	-1.00
PGW 06-2	-1.0	-	-	-	-	-	-	-	-	-	-	-	-	-	-	-	
PGW 06-3	-1.5	19.6	981	6.88	4.7	-4.8	-29.4	-4.6	4.3	4.3	0.03	4.60	1.98	0.02	0.06	0.19	-1.70
PGW 06-4	-2.0	-	-	-	-	-	-	-	-	-	-	-	-	-	-	-	-
2007																	
Lake water																	
Monsanto Lake	-	27.4	258	7.78	2.2	-8.8	-20.0	-2.0	2.1	0.2	0.02	0.75	0.60	0.04	0.03	0.17	-2.61
Pim Lake	-	24.6	314	7.74	2.2	-9.3	-18.4	-1.7	2.1	0.5	0.04	0.85	0.76	0.06	0.05	0.17	-2.59
Joe Lee Lake	-	25.5	207	7.66	1.9	-8.4	-20.2	-2.0	1.9	0.2	0.02	0.58	0.48	0.03	0.05	0.17	-2.58
Groundwater																	
MW 01_42	-0.8	19.5	810	7.19	5.8	-7.4	-19.9	-1.2	5.1	1.9	0.05	2.19	2.28	0.07	0.22	0.51	-1.72
MW 01_60	-1.1	20.5	921	7.21	2.2	-7.2	-8.4	0.1	1.9	3.5	0.78	0.89	3.17	1.06	0.46	0.10	-2.15
MW 03_62	-10.6	19.8	3219	7.65	1.3	-7.7	-33.7	-5.3	1.2	16.8	6.54	3.84	13.35	7.37	0.57	0.09	-2.79
MW 03_72	-13	19.1	2832	7.39	1.5	-8.9	-34.8	-5.2	1.3	13.4	6.55	3.41	10.6	6.96	0.59	0.14	-2.49

Sample ID	Water level bgs	Temp.	SPC	pH	DIC	$\delta^{13}C_{DIC}$	δD	$\delta^{18}O$	HCO_3^-	SO_4^{2-}	Cl	Ca	Mg	Na	K	Si	Log pCO_2
	(m)	(°C)	(uS/cm)		(mM C/L)	(‰)	(‰)	(‰)	(mM/l)	(mM/L)	(mM/L)	(mM/L)	(mM/L)	(mM/L)	(mM/L)	(mM/L)	(atm)
MW 04_101	-11	19.6	1600	7.53	2.7	-8.6	-29.8	-4.2	2.6	5.1	3.84	1.27	5.68	3.38	0.47	0.14	-2.31
MW 04_80	-10	16.3	2859	7.01	4.1	-7.5	-14.3	-0.4	3.3	14.4	3.19	4.95	11.07	5.56	0.59	0.31	-1.72
MW 05_58	-5.1	25.4	1248	6.89	5.7	-7.1	-21.3	-2.9	4.5	5.8	0.04	3.96	3.74	0.26	0.29	0.54	-1.43
MW 06_53	-1.9	15.5	944	7.19	3.0	-5.3	-42.2	-5.9	2.6	3.8	0.04	3.23	2.05	0.03	0.33	0.22	-2.01
MW 06_94	-1.4	13.4	1739	7.04	7.2	-12.5	-26.6	-2.6	5.8	6	2.45	2.35	6.18	3.33	0.47	0.39	-1.53
MW 07_20	-4.2	20.1	753	7.11	6.6	-2.9	-17.9	-0.5	5.6	1.6	0.02	2.44	1.88	0.02	0.09	0.46	-1.58
MW 07_70	-7.3	23.4	918	6.85	5.8	-4.5	-15.9	0.0	4.4	3.2	0.03	2.96	2.41	0.03	0.15	0.37	-1.42
MW 08_11	-0.9	15.9	884	7.14	5.2	-7	-10.3	-0.1	4.4	2.9	0.04	1.96	2.90	0.04	0.39	0.49	-1.72
MW 08_20	-0.8	14.7	777	7.23	4.6	-7.9	-7.7	1.1	4.0	2.2	0.04	1.10	3.10	0.05	0.34	0.39	-1.90
MW 08_52	-1.1	17.5	966	6.86	7.1	-6.8	-17.2	-0.7	5.4	0.9	2.71	1.05	2.44	2.85	0.36	0.22	-1.37
Soil water																	
PW 01	-0.5	23.1	928	7.01	5.0	-4.4	-40.1	-6.3	4.2	3.1	0.07	2.96	1.90	1.13	0.09	0.33	-1.61
PW 02	-6.0	21.1	2068	6.5	8.6	-3.1	-31.5	-5.2	5.0	12.4	0.04	11.08	4.18	0.03	0.10	0.36	-1.01
Perched groundwater																	
PGW 01-3	-1.5	23	859	7.09	5.0	-4.5	-25.7	-2.4	4.2	2.4	0.05	2.84	1.82	0.33	0.07	0.23	-1.68
PGW 03-3	-1.5	20.1	2601	6.28	22.8	-5.3	-14.4	-0.7	10.3	13.4	0.03	13.22	5.81	0.04	0.16	0.39	-0.49
PGW 06-2	-1.0	20.5	1903	6.4	10.1	-4.1	-9.0	1.0	5.2	8.9	0.02	8.69	3.75	0.04	0.10	0.22	-0.90
PGW 06-3	-1.5	18.5	1256	6.45	8.7	-5.8	-14.1	0.4	4.7	5.3	0.01	5.40	2.36	0.04	0.08	0.25	-1.01
PGW 06-4	-2.0	18.6	1151	6.84	6.0	-4.5	-9.6	0.1	4.5	4.8	0.01	4.64	2.20	0.04	0.09	0.29	-1.42

- = Not determined

Table II-2: Sample depth, concentration of $CO_{2(g)}$, and the stable C-isotope ratio of CO_2 ($\delta^{13}C_{CO2}$) in gas samples from the vadose zone and background soil gas from the Federal Tailings Pile, St Joe State Park, SE Missouri, USA.

Sample ID	Sampling depth (m)	log pCO_2 (atm)	$\delta^{13}C_{CO2(g)}$ (‰)
2006			
SJGW 1-1	-1.0	-2.82	-15.6
SJGW 1-3	-0.5	-2.22	-14.4
SJGW 1-4	-3.0	-2.30	-15.4
SJGW 2-1	-1.5	-2.20	-12.2
SJGW 2-2	-1.0	-2.28	-11.4
SJGW 2-3	-0.5	-1.57	-13.1
SJGW 2-4	-3.0	-3.05	-13.7
SJGW 3-1	-1.0	-1.25	-15.6
SJGW 3-2	-0.5	-1.56	-16.0
2007			
SJGW1-4	-1.0	-2.38	-14.9
SJGW3-3	-0.5	-1.35	-14.3
SJGW6-1	-1.0	-1.87	-13.7
SJGW3-1	-1.0	-1.83	-16.4
SJGW3-4	-2.0	-3.12	-
Background			
Background_01	-0.25	-2.08	-22.0
Background_02	-0.50	-1.72	-22.3

= Not determined

Table III-3: Saturation indices of mineral phases modeled using the computer program PHREEQCI (Parkhurst and Appelo, 1999) for lake water, soil water, perched groundwater, and groundwater samples from the Federal Tailings Pile, St Joe State Park SE, Missouri USA.

Sample ID	Alunite	Anglesite	Anhydrite	Gypsum	Melanterite	Jarosite-K	Aragonite	Cerrusite	Otavite	Siderite	Rhodochr.	Aragonite	Calcite	Dolomite	Goethite	Fe(OH)3	Gibbsite	Smithsonite	Pb(OH)2	Anorthite	Ca-Mont.
2007																					
Lake water																					
Monsanto Lake	-3.22	-5.00	-2.71	-2.50	-10.4	-9.38	-0.19	-1.12	-0.63	-3.15	-1.82	-0.19	-0.04	-0.03	6.67	0.70	2.23	-2.60	-1.46	-0.03	4.42
Pim Lake	-1.30	-4.57	-2.36	-2.14	-9.72	-8.13	-0.25	-1.09	-0.66	-2.92	-2.03	-0.25	-0.11	-0.14	6.73	0.85	2.50	-2.65	-1.55	0.28	5.12
Joe Lee Lake	-2.13	-5.04	-2.93	-2.71	-9.33	-6.82	-0.49	-1.24	-0.81	-2.18	-2.09	-0.49	-0.35	-0.64	7.39	1.48	2.44	-2.75	-1.71	-0.06	4.92
Groundwater																					
MW 01_42	5.53	-3.89	-1.61	-1.38	-7.75	-6.29	-0.20	-1.06	-1.09	-1.71	-2.54	-0.20	-0.05	-0.02	6.24	0.55	3.64	-3.00	-2.63	2.39	9.58
MW 01_60	5.99	-3.28	-1.75	-1.51	-7.54	-5.32	-1.08	-1.21	-1.53	-2.24	-2.78	-1.08	-0.94	-1.25	6.29	0.56	3.53	-3.48	-2.22	0.45	6.64
MW 03_62	4.28	-3.60	-0.86	-0.62	-5.92	1.64	-0.55	-1.88	-1.72	-0.99	-2.55	-0.55	-0.40	-0.21	8.72	3.02	3.07	-3.47	-2.15	0.69	5.64
MW 03_72	5.20	-	-0.94	-0.70	-5.59	1.03	-0.69	-	-	-0.72	-	-0.69	-0.54	-0.53	8.29	2.61	3.14	-	-	0.63	6.44
MW 04_101	3.99	-	-1.57	-1.33	-6.95	-1.89	-0.51	-	-	-1.27	-	-0.51	-0.36	-0.01	7.69	2.00	3.12	-	-	0.60	6.37
MW 04_80	8.62	-	-0.77	-0.53	-5.52	-1.60	-0.54	-	-	-0.71	-	-0.54	-0.39	-0.41	6.98	1.41	3.84	-	-	1.93	9.35
MW 05_58	6.76	-3.52	-1.03	-0.81	-7.07	-5.23	-0.32	-1.45	-1.44	-1.65	-1.15	-0.32	-0.18	-0.25	6.04	0.14	3.53	-3.39	-3.02	2.20	9.17
MW 06_53	6.96	-3.28	-1.19	-0.94	-5.69	-1.03	-0.46	-1.09	-1.42	-0.41	-2.49	-0.46	-0.31	-0.81	7.69	2.14	3.80	-3.32	-2.49	1.81	8.76
MW 06_94	9.05	-3.49	-1.28	-1.02	-5.49	-1.74	-0.49	-1.22	-1.44	-0.19	-2.64	-0.49	-0.34	-0.29	7.15	1.69	4.18	-3.28	-3.21	2.42	10.56

Sample ID	Alunite	Anglesite	Anhydrite	Gypsum	Melanterite	Jarosite-K	Aragonite	Cerrusite	Otavite	Siderite	Rhodochr.	Aragonite	Calcite	Dolomite	Goethite	Fe(OH)3	Gibbsite	Smithsonite	Pb(OH)2	Anorthite	Ca-Mont.
MW 07_20	5.25	-4.03	-1.62	-1.38	-7.27	-5.53	-0.16	-1.16	-1.10	-1.18	-2.26	-0.16	-0.01	-0.07	6.58	0.87	3.64	-3.28	-2.84	2.25	9.39
MW 07_70	6.57	-3.66	-1.30	-1.07	-6.85	-5.28	-0.44	-1.43	-1.50	-1.32	-2.49	-0.44	-0.30	-0.58	6.19	0.35	3.62	-3.36	-3.13	1.76	8.81
MW 08_11	7.02	-3.69	-1.51	-1.26	-5.79	-1.37	-0.44	-1.17	-1.20	-0.17	-2.40	-0.44	-0.29	-0.41	7.58	2.03	3.82	-3.18	-2.86	2.29	10.04
MW 08_20	6.62	-3.62	-1.83	-1.58	-6.23	-2.33	-0.65	-0.97	-1.13	-0.50	-2.48	-0.65	-0.49	-0.55	7.42	1.91	3.85	-3.17	-2.57	2.00	9.75
MW 08_52	7.42	-3.92	-2.23	-1.99	-7.67	-7.89	-0.83	-1.08	-1.36	-1.68	-2.24	-0.83	-0.68	-0.96	5.49	-0.13	4.05	-3.22	-3.09	1.38	9.10
Soil water																					
PW 01	5.18	-3.86	-1.31	-1.08	-7.71	-7.16	-0.30	-1.47	-1.35	-2.03	-2.15	-0.30	-0.16	-0.41	5.80	-0.02	3.39	-2.29	-3.01	1.50	8.16
PW 02	9.93	-2.76	-0.45	-0.22	-6.99	-8.89	-0.40	-1.30	-1.97	-2.30	-2.06	-0.40	-0.26	-0.86	4.39	-1.36	4.14	-2.45	-3.46	2.33	10.01
Perched groundwater																					
PGW 01-3	5.25	-3.34	-1.40	-1.17	-7.72	-6.73	-0.24	-0.80	-	-1.88	-0.76	-0.24	-0.09	-0.28	6.12	0.30	3.60	-0.99	-2.24	1.75	8.08
PGW 03-3	9.71	-2.80	-0.41	-0.17	-4.73	-3.41	-0.24	-1.22	-	0.06	-1.23	-0.24	-0.10	-0.49	5.93	0.21	3.77	-2.09	-3.97	1.21	9.24
PGW 06-2	9.38	-2.24	-0.63	-0.40	-7.40	-10.71	-0.53	-0.72	-	-2.66	-1.24	-0.53	-0.38	-1.06	3.75	-1.98	3.92	-0.77	-3.05	1.16	8.69
PGW 06-3	8.85	-2.53	-0.93	-0.68	-5.20	-4.12	-0.68	-0.86	-	-0.35	-1.31	-0.68	-0.53	-1.38	6.10	0.45	3.88	-2.09	-3.17	1.01	8.86
PGW 06-4	7.22	-	-1.00	-0.76	-5.37	-2.18	-0.36	-	-	-0.12	-1.37	-0.36	-0.21	-0.70	7.14	1.48	3.73	-2.77	-	1.57	8.85

- - = Not determined

Table II-4: Modeled stable C-isotope ($\delta^{13}C_{DIC}$) results for groundwater samples from the Federal Tailings Pile, St Joe State Park SE, Missouri USA.

Sample ID	Modeled $\delta^{13}C_{DIC}$ (‰)	Measured $\delta^{13}C_{DIC}$ (‰)	Dissolving phases	Evaporation or Dilution	Precipitating phases
MW 08_11	-7.0	-7.0	Dolomite, CO_2	dilution	Ca-Mont
MW 08_20	7.9	7.9	Dolomite, CO_2	dilution	Ca-Mont
MW 08_52	-6.8	-6.8	Dolomite, CO_2	dilution	Ca-Mont
MW 01_42	-6.7	-7.4	Dolomite, CO_2	dilution	Calcite, Ca-Mont
MW 01_60	-7.2	-7.2	Dolomite, CO_2	dilution	Ca-Mont
MW 06_53	-5.6	-5.3	CO_2	dilution	Ca-Mont
MW 06_94	-	-12.5	-	-	Model failed
MW 07_20	2.9	-2.9	Dolomite, calcite, CO_2	dilution	Ca-Mont
MW 07_70	-4.5	-4.5	Dolomite, Calcite, CO_2	dilution	Ca-Mont
MW 04_101	-8.6	-8.6	Dolomite, CO_2	dilution	/
MW 04_80	-7.4	-7.5	/	dilution	Calcite
MW 05_58	-7.4	-7.1	Dolomite, CO_2	dilution	Calcite
MW 03_62	-8.1	-7.7	Dolomite,	dilution	CO_2, Ca -Mont
MW 03_72	-8.6	-8.9	/	dilution	CO_2, Ca-Mont

/ = no reacting phases

- = not determined

CHAPTER III

DISSOLVED INORGANIC CARBON EVOLUTION IN NEUTRAL DISCHARGE FROM MINE TAILINGS PILES

Abstract

We measured the spatial concentrations of DIC, major ions, and stable carbon isotope ratios of DIC in two tailings piles producing neutral mine drainage. The objective was to investigate DIC and $\delta^{13}C_{DIC}$ evolution during the outgassing of $CO_{2(g)}$ from the tailings discharge. Results show that over the 620 m reach of one of the discharges, DIC decreased by 0.9 mM C/L to 1.1 mM C/L for a $\delta^{13}C_{DIC}$ enrichment of ~4.0‰. At the other discharge no significant decrease in DIC and only a small change in the $\delta^{13}C_{DIC}$ were observed over a 980 m reach. The DIC decrease was due to loss of excess $CO_{2(aq)}$ in water as discharge flowed downstream. The mechanism of $CO_{2(g)}$ loss is kinetic and leads to a kinetic $\delta^{13}C_{DIC}$ enrichment. The magnitude of the downstream $\delta^{13}C_{DIC}$ enrichment depends on the initial concentration of excess $CO_{2(aq)}$ in the discharge water and the amount and rate of $CO_{2(g)}$ lost from the discharge.

Keywords: Dissolved inorganic carbon; excess $CO_{2(aq)}$; stable carbon isotopes; $\delta^{13}C_{DIC}$; carbonate-rich tailings pile.

1. Introduction

Investigations of carbon transfer from DIC in water discharged to the surface using stable carbon isotopes of the DIC ($\delta^{13}C_{DIC}$) has gained attention in the last decades (e.g., Doctor et al., 2008). This is because changes in DIC and $\delta^{13}C_{DIC}$ can provide greater insights into our understanding of processes that control the movement of carbon between the discharge and the atmosphere (e.g., Doctor et al., 2008). The DIC in the groundwater that is discharged will have a carbon isotopic signature that is indicative of the sources of carbon and the relative contribution from each source. DIC in groundwater discharged to the surface can contain excess free dissolved $CO_{2(aq)}$ (Worral and Lancaster, 2005) that is in excess of the CO_2 partial pressure in the water (pCO_2) in equilibrium with atmospheric $CO_{2(g)}$. The transfer of the excess $CO_{2(aq)}$ to the atmosphere can occur via (1) equilibrium open system conditions in which there is exchange of carbon between the DIC and atmospheric $CO_{2(g)}$; which will result in equilibrium isotope exchange or (2) irreversible kinetic transfer of carbon from DIC by the outgassing of $CO_{2(g)}$ that would lead to kinetic isotope effects (e.g., Mills and Urey, 1940; Deines, 1970; Mook et al., 1974).

In environments where there is excess $CO_{2(aq)}$ in the discharge water, relative to atmospheric $CO_{2(g)}$, the extent to which $CO_{2(g)}$ escapes from the water is controlled by the rate of diffusion across the water/air interface (e.g., Michaelis et al., 1985), the initial excess $CO_{2(aq)}$ and the extent to which the DIC species are converted to $CO_{2(aq)}$ ($CO_3 \Rightarrow HCO_3 \Rightarrow H_2CO_3 \Rightarrow CO_{2(aq)}$). Thus, for an aqueous system exposed to the atmosphere, the partial pressure of carbon dioxide in water($pCO_{2(aq)}$) controls the

ultimate fate of the CO_2 that is lost. The carbonate reactions describing the transformation of DIC species in aqueous system exposed to the atmosphere are shown in equations 1-3.

$$CO_{2(g)} \leftrightarrow CO_{2(aq)} + H_2O \leftrightarrow \quad H_2CO_3 \qquad (1)$$

$$H_2CO_3 \leftrightarrow HCO_3^- + H^+ \qquad (2)$$

$$HCO_3^- \rightarrow CO_3^{2-} + H^+ \qquad (3)$$

Shifts in the isotopic composition of DIC ($\delta^{13}C_{DIC}$) will occur due to the fractionation caused by the preferential release of ^{12}C as $CO_{2(g)}$. The kinetic enrichment (ε_k) during the transfer of $CO_{2(g)}$ from water has been reported by several studies and shows a wide range. For example, Wanninkhof (1985) and Inoue and Sugimura (1985) determined ε_k in the range -1 to -4‰, Zhang et al. (1995) determined ε_k of -0.81±0.16‰ at 21^{o}C and 0.95±0.2‰ at 5^{o}C and Usdowski and Hoefs, (1990) calculated ε_k of -4‰. The range in the kinetic isotopic enrichment for the outgassing of $CO_{2(g)}$ in these studies may result from differences in the initial DIC concentrations, rates and different amounts of $CO_{2(g)}$ released from the water. The mechanism of CO_2 loss may be important in our understanding of the anthropogenic effects of neutral drainage on carbon transfer during DIC evolution at surface conditions.

The goal of this study is to investigate the downstream evolution of DIC and $\delta^{13}C_{DIC}$ changes in neutral mine discharge from the outgassing of $CO_{2(g)}$ to the atmosphere. The objective was to (1) investigate the effects of downstream changes of DIC and $\delta^{13}C_{DIC}$ composition of the discharge from two carbonate-rich mine tailings piles producing neutral drainage and (2) determine the nature of DIC speciation and

stable isotope composition ($\delta^{13}C_{DIC}$) shifts during this evolution. To accomplish our objectives, we measured the concentrations of DIC, major ions, and stable carbon isotope composition of the DIC in neutral mine discharge from two tailings piles to assess the DIC and $\delta^{13}C_{DIC}$ evolution in the discharge.

2. Study Site

The Elvin's Tailings Pile (ETP) and the Leadwood Tailings Pile (LTP) are two of several tailings piles found in St. Francois County, SE Missouri, USA (Fig. III-1). The tailing piles are located near the cities of Park Hills, MO and Leadwood, MO, respectively. The region has a temperate climate with mean annual precipitation and temperature for 1971-2007 of 1,086 mm and 12.7 $^{\circ}$C, respectively (Midwest Regional Climate Center, 2009). The ETP covers approximately 1.1 km^2 and is approximately 73 m at its highest elevation relative to the surrounding topography. The LTP covers 2.2 km^2 and 22 m higher than the surrounding topography. The SE portion of the ETP is drained by a small creek (ETP Creek) that collects water discharged directly from the tailings pile. The ETP Creek flows southeastwards for about 650 m to join the Flat River (FR). The Flat River is the largest tributary to the Big River (Kramer, 1976). At the LTP, the northern section is drained by a small creek (LTP Creek) that is collects seeps discharged from the tailings pile. The LTP Creek flows northeastwards for about 980 m to join the Big River (BR). The Big River is a perennial stream that flows northwards and then westwards through the study area (Fig. III-1).The BR is the major stream that drains the region (Kramer, 1976). The ETP Creek and LTP Creek are shallow and vary in depth

from less than 5 cm to 10 cm deep and have average discharge rates that range from 0.004 m^3/s to 0.01 m^3/s (http://waterdata.usgs.gov/mo/nwis/qwdata, Dec., 2009)

3. Method

3.1. Water sampling and field measurements

The sampling locations selected for this study include six locations along the ETP Creek (620 m), starting at the seep source (ETP1) downstream to location (ETP 6) and 5 locations along LTP Creek starting at 160 m (LTP1) from the seep source to location at LTP5 (980 m) downstream before the creek flows into the BR. It was not possible to sample LTP Creek at its seep source because of a drain pipe built at the seep source. AT the ETP Creek, the sampling distances between the stations ranged from 10 m to 200 m, while along the LTP Creek, the sampling distances between the stations ranged from 120 to 340 m (Table 1)

Water samples from both the ETP Creek and LTP Creek were collected in June 2006 and June 2007. The water samples were collected by the grab technique. Prior to collecting water samples, the temperature, pH, dissolved oxygen (DO), oxidation reduction potential (ORP), and specific conductance (SPC) were measured using a Yellow Spring Instrument (YSI) multi-parameter probe that was calibrated to manufacturers specifications. All water samples were filtered through a 0.45 μm syringe filter during collection. The water samples were collected in high density polyethylene (HDPE) bottles that were unacidified for anion samples and acidified to a pH <2 with high purity HNO_3 for cation and metal samples. All water samples were cooled on ice while in the field and transported to the laboratory where they were stored at 4^oC until

analysis. Water samples for DIC analysis were collected as described by Atekwana and Krishnamurthy (1998).

3.2. Sample analyses

The alkalinity of the water samples was measured by acid titration (Hach, 1992) immediately after sampling in the field. Anions were analyzed by Dionex ICS 3000 ion chromatography and cations and metals were analyzed by a PerkinElmer Optima 2100DV inductively coupled plasma optical emission spectrometer (ICP-OES). Water samples collected for DIC were extracted for $CO_{2(g)}$ as described by Atekwana and Krishnamurthy (1998). The DIC concentration was calculated from the $CO_{2(g)}$ yields measured by a pressure transducer. The $CO_{2(g)}$ was sealed in Pyrex tubes for later isotope analysis. Stable carbon isotope ratios of the $CO_{2(g)}$ was measured by isotope ratio mass spectrometry at Western Michigan University, Kalamazoo Michigan. The isotope ratios are reported in the delta notation in per mil:

$$\delta\ (‰) = ((R_{sample} / R_{standard}) -1) \times 10^3$$

Where R is the ratio $^{13}C/^{12}C$. The delta values are reported relative to VPDB international carbon standard. Routine $\delta^{13}C$ measurements have an overall precision of < 0.1‰.

4. Results

4.1. Spatial variability of physical parameters in tailings discharge

The results for pH, ORP, DO and SPC for the samples are presented in Table III-1. Although measurements varied between the two sampling periods and sites, the samples from the tailing piles show similar trends for pH, DO and SPC. In general there

is a marked increase in pH, DO and SPC and decrease in ORP between the ETP1 (seep source) and the second sampling station ETP2 at 127 m from where all the parameters remain nearly constant beyond ETP2. The pH increases from 6.5 to 7.1 (Fig. III-2a), DO from 3.8 to 4.5 mg/l (Fig. III-2e) and SPC from 1112 to 1294 μs/cm (Fig. III-2g). In 2006, the ORP decreases from 218 mV to 173 mV between ETP1 and ETP2 and continued to decrease to 146 at ETP6 (Fig. III-2c), while in 2007 there is a slight increase in ORP after ETP2 before decreasing slightly downstream.

Water samples from LTP Creek show that spatial changes in the pH, ORP, DO and SPC are different from the ETP samples (Fig. III-2b, d, f and h). The pH fluctuates between 7.6 and 8.1. The lowest pH (7.6) is measured for LTP5, while the highest pH (8.1) is measured for LTP1 and LTP4 for 2006 and 2007, respectively (Fig. III-2b). The DO at LTP Creek decreased between LTP1 and LTP2 from 9.7 to 7.8 mg/l (Fig. III-2f) and then increased to 10.4 mg/l at LTP4 before decreasing. In 2007, SPC increases slightly from 906 to 1106 μs/cm between LTP1 and LTP2 and then remained nearly constant beyond (Fig. III-2h). The ORP shows an increasing trend between 185 mV to 242 mV for 2006 and a decreasing trend between 196 and 115 mV (Fig. III-2d) for 2007 between LTP1 and LTP2 after which the change was small.

4.2. Spatial variability of SO_4, Mg, Ca and Al in tailings discharge

Variations in concentrations of SO_4, Mg, Ca, and Al are presented in Table III-1. Concentrations of SO_4 range between 6.4 to 8.6 mM/L, Mg range between 2.5 and 3.7 mM/L, Ca range between 4.5 and 6.0 mM/L, and Al is nearly constant at ~ 0.2 mM/L for 2007 but increases slightly between ETP1 and ETP2 from 0.15 mM/L before fluctuating

slightly downstream. The trends in the downstream variation of SO_4, Ca, and Mg for ETP are shown (Fig. III-3a, c, and e).

. The water samples from the LTP Creek, range in SO_4 concentrations range between 3.4 and 4.0 mM/L (Fig. III-3b), Mg range between 1.9 and 2.2 mM/L, Ca range between 3.3 and 4.4 mM/L, and Al is nearly constant at ~ 0.1 mM/L. Concentrations of SO_4, Ca, and Mg show comparatively smaller increases relative to ETP between LTP1 and LTP2, beyond which the concentrations also remain nearly constant. In general, for all species, ETP samples have relatively higher concentrations compared to LTP samples. The trends in the downstream variation of SO_4, Ca, and Mg for LTP are shown (Fig. III-3b, d, f, and h).

4.3. Spatial variability of HCO_3, DIC, logpCO_2 and $\delta^{13}C_{DIC}$ in tailings discharge

The results of variations in HCO_3, DIC, logpCO_2 and $\delta^{13}C_{DIC}$ are presented in Table III-1. For ETP Creek samples, HCO_3 concentrations are nearly constant while DIC concentrations and log pCO_2 values show an overall decrease downstream. Meanwhile, the $\delta^{13}C_{DIC}$ is enriched downstream from the source. The HCO_3 concentrations range between 2.5 and 3.2 mM C/L, DIC concentrations range between 2.1 mM C/L and 3.3 mM C/L, while logpCO_2 values ranged between -3.0 and -1.3 atm. The $\delta^{13}C_{DIC}$ values range between -8.7‰ and -4.4‰. The trends in the downstream variation of HCO_3, DIC, logpCO_2 and $\delta^{13}C_{DIC}$ for ETP are shown (Fig. III-4a, c, and e).

For LTP Creek samples, HCO_3 concentrations also remain nearly constant between 4.1 and 4.3 mM/L, whereas DIC and logpCO_2 concentrations fluctuate with slight increases downstream, ranging between 3.7 and 4.6 mM C/L for DIC and the

logpCO_2 for LTP samples ranges between 2.2 and 2.7 atm. The $\delta^{13}C_{DIC}$ for the LTP Creek samples varied between -9.2‰ and -11.5‰. Compared to ETP Creek samples, LTP Creek concentrations of HCO_3, DIC and logpCO_2 values are overall higher. On the other hand, the LTP Creek values for $\delta^{13}C_{DIC}$ are more depleted and remain nearly constant compared to the $\delta^{13}C_{DIC}$ values of ETP Creek samples. The trends in the downstream variation of HCO_3, DIC, logpCO_2 and $\delta^{13}C_{DIC}$ for LTP are shown (Fig. III-4b, d, f, and h).

5. Discussion

5.1. DIC and $\delta^{13}C_{DIC}$ evolution in discharge water

DIC at the ETP and LTP tailings piles is produced from the neutralization of H_2SO_4 by carbonate minerals in the tailings. The ETP and LTP are composed of trace amounts of metal sulfides, carbonate minerals, dominantly dolomite with small quantities of calcite and other carbonates (Smith and Schumacher, 1993) that can generate acidity and neutralize carbonates. The production of acid by sulfide minerals and neutralization of carbonates, particularly dolomite is evidenced by the high concentrations of SO_4, Ca, and Mg in the water samples (Table 1) (e.g., Singer and Stumm, 1970). The H_2SO_4 reacts with the dolomite according to equation 4 to release HCO_3, SO_4, Ca, and Mg in the tailings water.

$$H_2SO_4 + MgCa(CO_3)_2 \rightarrow SO_4^{2-} + Mg^{2+} + Ca^{2+} + 2HCO_3^- \quad (4)$$

If HCO_3 is the dominant DIC species produce from the neutralization reaction (Equation 4), the DIC and HCO_3 in the water samples should be correlated. The cross plot for DIC

vs. HCO_3 (Fig. III-6a and b) for the ETP and LTP samples however, do not show any relationship. The lack of a linear relationship between DIC and HCO_3 suggest the presence of significant amounts of DIC species in the form of $CO_{2(aq)}$ in the water samples. The dissolved $CO_{2(aq)}$ is produced in excess, if HCO_3 further reacts with protons according to reverse Equation 2 (Drever, 1997). The excess $CO_{2(aq)}$ that is produced from the HCO_3 dehydration can be lost to the atmosphere as water discharges from the tailings pile. Although Figure III-5c and III-5d show that the ETP samples consistently have higher pCO_2 compared to LTP samples, both tailings piles have relatively higher $logpCO_{2(aq)}$ compared to atmospheric. The dissolved CO_2 could therefore be lost from both sites. However, rate of loss of DIC as $CO_{2(g)}$ from solution depend on the amount of excess $CO_{2(aq)}$ present in the water samples. The fraction of excess $CO_{2(aq)}$ in the water samples at the ETP and LTP Creeks are shown in Table III-1. The percent excess CO_2 in the DIC was estimated according to the relation

$$\%\ excess\ CO_2 = \left(\frac{DIC - HCO_3}{DIC}\right) x100 \qquad (5)$$

Higher excess $CO_{2(aq)}$ at the ETP site means that more DIC loss should occur at ETP compared to LTP site. The downstream decrease in DIC concentrations at the ETP whereby HCO_3 remains nearly constant, support the observation of loss of mainly excess $CO_{2(aq)}$ from the samples. At the LTP, DIC and HCO_3 concentrations remain nearly constant indicating that little excess $CO_{2(aq)}$ is lost from these samples.

The plots of $logpCO_2$ vs. $\delta^{13}C_{DIC}$ (Fig. III-5e and f) show a negative relationship for samples at the ETP Creek described by the least square regression equation: y= -0.34x-4.37; R^2 =0.95 and -0.23x-4.1; R^2=0.89 for 2006 and 2007 samples, respectively. The relationship between $logpCO_2$ vs. $\delta^{13}C_{DIC}$ show that downstream DIC enrichment

depends on the rate of loss of $CO_{2(g)}$ from the discharge. The $\delta^{13}C_{DIC}$ enrichment trend is consistent with observations from previous studies that show the downstream enrichment of $\delta^{13}C_{DIC}$ with decreasing pCO_2 in stream water (e.g., Doctor et al., 2008; Fonyuy and Atekwana, 2008a). No relationship of $logpCO_2$ vs. $\delta^{13}C_{DIC}$ is observed for LTP samples. The relationship between $\delta^{13}C_{DIC}$ vs. Ct/Co (where Co is initial concentration of DIC in water sample at the seep source and Ct is the fraction of DIC remaining as the discharge flows downstream) (Fig. III-5g and h), show a decrease in DIC corresponding to $\delta^{13}C_{DIC}$ enrichment for samples at the ETP. The LTP Creek, samples show no relationship between $\delta^{13}C_{DIC}$ vs. Ct/Co and the DIC remains nearly constant. The relationship between $\delta^{13}C_{DIC}$ vs. Ct/Co and $logpCO_{2(aq)}$ vs. $\delta^{13}C_{DIC}$ show that the change in $\delta^{13}C_{DIC}$ composition in the water during the outgassing of CO_2 depends on the rate of loss (slope of regression) and the concentration of excess $CO_{2(aq)}$ that is present in the water at the source and at any time during flow. At the LTP, where the DIC concentrations and $logpCO_{2(aq)}$ are initially lower compared to samples from the ETP Creek, there is no downstream decrease in DIC and $logpCO_{2(aq)}$ and no corresponding changes downstream in the $\delta^{13}C_{DIC}$ of the samples that remain nearly constant. This means that no excess CO_2 is lost from the DIC at the LTP site.

5.2. Effect of CO_2 outgassing on $\delta^{13}C_{DIC}$

The highest decrease in DIC for ETP Creek occurs between ETP1 and ETP2. This is because the DIC in samples discharged at the source is in greater disequilibrium with atmospheric CO_2 due to significantly higher excess CO_2 and thus $logpCO_2$ relative to atmospheric. For both sampling periods the greatest change in $\delta^{13}C_{DIC}$ (2.1‰ and 2.0‰)

occurs between the first and second sampling sites (ETP1 and ETP2). These are also the sites for which the greatest amount of DIC loss of 0.6 mM C/L and 0.4 mM C/L for 2006 and 2007 respectively. The tailings groundwater discharging at the seep would tend to lose the excess CO_2 more rapidly compared to downstream stations. Meanwhile, the outgassing of $CO_{2(g)}$ between the seep at ETP1 and downstream station ETP6 produced a total shift in $\delta^{13}C_{DIC}$ of 4.3‰ and 3.4‰ for 2006 and 2007 samples, respectively. The total amount of downstream DIC loss at ETP Creek increased to 0.9 mM C/L and 1.1 mM C/L for 2006 and 2007 respectively and so did the enrichment in $\delta^{13}C_{DIC}$ also increase from 2.1 to 4.3‰ and 2.0 to 3.4‰ for 2006 and 2007 respectively. The increase in $\delta^{13}C_{DIC}$ per unit decrease in logpCO_2 given by the slope of the regression line is: 0.23‰ and 0.35‰ (Fig. III-5d) for 2006 and 2007 respectively. This suggest that magnitude of $\delta^{13}C_{DIC}$ enrichment depends on the rate of loss of excess $CO_{2(g)}$ from water. Also the initial amount of excess $CO_{2(aq)}$ (intercept of the regression line) will affect the extent of $\delta^{13}C_{DIC}$ enrichment. The LTP Creek samples, on the other hand, show very little loss in DIC concentrations over the entire downstream segment and comparatively very little shift in the $\delta^{13}C_{DIC}$. Thus higher concentrations of excess $CO_{2(g)}$ loss in water at the ETP Creek leads to greater $\delta^{13}C_{DIC}$ shift compared to the LTP Creek.

The mechanism of excess $CO_{2(aq)}$ loss to atmosphere at the ETP site is kinetic, and leads to a kinetic $\delta^{13}C_{DIC}$ enrichment. There is experimental evidence for the kinetic enrichment of DIC due to loss of $CO_{2(g)}$ from solution. For example, Zhang et al., (1995) reported a kinetic enrichment of 1‰ for $CO_{2(g)}$ outgassing from an acidic solution, Fonyuy and Atekwana (2008a,b) reported a kinetic enrichment of 1‰ to 3‰ in a study on acid mine drainage contaminated stream and Ali and Atekwana (2009) reported

enrichment of 1‰ to 6‰ for the acidification of water samples. Field studies have also reported kinetic enrichment of DIC. For example Atekwana and Fonyuy (2009) reported downstream enrichment of DIC of up to 8‰ in acid mine drainage (AMD) contaminated stream water, Doctor et al., (2008) report downstream DIC enrichment of nearly 4‰ for a headwater stream over a 600 m transect while Michaelis et al. (1985) reported $\delta^{13}C_{DIC}$ enrichment of 5‰, in a study of CO_2 outgassing from a carbonate rich groundwater discharge. The wide range in the kinetic enrichment in $\delta^{13}C_{DIC}$ observed in these studies show that the kinetic enrichment during excess CO_2 outgassing may best be explained by a physical process dependent on the rate and amount of excess CO_2 that is released from the water. The absence of downstream variation in the HCO_3 concentrations and the saturation state of carbonate minerals (Table A-5) in the water samples indicates that there is neither HCO_3 dehydration nor carbonate dissolution occurring at the ETP and LTP sites. This suggest that the fate of the excess $CO_{2(aq)}$ in the water samples is not chemically controlled. The loss of $CO_{2(g)}$ from the water samples at the ETP Creek is therefore a physical process driven only by the difference in the concentration gradient of $CO_{2(aq)}$ across the water/air interface. Thus the factors that influence the $\delta^{13}C_{DIC}$ shifts during excess CO_2 loss from the water can be summarized thus:(1) the initial amount of excess $CO_{2(aq)}$ in the discharge water at the source and (2) the rate and amount of $CO_{2(g)}$ that is being lost to the atmosphere.

6. Conclusion

Groundwater that is discharged from carbonate-rich tailings piles contains high DIC and excess $CO_{2(aq)}$. The loss of the excess CO_2 from discharges is responsible for

isotopic enrichment during downstream flow. The mechanism of $CO_{2(g)}$ loss from the water to the atmosphere is kinetic and the rate and magnitude of the kinetic $\delta^{13}C_{DIC}$ enrichment depends on initial amount of excess $CO_{2(aq)}$ that is present at the source and the amount and rate of $CO_{2(g)}$ loss to the atmosphere. The excess $CO_{2(aq)}$ in the discharge water is lost to the atmosphere due to a difference in the partial pressure ($logpCO_{2(aq)}$) in the water relative to the atmosphere. The amount of excess $CO_{2(g)}$ that is lost is initially high and decreases downstream from the source. The loss of $CO_{2(g)}$ from the water samples is a physical process that results in the downstream kinetic enrichment in $\delta^{13}C_{DIC}$ due to the irreversible nature of the outgassing of excess $CO_{2(g)}$ from the water. The magnitude of the enrichment of $\delta^{13}C_{DIC}$ during the outgassing $CO_{2(g)}$ depends on the initial concentration of excess $CO_{2(g)}$ in the water sample at the source and the amount of $CO_{2(g)}$ that is lost. At the ETP and the LTP Creeks, the total DIC decrease by 0.9 mM C/L and 1.1 mM C/L and a total shift in $\delta^{13}C_{DIC}$ of 4.3‰ and 3.4‰ for 2006 and 2007 respectively. The enrichment in $\delta^{13}C_{DIC}$ per unit decrease in $logpCO_2$ was 0.23‰ and 0.35‰ for initial $logpCO_2$ values of -2.0 and -1.8 atm respectively at the ETP and no significant change in DIC or rate of $\delta^{13}C_{DIC}$ enrichment was measured for LTP creek samples. In general, the water samples at ETP had more excess $CO_{2(g)}$ and showed more shifts in $\delta^{13}C_{DIC}$ compared to LTP Creek samples that showed no change in DIC concentrations and no shifts in $\delta^{13}C_{DIC}$.

Acknowledgements

This work was funded by the US National Science Foundation Award EAR-0510954. Acknowledgment is also made to the National Association of Black Geologist and

Geophysicists for financial support for HA. We thank A. Mukherjee and E. Fonyuy for field help.

References

Ali, H.N. and Atekwana, E.A., 2009. Effect of progressive acidification on stable carbon isotopes of dissolved inorganic carbon in surface waters. Chem. Geol. 260, 102-111.

Atekwana, E.A. and Fonyuy, E.W., 2009. Dissolved inorganic carbon concentrations and stable carbon isotope ratios in streams polluted by variable amounts of acid mine drainage. J. Hydrol. 372, 136-148.

Atekwana, E.A. and Krishnamurthy, R.V., 1998. Seasonal variations of dissolved inorganic carbon and $\delta^{13}C$ of surface waters: application of a modified gas evolution technique. J. Hydrol. 205, 265-278.

Deines, P., 2004. Carbon isotope effects in carbonate systems. Geochim.Cosmochim. Acta 68, 2659-2679.

Doctor, D.H., Kendall, C., Sebestyen, S.D., Shanley, J.B., Ote, N., and Boyer, E.W., 2008. Carbon isotope fractionation of dissolved inorganic carbon (DIC) due to outgassing of carbon dioxide from a headwater stream. Hydrol. Process. 22, 2410-2423

Drever, J.I., 1997. The Geochemistry of Natural Waters: Surface and Groundwater environments. 3rd Ed, Prentice-Hall, Englewood Cliffs, NJ.

Fonyuy, E.W. and Atekwana E.A., 2008a. Effects of acid mine drainage on dissolved inorganic carbon and stable carbon isotopes in receiving streams. Appl. Geochem. 23, 743-764.

Fonyuy, E.W. and Atekwana, A.E., 2008b. Dissolved inorganic carbon evolution and stable carbon isotope fractionation in acid mine drainage impacted streams: insights from a laboratory study. Appl. Geochem. 23, 2634-2648.

Hach Company, 1992. Water Analysis Handbook. Hach Company, Loveland, Co.

Inoue, H., and Sugimura, Y., 1985. Carbon isotopic fractionation during the CO_2 exchange process between air and sea water under equilibrium and kinetic conditions. Geochim. Cosmochim. Acta 49, 2453-2460.

Kramer R.L., 1976. Effects of century old Missouri lead mining operation upon the water quality, sediments and biota of the Flat River Creek: M.S. Thesis, University of Missouri Rolla, 111p.

Michaelis, J., Usdowski, E., and Menschel, G., 1985. Partitioning of C-13 and C-12 on the degassing of CO_2 and the precipitation of calcite - rayleigh-type fractionation and a kinetic-model. Am. J. Sci. 285, 318-327.

Mills, G.A. and Urey, H.C., 1940. The kinetics of isotopic exchange between carbon dioxide, bicarbonate ion, carbonates ion and water. J. Am. Chem. Soc. 62, 1019-1026.

Mook, W.G., Bommerson, J.C. and Staverman, W.H., 1974. Carbon isotope fractionation between dissolved bicarbonate and gaseous carbon dioxide. Earth Planet. Sci. Lett. 22, 169-176.

Singer, P.C., and Stumm, W., 1970. Acidic mine drainage: The rate-determining step. Science 167, 1121-1123.

Smith, B. J., and Schumacher, J. G., 1991. Hydrochemical and sediment data for the old lead belt, Southeastern Missouri-1988-89. U.S. Geol. Surv. Open File Rep. 91-211, 1-98.

Smith, B. J., and Schumacher, J. G., 1993. Surface-water and sediment quality in the old lead belt, Southeastern Missouri-1988-89. U.S. Geol. Surv. Water Resour. Investig. Rep. 93-4012, 1-92.

Usdowski, E., and Hoefs, J., 1990. Kinetic $^{13}C/^{12}C$ and $^{18}O/^{16}O$ effects upon dissolution and outgassing of CO_2 in the system CO_2-H_2O. Chem. Geol. Isotope Geoscience section 80, 109-118.

Wanninkhof, R., 1985. Kinetic fractionation of the carbon isotopes C-13 and C-12 during transfer of CO_2 from air to seawater. Tellus Ser. B-Chem. Phys. Meteorol. 37, 128-135.

Worrall, F and Lancaster, A., 2005. The release of CO_2 from river waters – the contribution of excess CO_2 from groundwater. Biogeochem. 76: 299-317

Zhang, J., Quay, P.D., and Wilbur, D.O., 1995. Carbon-isotope fractionation during gas-water Exchange and dissolution of CO_2. Geochim. Cosmochim. Acta 59, 107-114.

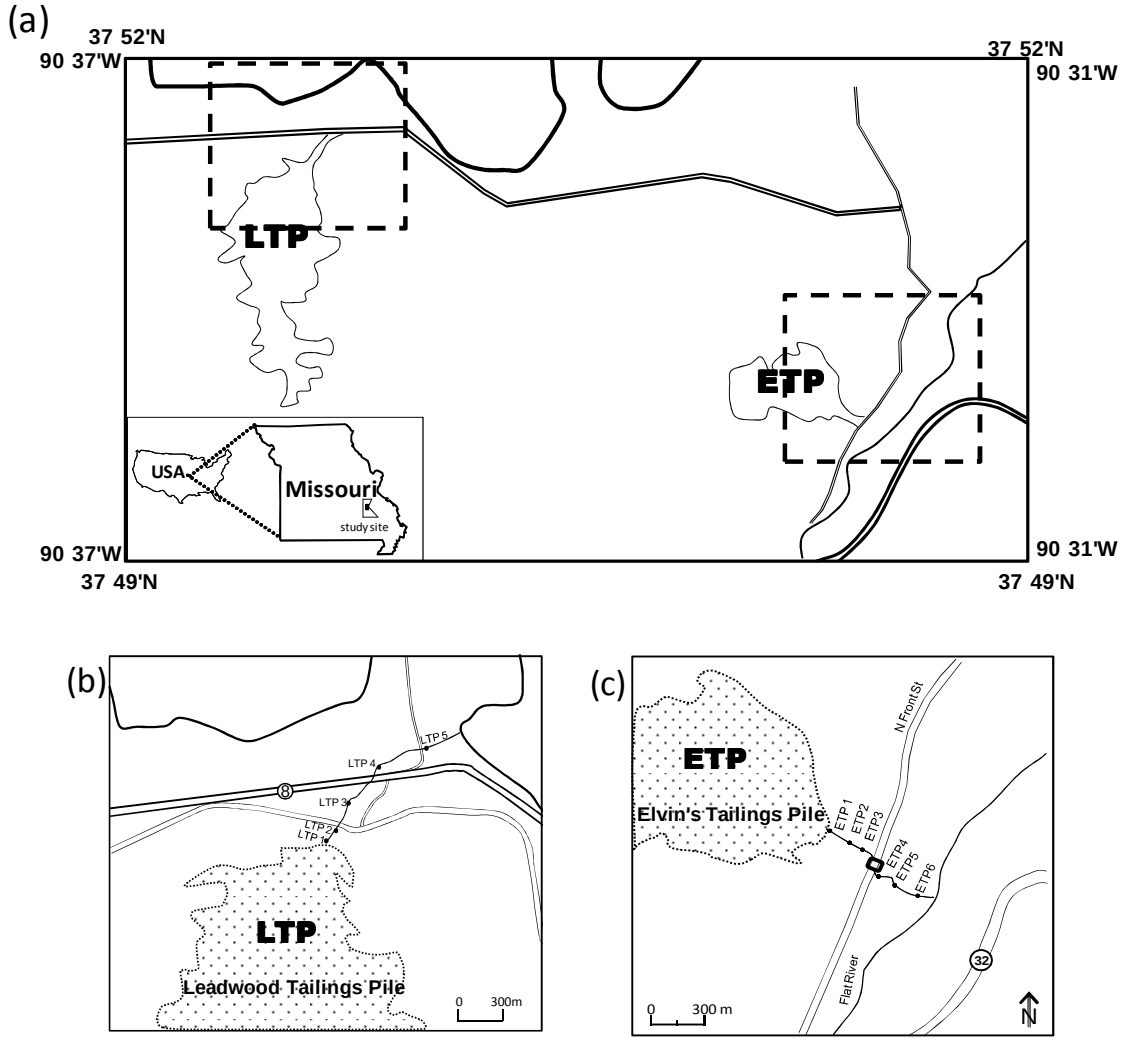

Figure III-1. Map of study site (a) showing locations of the Elvin's Tailings Pile and Leadwood Tailings Pile and (b), (c) show the sampling locations along the Elvin's Tailings Pile discharge and the Leadwood Tailings Pile discharge (LTP Creek). Maps are adapted from Google Earth (2009).

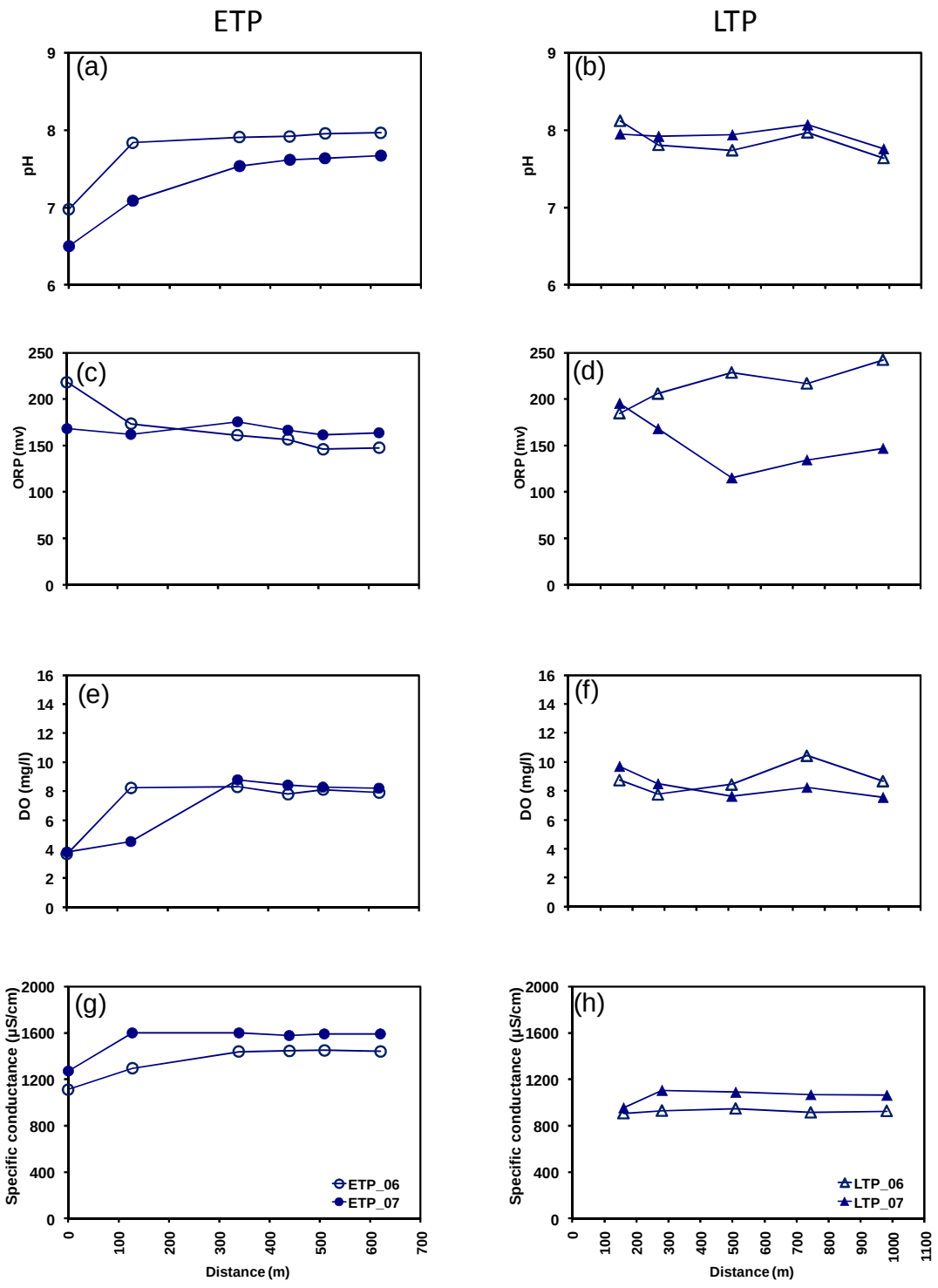

Figure III-2. Plots of spatial variation of pH, ORP, DO and SPC along the Elvin's Tailings Pile discharge Creek and along the Leadwood Tailings Pile discharge (LTP Creek).

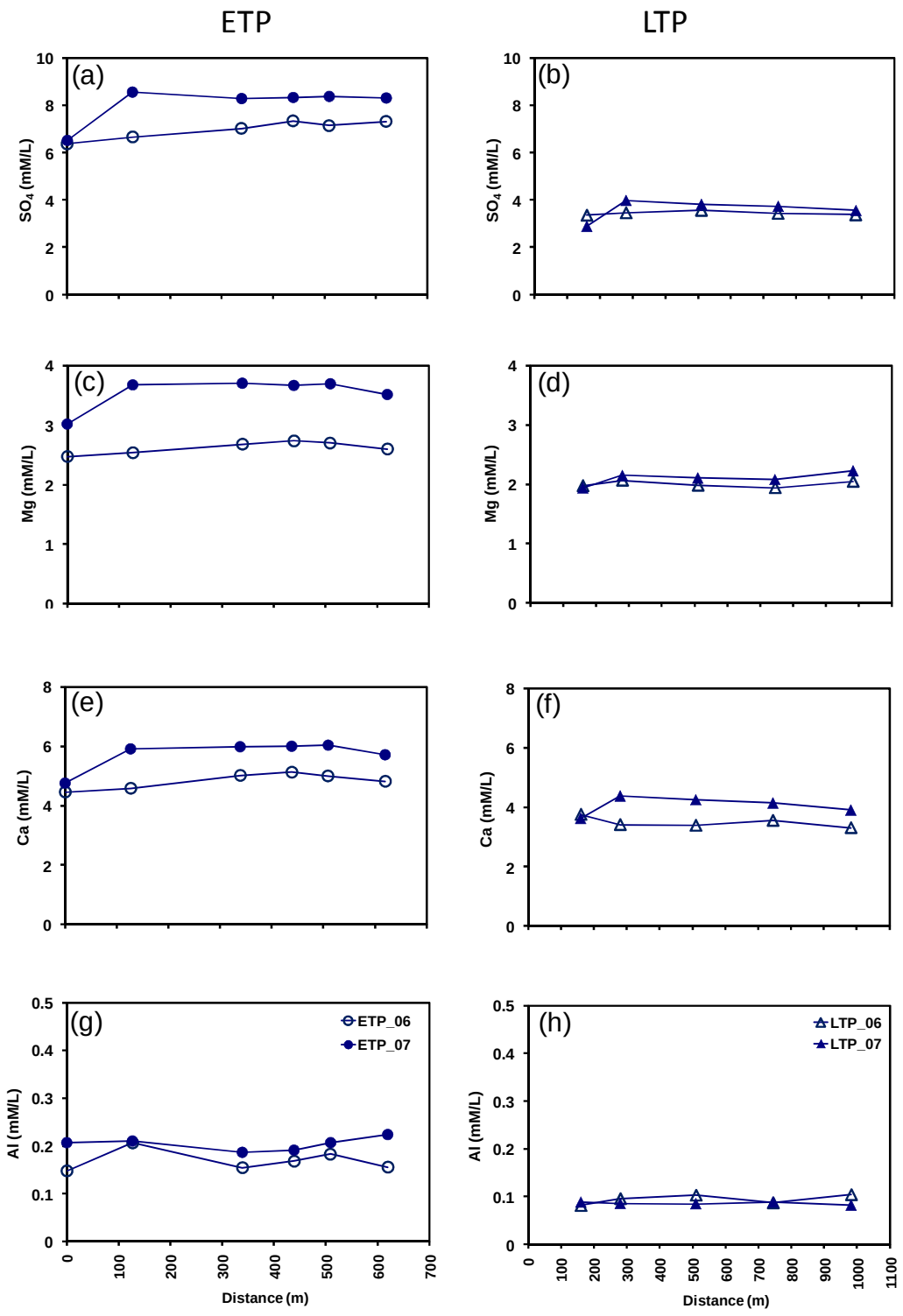

Figure III-3. Plots of spatial distribution of SO_4, Ca, Mg and Al along the Elvin's Tailings Pile and the Leadwood Tailings Pile discharge Creeks.

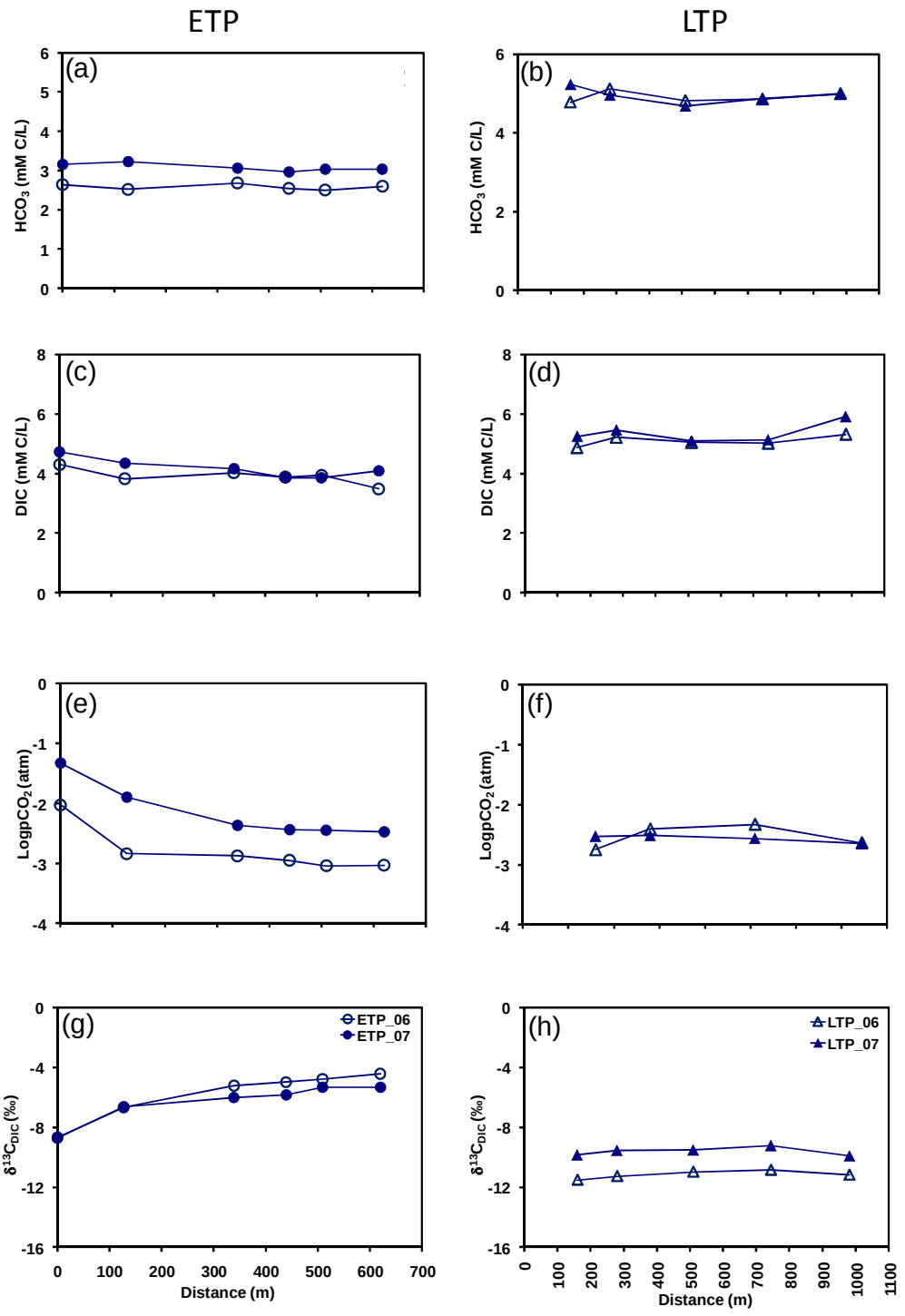

Figure III-4: Plots of spatial variation of HCO_3, DIC, $logpCO_2$ and $\delta^{13}C_{DIC}$ along the Elvin's Tailings Pile the Leadwood Tailings Pile discharge.

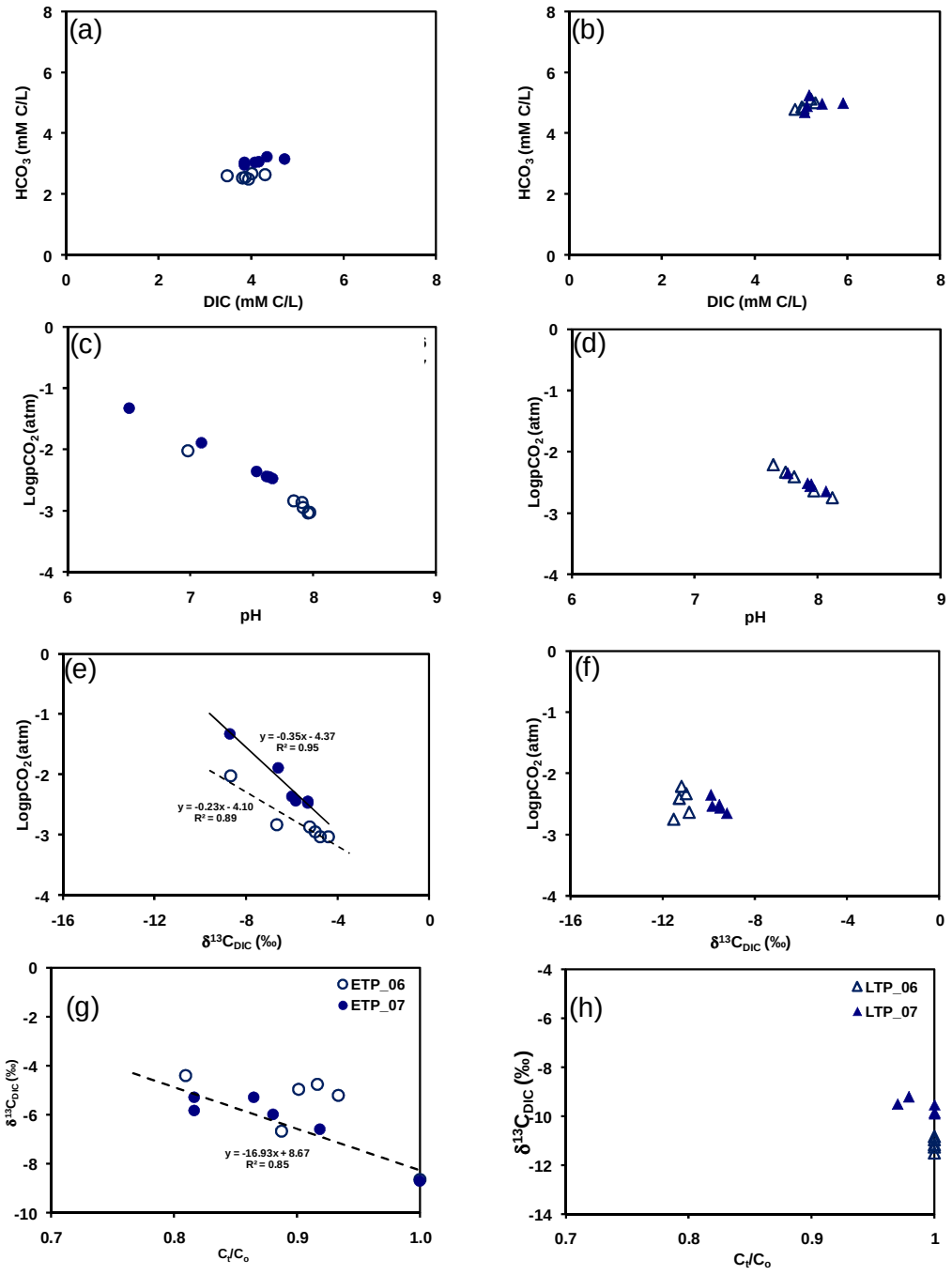

Figure III-5: Cross plots of HCO_3 vs. DIC, $logpCO_2$ vs. pH and $logpCO_2$ vs. $\delta^{13}C_{DIC}$ and $\delta^{13}C_{DIC}$ vs. Ct/Co along the Elvin's Tailings Pile (ETP Creek) and the Leadwood Tailings Pile discharge (LTP Creek). (Where Co is the DIC concentration at the source and Ct is the DIC concentration at station t downstream) .

Table III-1: Results of the physical, chemical, and stable isotope analyses for discharge water from the Elvin's Tailings Pile and Leadwood Tailings Pile, St. Francoise County, SE Missouri, USA

Sample ID	Distance (m)	Temp. (^{o}C)	SPC (µs/cm)	DO (mg/L)	pH	ORP (mV)	HCO3 (mM/L)	DIC (mMC/L)	$\delta^{13}C_{DIC}$ (‰)	Cl (mM/L)	SO_4 (mM/L)	Al (mM/L)	Ca (mM/L)	K (mM/L)	Mg (mM/L)	Na (mM/L)	eCO_2 %	$logpCO_2$ (atm)
2006																		
ETP CreeK																		
ETP 1	0.0	18.9	1112	3.7	7.0	218	2.6	4.3	-8.7	0.3	6.4	0.2	4.5	0.2	2.5	0.2	39	-20
ETP 2	127	25.7	1294	8.2	7.8	173	2.5	3.8	-6.7	0.3	6.7	0.2	4.6	0.2	2.5	0.2	34	-2.8
ETP 3	339	27.8	1440	8.3	7.9	161	2.7	4.0	-5.2	0.3	7.0	0.2	5.0	0.2	2.7	0.2	33	-2.9
ETP 4	439	27.7	1446	7.8	7.9	157	2.5	3.9	-5.0	0.3	7.3	0.2	6.0	0.2	3.2	0.3	35	-3.0
ETP 5	509	27.7	1450	8.1	8.0	146	2.5	3.9	-4.8	0.3	7.1	0.2	5.0	0.2	2.7	0.2	37	-3.0
ETP 6	620	27.4	1441	7.9	8.0	148	2.6	3.5	-4.4	0.3	7.3	0.2	4.8	0.2	2.6	0.2	25	-3.0
LTP Creek																		
LTP 1	0	21.1	906	8.8	8.1	185	4.8	4.9	-11.5	0.1	3.4	0.1	3.7	0.1	2.0	0.2	2	-2.7
LTP 2	120	20.6	928	7.8	7.8	206	4.1	5.2	-11.3	0.2	3.5	0.1	3.4	0.1	2.1	0.2	2	-2.4
LTP 3	350	20.8	947	8.5	7.7	229	4.8	5.1	-11.0	0.2	3.6	0.1	3.4	0.1	2.0	0.2	5	-2.3
LTP 4	585	21.1	913	10.4	8.0	217	4.9	5.0	-10.8	0.2	3.4	0.1	3.5	0.1	1.9	0.2	3	-2.6
LTP 5	822	20.9	926	8.7	7.6	242	5.0	5.3	-11.2	0.3	3.4	0.1	3.3	0.1	2.0	0.3	6	-2.2
2007																		
ETP CreeK																		
ETP 1	0	15.2	1273	3.8	6.5	168	3.2	4.7	-8.7	0.3	6.5	0.1	4.8	0.2	3.0	0.4	33	-1.3
ETP 2	127	18.1	1600	4.5	7.1	162	3.2	4.3	-6.6	0.3	8.6	0.2	5.9	0.2	3.7	0.3	26	-1.9
ETP 3	339	20.6	1600	8.8	7.5	176	3.1	4.2	-6.0	0.3	8.3	0.2	6.0	0.2	3.7	0.3	27	-2.4
ETP 4	439	22.3	1580	8.4	7.6	167	3.0	3.9	-5.8	0.3	8.3	0.2	6.0	0.2	3.7	0.3	23	-2.4
ETP 5	509	22.5	1592	8.3	7.6	162	3.0	3.9	-5.3	0.3	8.4	0.2	6.0	0.2	3.7	0.3	21	-2.5
ETP 6	620	22.4	1593	8.2	7.7	164	3.0	4.1	-5.3	0.3	8.3	0.2	5.7	0.2	3.5	0.3	26	-2.3
LTP Creek																		
LTP 1	0	19.9	955	9.7	8.0	196	5.2	5.2	-9.8	0.1	2.9	0.1	3.6	0.1	1.9	0.3	0	-2.5
LTP 2	120	22.1	1106	8.5	7.9	168	5.0	5.5	-9.5	0.2	4.0	0.1	4.4	0.1	2.2	0.3	9	-2.5
LTP 3	350	23.0	1089	7.6	7.9	1150	4.7	5.1	-9.5	0.2	3.8	0.1	4.2	0.1	2.1	0.3	8	-2.6
LTP 4	585	24.7	1068	8.2	8.1	135	4.9	5.1	-9.2	0.2	3.7	0.1	4.1	0.1	2.1	0.3	5	-2.7
LTP 5	822	22.6	1063	7.6	7.8	147	5.0	5.9	-9.9	0.2	3.6	0.1	3.9	0.1	2.2	0.3	6	-2.4

CHAPTER V

CONCLUSION

This work presents three separate but related research projects on the carbon cycling. It focuses on the use of stable isotopes of carbon, hydrogen and oxygen to understand processes and mechanisms that transform dissolved inorganic carbon during evolution in ground and surface waters impacted by acidification and/or neutralization. The research objective was to conduct field and laboratory experiments to investigate:

1) the DIC speciation and carbon isotopic shifts during progressive acidification

2) DIC production and fate in groundwater and soil water affected by acidification and neutralization

3) DIC and $\delta^{13}C_{DIC}$ evolution in discharged from neutral mine tailings piles

The following products result from the experiments conducted in this study:

1) A model of $\delta^{13}C_{DIC}$ and $\delta^{13}C_{CO2}$ evolution of surface waters during acidification.

2) Information on DIC partitioning and $\delta^{13}C_{DIC}$ and $\delta^{13}C_{CO2}$ shifts in groundwater and soil water during acid neutralization of sulfuric acid.

3) Information on DIC evolution and $\delta^{13}C_{DIC}$ shifts during downstream evolution of neutral mine discharged from mine tailings piles.

1. A model of $\delta^{13}C_{DIC}$ and $\delta^{13}C_{CO2}$ evolution of surface waters during acidification

The first experiment involved the progressive acidification of natural and artificial water samples to study the effects of acidification on carbon isotope shifts. From the results of the laboratory experiments, the $\delta^{13}C_{DIC}$ measured for samples undergoing acidification show variable enrichment or depletion. The $\delta^{13}C_{DIC}$ was enriched during the HCO_3^- dehydration phase and was depleted after HCO_3^- was exhausted. The trends in enrichment and depletion of the $\delta^{13}C_{DIC}$ mimicked those of the pCO_2. However, the rate of isotopic enrichment and depletion in each acidified sample was different and depended on the initial HCO_3^-:$CO_{2(aq)}$ ratio. The concentration of $CO_{2(aq)}$ in each sample controls the extent of isotopic exchange of carbon between the un-dehydrated HCO_3^- and the $CO_{2(aq)}$. The $\delta^{13}C$ of $_{CO2}$ captured from the acidified samples showed a steep enrichment trend with progressive acidification consistent with continous enrichment from addition of carbon-13. The $\delta^{13}C_{CO2}$ evolved was identical to the $\delta^{13}C_{DIC}$ of samples at the point where all HCO_3^- was exhausted. Higher concentrations of $CO_{2(aq)}$ results in greater exchange of carbon between HCO_3^- and $CO_{2(aq)}$ which minimizes the enrichment in $\delta^{13}C_{DIC}$ from HCO_3^--$CO_{2(g)}$ fractionation during progressive acidification. The depletion of the $\delta^{13}C_{DIC}$ after HCO_3^- was exhausted in the samples was governed by isotopic fractionation controlled by the solubilities of ^{13}C vs.^{12}C during water-gas exchange. The slightly more soluble and reactive ^{12}C is retained in solution causing the observed ^{13}C depletion.

Whether enrichments or depletion in the $\delta^{13}C_{DIC}$ are measured for field samples will depend on the extent to which the acidification process occurred before sampling. If samples are collected during the HCO_3^- dehydration phase, enrichment in the $\delta^{13}C_{DIC}$ will

be observed, the magnitude of which will depend on the extent of HCO_3^- dehydration. Alternatively, if samples are collected after all HCO_3^- is dehydrated, a depletion in the $\delta^{13}C_{DIC}$ will be measured, the magnitude of which will also dependent on the progress of acidification. The DIC speciation and $\delta^{13}C$ shifts is important for studies involving carbon cycling in acid mine drainage contamination or acidic input from acid rains that cause highly acidic solutions.

2. Information on DIC partitioning and stable isotope fractionation $\delta^{13}C$ groundwater and soil water in a tailings

Acidification and neutralization are the dominant controls of the chemical and carbon isotope evolution in a metal sulfide-rich and carbonate-rich tailings pile. The results of this study show that acid neutralization produces "leachate" with relatively high concentrations of DIC, SO_4 and Ca+Mg, and enriched $\delta^{13}C_{DIC}$. The DIC in samples from the vadose zone is characterized by high $CO_{2(aq)}$ relative to HCO_3. Additional neutralization of protons by HCO_3 and degassing of CO_2 create high amounts of CO_2 in the vadose zone, evident in the enriched $\delta^{13}C_{CO2}$ and clearly distinguishable from lighter $\delta^{13}C_{CO2}$ in a background soil zone. This CO_2 is in part responsible for the carbonate evolution of the groundwater. DIC in the groundwater is characterized by higher HCO_3 concentrations relative to $CO_{2(aq)}$. In addition, $\delta^{13}C_{DIC}$ modeling indicates that besides mixing or dilution of leachate with infiltration and lateral groundwater recharge, the carbonate evolution is regulated by the CO_2 in the vadose zone.

These results are important for interpreting DIC and stable carbon isotope evolution of groundwater. We provide chemical and isotopic evidence that suggests that in natural

and anthropogenic settings where sulfuric acid production by metal sulfides and neutralization by carbonates occur, the carbonate evolution of shallow groundwater is not described by the classical model ascribed to soil zone $CO_{2(g)}$.

3. Information on DIC evolution and $\delta^{13}C_{DIC}$ shifts during downstream evolution of neutral mine discharged from mine tailings piles.

The results of this study show that neutral mine discharge from carbonate-rich tailings piles contains high DIC and excess $CO_{2(aq)}$. The loss of the excess CO_2 from discharges is responsible for isotopic enrichment during downstream flow. The mechanism of $CO_{2(g)}$ loss from the water to the atmosphere is kinetic and the rate and magnitude of the kinetic $\delta^{13}C_{DIC}$ enrichment depends on initial amount of excess $CO_{2(aq)}$ that is present at the source and the amount and rate of $CO_{2(g)}$ loss to the atmosphere. The excess $CO_{2(aq)}$ in the discharge water is lost to the atmosphere due to a difference in the partial pressure ($\log pCO_{2(aq)}$) in the water relative to the atmosphere. The amount of excess $CO_{2(g)}$ that is lost is initially high and decreases downstream from the source. The loss of $CO_{2(g)}$ from the water samples is a physical process that results in the downstream kinetic enrichment in $\delta^{13}C_{DIC}$ due to the irreversible nature of the outgassing of excess $CO_{2(g)}$ from the water. The magnitude of the enrichment of $\delta^{13}C_{DIC}$ during the outgassing $CO_{2(g)}$ depends on the initial concentration of excess $CO_{2(g)}$ in the water sample at the source and the amount of $CO_{2(g)}$ that is lost.

4. Suggestion and recommendations

Investigations of dissolve inorganic carbon evolution in surface and groundwater offer important insights into carbon evolution and the use of stable isotopes in the study

of carbon cycling in environments impacted by neutral mine drainage. Field experiment to quantify the amount of CO_2 that is loss from tailings environment from contributions from acid neutralization to the atmosphere are important in assessing the overall effect on local carbon budgets.

In order to adequately assess the effects of acidification on the stable carbon isotopes of DIC in surface waters, time series measurements may be necessary to capture the progressive changes. When spatial and time series measurements are made, DIC species and the $\delta^{13}C_{DIC}$ should be measured along with routine physical and chemical parameters, as this would provide adequate input to model the process of acidification and its effect on stable carbon isotopes.

Further field investigations on (1) high resolution spatial and temporal sampling of soil, groundwater, surface water samples and sediments for geochemical parameters DIC, DOC, stable isotope analysis of surface discharge from the tailings piles and (2) diel variations of neutral mine discharge are needed to provide data that can capture detailed stable isotope changes and DIC variations in field settings. For adequate characterization of mechanisms and processes affecting the inorganic carbon evolution in water impacted by neutral mine drainage The data will provide information to fill knowledge gaps in (1) depth and spatial evolution of DIC and $\delta^{13}C_{DIC}$ in carbonate rich tailings environment and (2) the impact of biological activities and temperature changes on DIC evolution in surface discharge from neutral mine drainage

Bibliography

Affek, H.P., Ronen, D., Yakir, D., 1998. Production of CO_2 in the capillary fringe of a deep phreatic aquifer. Water Resources Research 34, 989-996.

Andrews, J. A., Schlesinger, W.H., 2001. Soil CO_2 dynamics, acidification, and chemical weathering in a temperate forest with experimental CO_2 enrichment. Global Biogeochemical Cycles 15, 149-162.

Falkowski, P., Scholes, R.J., Boyle, E., et al., 2000. The global carbon cycle: A test of our knowledge of Earth as a system. Science 290, 291-296.

House, J.I., Prentice, I.C., Ramankutty, N., et al., 2003. Reconciling apparent inconsistencies in estimates of terrestrial CO_2 sources and sinks. Tellus 55B, 345-363.

Karim, A., Veizer, J. 2000. Weathering processes in the Indus River Basin: implications from riverine C, S, O, and Sr isotopes. Chemical Geology 170, 153-177.

Schimel, D.S., House, J.I., Hibbard, K.A., et al., 2001. Recent patterns and mechanisms of carbon exchange by terrestrial ecosystems. Nature 414, 169-172.

Takahashi, T., 2004. The fate of industrial carbon dioxide. Science 305, 352-353

Telmer, K., Veizer, J., 1999. Carbon fluxes, pCO_2, and substrate weathering in a large northern river basin, Canada: C- isotope perspectives. Chemical Geology 159, 61-86.

Webb, J.A., Sasowsky, I.D., 1994. The interaction of acid mine drainage with a carbonate terrain: evidence from the Obey River, north-central Tennessee. Journal of Hydrology 161, 327-346.

Wicks, C.M., Groves, C.G., 1993. Acidic mine drainage in carbonate terrains: Geochemical processes and rates of calcite dissolution. Journal of Hydrology 146, 13

APPPENDICES

Table A-1: Results of physical, chemical, and isotopic analyses of closed and open acidification and for unacidified samples of tap water

Date	Time	Sample	Temp (^{o}C)	SPC (us/cm3)	DO (mg/L)	pH	ORP	H_2SO_4 (ml)	DIC (mMC/L)	Alk (mg/L)	$\delta^{13}C_{DIC}$ (‰)	CO_2 (mMC/L)	$\delta^{13}C_{CO2}$ (‰)
Tap water-Unacidified													
4/9/06	10:30	TW1-1	17.6	496	4.64	7.4	467	0	4.6	234	-12.5	-	-
4/12/06	22:30	TW1-2	23.2	483	5.57	7.6	531	0	4.4	232	-11.6	-	-
4/15/06	11:30	TW1-3	24.4	495	5.34	8.0	540	0	4.3	231	-11.0	-	-
4/19/06	9:30	TW1-4	24.2	487	5.9	8.1	456	0	4.4	222	-10.6	-	-
4/22/06	21:00	TW1-5	24.2	485	5.49	8.2	389	0	4.3	228	-9.8	-	-
4/26/06	10:30	TW1-6	23.5	477	6.13	8.3	257	0	4.0	222	-9.5	-	-
4/29/06	8:00	TW1-7	22.6	456	6.95	8.3	259	0	4.4	224	-9.0	-	-
5/5/06	12:00	TW1-8	22.9	434	5.83	8.1	281	0	3.8	199	-8.5	-	-
5/8/06	8:45	TW1-9	25.0	441	6.21	8.1	214	0	3.7	192	-7.9	-	-
5/13/06	10:45	TW1-10	24.9	426	5.75	8.1	213	0	3.6	185	-7.3	-	-
5/16/06	16:00	TW1-11	24.2	414	5.45	8.1	243	0	3.6	169	-6.8	-	-
5/19/06	10:30	TW1-12	25.3	418	5.61	8.0	263	0	3.7	167	-6.4	-	-
Tap water-Unacidified													
4/9/06	11:00	TW2-1	16.1	490	4.88	7.4	532	0	3.9	236	-12.6	-	-
4/12/06	23:00	TW2-2	23.2	484	5.58	7.7	586	0	4.4	230	-11.5	-	-
4/15/06	12:00	TW2-3	24.4	497	5.14	8.0	557	0	4.3	230	-10.9	-	-
4/19/06	10:00	TW2-4	24.3	491	5.47	8.2	508	0	4.5	232	-10.2	-	-
4/22/06	21:00	TW2-5	24.0	476	5.47	8.1	466	0	4.1	223	-9.6	-	-
4/26/06	11:00	TW2-6	23.4	453	5.9	8.1	395	0	4.2	211	-9.0	-	-
4/29/06	8:30	TW2-7	22.4	433	6.48	8.1	485	0	4.2	208	-8.5	-	-
5/5/06	12:10	TW2-8	22.9	417	5.44	8.2	346	0	3.4	195	-8.3	-	-
5/8/06	9:00	TW2-9	25.0	427	5.27	8.1	211	0	3.6	183	-7.1	-	-
5/13/06	11:20	TW2-10	24.8	415	5.87	8.2	202	0	3.5	182	-6.6	-	-

Date	Time	Sample	Temp (^{o}C)	SPC (us/cm3)	DO (mg/L)	pH	ORP	H_2SO_4 (ml)	DIC (mMC/L)	Alk (mg/L)	$\delta^{13}C_{DIC}$ (‰)	CO_2 (mMC/L)	$\delta^{13}C_{CO2}$ (‰)
5/16/06	16:40	TW2-11	24.3	404	5.44	8.1	237	0	3.5	176	-6.1	-	-
5/19/06	10:45	TW2-12	25.3	410	5.58	8.2	247	0	3.7	169	-5.8	-	-
Tap water -Closed Acidification													
7/1/06	11:00	ATW1-1	22.9	486	6.37	7.3	605	0	4.6	230	-12.2	0.0	-19.6
7/1/06	1:30	ATW1-2	22.4	499	4.63	7.0	636	0.3	4.4	205	-11.8	0.1	-18.2
7/1/06	12:30	ATW1-3	22.4	505	3.07	6.8	653	0.3	3.9	168	-11.2	0.2	-17.0
7/1/06	14:10	ATW1-4	22.9	512	2.64	6.6	656	0.3	3.4	137	-10.6	0.3	-15.0
7/1/06	15:45	ATW1-5	22.9	513	1.78	6.6	638	0.3	2.7	106	-9.1	0.3	-13.3
7/1/06	17:30	ATW1-6	23.1	525	1.7	6.4	342	0.3	2.4	78	-8.7	0.2	-13.3
7/1/06	22:45	ATW1-7	23.2	533	3.06	6.2	309	0.3	1.5	39	-7.5	0.3	-11.1
7/1/06	0:05	ATW1-8	23.2	552	5.21	5.8	291	0.3	1.3	17	-7.3	0.3	-10.0
7/2/06	10:30	ATW1-9	22.4	589	4.77	3.7	457	0.2	0.9	0	-8.0	0.1	-7.2
7/2/06	13:00	ATW1-10	22.6	675	4.73	3.3	459	0.1	0.5	0	-8.2	0.2	-7.2
7/2/06	13:45	ATW1-11	22.7	776	2.65	3.1	456	0.1	0.3	0	-8.4	0.2	-8.1
7/2/06	16:30	ATW1-12	22.3	920	3.78	2.9	470	0.2	0.1	0	-8.8	0.1	-8.4
7/2/06	19:30	ATW1-13	22.4	1178	2.67	2.7	468	0.3	0.0	0	-9.3	0.0	-9.2
Tap water- Open Acidification													
4/9/06	20:30	ATW2-1	21.4	463	3.7	7.1	602	0	4.9	231	-12.4	-	-
4/9/06	21:00	ATW2-2	21.6	475	4.5	6.5	661	0.5	4.8	187	-12.1	-	-
4/9/06	21:15	ATW2-3	21.7	484	5.3	6.1	692	0.5	3.9	145	-11.9	-	-
4/9/06	21:45	ATW2-4	21.8	498	6.1	5.8	711	0.5	4.1	96	-11.7	-	-
4/9/06	22:00	ATW2-5	21.9	507	6.8	5.6	724	0.3	3.5	69	-12.0	-	-
4/9/06	22:15	ATW2-6	22.0	515	6.7	5.4	676	0.3	3.5	40	-11.4	-	-
4/9/06	22:45	ATW2-7	22.1	527	7.1	4.6	754	0.3	3.1	8	-11.5	-	-
4/9/06	23:05	ATW2-8	22.2	683	6.8	3.1	758	0.3	2.6	0	-11.8	-	-
4/9/06	23:20	ATW2-9	22.2	868	7.1	2.8	794	0.3	2.0	0	-11.9	-	-
4/9/06	23:45	ATW2-10	22.2	1082	7	2.6	810	0.3	1.3	0	-12.1	-	-

Table A-2: Results of chemical analysis of closed and open acidification and for unacidified samples of tap water, groundwater, AMD spring and $NaHCO_3$ solution

Sample ID	Fl	Cl	SO_4	Na	K	Mg	Ca
	mg/L	mg/L	mg/L	mg/L	mg/L	mg/L	mg/L
Tap water-Unacidified							
TW1-1	1.1	3.6	31.8	3.5	0.7	33.3	55.4
TW1-2	1.1	3.7	31.4	3.5	0.6	33.5	57.1
TW1-3	0.7	-	31.5	3.6	0.6	33.3	56.8
TW1-4	1.1	3.7	31.6	3.6	0.6	33.5	57.1
TW1-5	1.1	3.7	31.1	3.7	0.6	33.9	57.9
TW1-6	0.9	3.7	31.8	3.7	0.6	33.8	57.4
TW1-7	1.1	3.8	31.6	3.7	0.5	33.7	53.9
TW1-8	1.0	3.8	32.1	3.7	0.6	33.6	45.9
TW1-9	1.0	3.8	31.9	3.7	0.5	33.5	42.3
TW1-10	0.9	3.8	31.7	3.7	0.5	33.6	39.6
TW1-11	0.9	3.8	31.8	3.7	0.6	34.5	37.6
TW1-12	0.9	3.8	31.7	3.7	0.5	35.4	37.3
Tap water-Unacidified							
TW2-1	-	-	32.8	5.6	3.4	44.4	57.6
TW2-2	1.1	3.8	31.8	3.6	0.5	33.2	59.4
TW2-3	1.1	3.7	31.7	3.7	0.5	33.1	56.7
TW2-4	1.1	3.7	31.8	3.6	0.5	33.6	57.3
TW2-5	1.0	5.6	31.9	3.7	0.8	50.3	67.8
TW2-6	1.1	3.8	32.0	3.7	0.5	33.2	42.8
TW2-7	1.0	3.7	32.2	3.7	0.5	33.7	40.5
TW2-8	1.1	3.8	32.2	3.7	0.5	33.3	40.4
TW2-9	0.9	3.8	32.5	3.7	0.5	33.3	37.2
TW2-10	0.9	3.8	32.1	3.7	0.5	33.3	35.2
TW2-11	0.9	3.8	31.6	3.7	0.5	33.4	33.7
TW2-12	0.9	4.1	32.5	3.8	0.5	33.2	32.4
Tap water-Closed Acidification							
ATW1-1	1.1	3.4	34.9	3.2	-	34.1	59.6
ATW1-2	1.2	3.3	64.2	3.2	-	34.7	61.0
ATW1-3	1.1	3.6	102.1	3.3	-	35.4	61.9
ATW1-4	1.2	3.4	126.9	3.2	-	35.1	62.1
ATW1-5	1.1	3.4	156.3	3.2	-	34.9	61.2
ATW1-6	0.9	3.4	185.5	3.2	-	34.8	61.1
ATW1-7	0.9	3.4	212.4	3.2	-	35.0	60.8
ATW1-8	1.1	3.6	259.2	3.2	-	35.2	61.0
ATW1-9	1.1	3.4	274.4	3.2	-	35.7	62.3
ATW1-10	1.2	3.6	288.8	3.2	-	35.9	62.4
ATW1-11	1.1	3.5	312.0	3.2	-	35.8	62.3

Sample ID	Fl	Cl	SO_4	Na	K	Mg	Ca
ATW1-12	1.1	3.5	330.4	3.3	-	36.4	62.7
ATW1-13	1.0	3.4	353.6	3.2	-	35.0	60.9
Tap water-Open Acidification							
ATW2-1	1.3	3.6	28.2	3.4	-	33.5	58.8
ATW2-2	1.2	3.5	63.0	3.4	-	33.7	58.8
ATW2-3	1.2	3.4	105.8	3.4	-	33.9	59.6
ATW2-4	1.2	3.6	156.9	3.4	-	34.0	59.2
ATW2-5	1.2	3.5	186.1	3.4	-	34.4	59.3
ATW2-6	1.1	3.6	218.0	3.5	-	34.5	59.4
ATW2-7	1.0	3.6	246.4	3.4	-	34.0	58.6
ATW2-8	1.0	3.5	274.1	3.5	-	34.8	60.6
ATW2-9	1.0	4.4	316.6	3.4	-	35.1	61.4
ATW2-10	0.9	3.5	329.1	3.5	-	34.8	60.3
Groundwater-Unacidified							
FTP1-1	0.5	1.8	382.5	0.8	10.5	56.7	136.7
FTP1-2	0.6	1.7	381.4	0.8	10.9	57.3	138.4
FTP1-3	0.5	1.8	386.0	0.8	10.8	57.3	137.1
FTP1-4	0.7	1.8	386.9	0.8	10.9	57.3	135.1
FTP1-5	0.5	1.8	386.3	0.8	10.6	56.9	133.6
FTP1-6	0.6	1.8	382.8	0.8	10.8	57.3	132.8
FTP1-7	0.5	1.8	385.9	0.8	10.8	57.5	131.4
FTP1-8	0.7	1.8	387.7	0.8	10.8	57.2	129.0
FTP1-9	0.6	1.8	388.3	0.8	10.8	56.9	127.8
FTP1-10	0.5	1.8	382.2	0.8	10.9	56.9	125.3
FTP1-11	0.5	1.8	381.2	0.8	10.8	56.7	123.1
Groundwater-Unacidified							
FTP2-1	0.7	2.8	380.7	0.7	11.0	55.9	135.0
FTP2-2	0.6	1.8	383.7	0.8	11.2	56.3	136.4
FTP2-3	0.5	1.8	382.9	0.8	10.9	56.6	136.6
FTP2-4	0.7	1.8	380.6	0.8	11.1	55.3	131.8
FTP2-5	0.5	1.8	380.0	0.8	10.8	55.4	130.9
FTP2-6	0.7	1.8	380.9	0.8	10.8	56.7	131.6
FTP2-7	0.6	1.8	384.3	0.8	10.7	56.0	128.3
FTP2-8	0.6	1.7	360.0	0.8	10.5	54.0	122.1
FTP2-9	0.6	1.7	365.2	0.7	10.4	53.1	118.9
FTP2-10	0.7	2.0	430.9	0.9	12.3	62.6	140.2
FTP2-11	0.4	1.4	282.9	0.6	8.2	43.1	94.3
Groundwater-Closed acidification							
AFTP1-1	0.8	2.7	395.8	0.7	9.8	57.0	138.8
AFTP1-2	0.8	1.7	417.1	0.7	9.6	57.4	141.2
AFTP1-3	0.8	1.7	439.3	0.7	9.8	57.6	140.6
AFTP1-4	0.8	1.7	463.7	0.7	9.8	58.2	140.9

Sample ID	Fl	Cl	SO_4	Na	K	Mg	Ca
AFTP1-5	0.8	1.7	486.1	0.7	9.7	57.8	140.5
AFTP1-6	0.8	1.7	518.0	0.7	9.8	57.9	140.4
AFTP1-7	0.8	1.7	529.3	0.7	9.7	57.6	139.4
AFTP1-8	0.8	1.7	542.7	0.7	9.6	57.7	139.0
AFTP1-9	0.8	1.7	557.1	0.7	9.7	57.9	140.0
AFTP1-10	-	-	570.2	-	-	-	-
AFTP1-11	0.7	1.7	586.8	0.7	9.7	58.1	139.0
AFTP1-12	0.7	1.7	612.4	0.7	9.7	57.8	138.7
AFTP1-13	0.7	1.7	643.4	0.7	9.5	57.8	138.9
AFTP1-14	0.8	1.7	683.2	0.7	9.7	57.5	138.1
Groundwater Open acidification							
AFTP2-1	0.9	2.9	393.6	0.7	10.4	56.6	141.1
AFTP2-2	0.9	1.8	413.6	0.7	10.5	57.1	142.6
AFTP2-3	0.7	1.7	428.6	0.7	10.4	56.9	142.3
AFTP2-4	0.8	1.7	451.2	0.8	10.4	57.0	141.8
AFTP2-5	0.9	1.7	470.7	0.7	10.5	57.1	142.4
AFTP2-6	0.7	1.9	492.6	0.7	10.3	57.0	142.6
AFTP2-7	0.8	1.7	512.8	0.7	10.3	57.2	142.6
AFTP2-8	0.8	1.6	531.8	0.7	10.4	56.9	142.1
AFTP2-9	0.7	1.8	542.6	0.7	10.2	56.6	141.5
AFTP2-10	0.5	1.4	551.8	0.7	10.5	56.9	142.8
AFTP2-11	-	1.8	559.9	-	-	-	-
AFTP2-12	0.5	1.7	578.4	0.8	10.4	57.4	146.5
AFTP2-13	0.6	1.8	592.9	0.7	10.2	57.1	149.4
AFTP2-14	0.5	1.7	613.3	0.8	9.5	56.9	151.8
AFTP2-15	0.5	1.7	654.6	0.8	10.5	56.7	156.4
AFTP2-16	0.5	1.7	698.3	-	1.1	0.2	-
AMD-Unacidified							
AMD1-1	1.8	15.7	1575.6	74.9	11.2	141.0	345.7
AMD1-2	0.5	18.7	1614.4	77.1	12.7	145.9	358.8
AMD1-3	0.4	20.5	1611.4	77.3	13.0	146.2	358.3
AMD1-4	0.4	21.6	1698.7	76.9	12.5	145.8	359.3
AMD1-5	0.4	20.2	1576.8	77.2	12.8	145.7	357.8
AMD1-6	0.5	21.4	1665.1	77.2	12.7	145.6	358.9
AMD1-7	1.4	20.0	1545.1	77.3	13.1	145.0	357.1
AMD1-8	0.3	20.9	1611.7	77.5	13.2	145.9	359.1
AMD1-9	0.5	25.5	1587.5	77.6	13.6	145.1	358.0
AMD-Unacidified							
AMD2-1	1.5	20.1	1569.1	74.5	12.2	139.0	341.5
AMD2-2	1.5	20.4	1609.7	76.2	12.3	142.1	349.3
AMD2-3	1.9	17.9	1403.9	66.3	11.0	123.4	303.0
AMD2-4	2.8	20.5	1606.8	76.3	12.7	142.4	349.7

Sample ID	Fl	Cl	SO_4	Na	K	Mg	Ca
AMD2-5	1.3	20.0	1542.5	74.1	12.4	138.3	338.9
AMD2-6	1.2	20.3	1577.0	75.0	12.9	140.8	347.1
AMD2-7	2.6	20.3	1588.6	75.4	12.8	141.6	349.6
AMD2-8	2.9	20.8	1596.5	76.3	13.3	143.4	352.5
AMD2-9	0.5	13.8	1575.0	75.8	13.6	142.8	351.5
AMD2-10	1.5	19.3	1498.1	75.6	12.8	142.3	350.1
AMD2-11	2.0	20.1	1564.1	74.5	12.3	140.3	344.9
AMD2-12	1.5	13.7	1591.5	76.0	13.0	143.2	351.7
AMD-Closed Acidification							
AAMD1-1	0.5	20.8	1607.1	75.7	13.3	152.2	353.0
AAMD1-2	0.8	20.3	1612.8	76.0	13.4	153.0	353.6
AAMD1-3	0.5	19.8	1649.0	75.9	13.1	153.0	353.8
AAMD1-4	0.5	19.7	1657.5	75.7	13.2	153.0	352.6
AAMD1-5	0.5	20.1	1683.0	76.3	13.9	153.7	354.0
AAMD1-6	0.5	20.2	1711.1	76.9	14.0	155.1	355.4
AAMD1-7	0.5	19.9	1710.9	75.9	13.7	153.2	353.0
AAMD1-8	0.5	20.0	1745.3	76.3	13.6	154.1	354.4
AAMD1-9	0.5	20.0	1759.3	76.1	13.9	154.0	353.8
AAMD1-10	0.5	20.4	1791.5	76.8	13.7	155.4	354.5
AAMD1-11	0.5	20.5	1831.2	77.4	13.9	156.9	357.3
AAMD1-12	0.9	19.9	1841.7	76.0	13.4	154.2	353.8
AMD-Open Acidification							
AAMD2-1	0.5	20.1	1609.4	76.3	14.3	154.2	354.7
AAMD2-2	0.5	20.2	1640.8	77.0	13.9	156.1	357.8
AAMD2-3	0.5	20.2	1641.7	76.8	14.6	154.9	353.9
AAMD2-4	0.5	20.1	1668.5	76.7	13.8	155.2	355.2
AAMD2-5	0.5	20.1	1673.2	76.2	14.5	154.1	354.5
AAMD2-6	0.5	20.1	1700.4	76.8	14.0	155.9	356.4
AAMD2-7	0.5	20.0	1702.0	76.0	14.6	154.0	353.8
AAMD2-8	0.5	20.1	1717.7	76.0	14.7	153.8	353.6
AAMD2-9	0.5	20.1	1730.4	76.4	14.8	154.6	354.8
AAMD2-10	0.4	15.7	1743.1	74.4	14.6	150.7	346.7
AAMD2-11	0.5	20.3	1757.7	76.2	14.9	154.0	354.3
AAMD2-12	0.4	20.0	1772.0	76.1	14.7	154.6	355.5
AAMD2-13	0.5	20.0	1782.9	76.2	14.9	154.5	355.6
AAMD2-14	0.4	20.0	1804.4	75.8	14.7	153.7	353.6
AAMD2-15	0.4	19.9	1842.4	76.1	15.0	153.8	353.8

Solid $NaHCO_3$

Date	Sample	CO_2 (mM/L)	$\delta^{13}C$ (‰)
5/8/2007	$NaHCO_3$-1	11.6	-3.6
5/8/2007	$NaHCO_3$-2	11.4	-3.4
5/8/2007	$NaHCO_3$-3	12.0	-3.4
5/8/2007	$NaHCO_3$-4	11.9	-3.6
5/9/2007	$NaHCO_3$-5	11.6	-3.6

Sample (ID)	Al (mg/L)	Mg (mg/L)	Na (mg/L)	Rb (mg/L)	Sr (mg/L)
$NaHCO_3$ Open Acidification					
AS1-1	1.1	0.2	99.8	3.4	2.3
AS1-2	1.1	0.2	100.7	3.4	2.3
AS1-3	1.2	0.3	100.5	3.8	2.5
AS1-4	1.4	0.3	100.9	4.4	2.9
AS1-5	1.0	0.2	100.5	3.3	2.2
AS1-6	1.3	0.3	101.3	4.1	2.7
AS1-7	1.0	0.2	103.2	3.3	2.2
AS1-8	1.0	0.2	104.2	3.2	2.1
AS1-9	0.8	0.2	104.0	2.6	1.7
AS1-10	1.2	0.2	103.0	3.8	2.5
AS1-11	1.1	0.2	100.7	3.4	2.2
AS1-12	1.1	0.2	103.8	3.4	2.2
AS1-13	1.1	0.2	101.9	3.5	2.3
AS1-14	1.1	0.2	102.7	3.6	2.4
AS1-15	1.1	0.2	102.6	3.5	2.3
AS1-16	1.1	0.2	100.6	3.3	2.2
AS1-17	1.2	0.2	104.8	3.7	2.5
$NaHCO_3$ Open Acidification					
AS3-1	1.3	0.3	98.7	3.3	2.4
AS3-2	1.1	0.2	101.6	2.9	2.1
AS3-3	0.9	0.2	103.2	2.4	1.7
AS3-4	1.3	0.2	100.6	3.3	2.4
AS3-5	1.0	0.2	101.9	2.7	1.9
AS3-6	0.9	0.2	103.4	2.4	1.7
AS3-7	0.9	0.2	88.3	2.3	1.7
AS3-8	1.1	0.2	103.5	2.8	2.0
AS3-9	1.4	0.3	104.1	3.7	2.7
AS3-10	1.1	0.2	104.9	3.0	2.2
AS3-11	1.0	0.2	105.6	2.7	2.0
AS3-12	1.4	0.3	102.2	3.6	2.6
AS3-13	1.3	0.2	102.8	3.3	2.4

Sample (ID)	Al (mg/L)	Mg (mg/L)	Na (mg/L)	Rb (mg/L)	Sr (mg/L)
AS3-14	1.0	0.2	96.3	2.6	1.9
AS3-15	1.6	0.3	105.7	4.1	3.0
AS3-16	1.4	0.3	103.0	3.5	2.6
$NaHCO_3$ closed acidification					
AC1-1	1.2	0.3	108.8	3.8	2.5
AC1-2	0.9	0.2	109.3	2.8	1.9
AC1-3	0.9	0.2	110.2	3.0	2.0
AC1-4	0.8	0.2	110.8	2.6	1.7
AC1-5	1.0	0.2	112.0	3.1	2.1
AC1-6	0.9	0.2	110.8	2.9	1.9
AC1-7	1.0	0.2	109.1	3.1	2.1
AC1-8	1.0	0.2	110.4	3.1	2.0
AC1-9	1.2	0.3	110.3	3.9	2.5
AC1-10	1.0	0.3	112.9	3.2	2.1
AC1-11	1.0	0.3	112.0	3.1	2.1
AC1-12	1.2	0.3	111.6	3.7	2.4
AC1-13	0.8	0.2	111.0	2.6	1.7
$NaHCO_3$ unacidified					
UAJ1-1	0.9	0.2	100.8	2.8	1.9
UAJ1-2	0.8	0.2	99.0	2.5	1.7
UAJ1-3	1.0	14.4	226.0	3.4	2.6
UAJ1-4	0.9	0.2	101.1	2.7	1.8
UAJ1-5	1.0	0.2	102.7	3.0	2.0
UAJ1-6	0.8	0.2	102.2	2.5	1.7
UAJ1-7	0.8	0.2	96.5	2.6	1.7
UAJ1-8	0.9	0.2	99.4	2.9	1.9
UAJ1-9	1.0	0.2	99.3	3.2	2.1
UAJ1-10	0.9	0.2	101.1	2.8	1.8
UAJ1-11	1.0	0.2	101.5	3.2	2.1
UAJ1-12	0.8	0.2	101.4	2.7	1.8
UAJ1-13	1.0	0.2	102.0	3.2	2.1
UAJ1-14	1.0	0.2	104.2	3.2	2.1
UAJ1-15	0.9	0.2	100.6	3.0	2.0
UAJ1-16	0.9	0.2	105.6	2.9	1.9
UAJ1-17	1.1	0.2	102.5	3.3	2.2
$NaHCO_3$ unacidified					
UAD1-1	0.9	0.2	111.6	2.9	1.9
UAD1-2	0.8	0.2	110.5	2.4	1.6
UAD1-3	0.9	0.2	113.3	2.8	1.9
UAD1-4	1.0	0.2	112.0	3.2	2.1
UAD1-5	1.0	0.2	110.7	3.1	2.1

Sample (ID)	Al (mg/L)	Mg (mg/L)	Na (mg/L)	Rb (mg/L)	Sr (mg/L)
UAD1-6	0.9	0.2	110.9	2.7	1.8
UAD1-7	0.9	0.2	114.0	3.0	2.0
UAD1-8	0.9	0.2	112.3	2.9	1.9
UAD1-9	1.0	0.2	112.3	3.2	2.1
UAD1-10	1.0	0.2	113.2	3.2	2.1
UAD1-11	1.0	0.2	112.5	3.0	2.0
UAD1-12	0.9	0.2	113.8	2.8	1.9
UAD1-13	1.0	0.2	117.5	3.0	2.0
UAD1-14	0.9	0.2	117.6	3.0	2.0
UAD1-15	1.0	0.2	114.8	3.1	2.1
UAD1-16	0.8	0.2	112.2	2.5	1.7
UAD1-17	0.9	0.2	111.5	2.9	2.0
UAD1-18	1.0	0.2	117.1	3.1	2.0
UAD1-19	0.9	0.2	117.4	2.7	1.8

Table A-3: δD and $\delta^{18}O$ data for the 2006 and 2007 samples from the Federal Tailings Pile, St Joe State Park, SE Missouri

	2007 data		2006 data	
Sample ID	07_ $\delta^{18}O$ (‰)	07_ δD (‰)	06_ δD (‰)	07_ $\delta^{18}O$ (‰)
Soil and perched groundwater				
PW01	-6.3	-40.1	-12.4	-1.7
PW02	-5.2	-31.5	-27.2	-4.1
PGW01-3	-2.4	-25.7	-	-
PGW03-3	-0.7	-14.4	-34.2	-5.1
PGW06-2	1.0	-9.0	-	-
PGW06-3	0.4	-14.1	-29.4	-4.6
PGW06-4	0.1	-9.6	-	-
Groundwater				
MW01-42	-1.2	-19.9	-38.3	-6.8
MW01-60	0.1	-8.4	-42.5	-7.5
MW08-11	-5.3	-33.7	-23.4	-2.9
MW08-20	-5.2	-34.8	-23.7	-2.9
MW08-52	-4.2	-29.8	-19.1	-1.8
MW06-53	-0.4	-14.3	-29.6	-4.6
MW06-94	-2.9	-21.3	-16.3	-1.6
MW07-20	-5.9	-42.2	-24.4	-2.8

Sample ID	07_ $\delta^{18}O$ (‰)	07_ δD (‰)	06_ δD (‰)	07_ $\delta^{18}O$ (‰)
MW07-70	-2.6	-26.6	-27.3	-3.3
MW05-58	-0.5	-17.9	-31.3	-5.6
MW04-101	0.0	-15.9	-	-
MW04-80	-0.1	-10.3	-	-
MW03-62	1.1	-7.7	-37.6	-7.4
MW03-72	-0.7	-17.2	-34.6	-6.8
Lakes				
Monsanto lake	-2.0	-20.0	-13.4	0.4
Pimp Lake	-1.7	-18.4	-8.6	0.0
Jo Lee Lake	-2.0	-20.2	-13.8	-1.4

- = Not determined

Federal Tailings Pile sediment analysis

Mass of sample digested=1000.1mg

Sample No	Fe mg/L	Pb mg/L	Zn mg/L	Mn mg/L
Sample 1	333.2	9.7	3.03	54.6
Sample 2	344.3	11.2	3.7	56.5
Sample 3	336.9	13.23	4.4	55.5

Table A-4: 2006 and 2007 metal data from the Federal Tailings Pile, St Joe State Park, SE Missouri

Sample ID	Al (mM/L)	Rb mM/L	Pb (µM/L)	Fe (µM/L)	Zn (µM/L)	Ag (µM/L)	Cd (µM/L)	Co (µM/L)	Cr (µM/L)	Mn (µM/L)	Ni (µM/L)	V (µM/L)
2006												
Lakes												
Monsanto Lake	0.04	0.04	0.11	0.18	0.13	0.01	0.05	0.23	0.40	0.04	0.08	0.34
Pim Lake	0.05	0.04	0.11	0.18	0.14	0.01	0.06	0.22	0.43	0.03	0.07	0.31
Joe Lee Lake	0.04	0.04	0.08	0.88	0.12	0.01	0.05	0.19	0.40	0.03	0.04	0.32
Groundwater												
MW 08_11	0.11	0.10	0.08	13.43	0.13	0.02	0.06	0.25	0.40	0.04	0.04	0.35
MW 08_20	0.12	0.11	0.12	5.80	0.12	0.02	0.06	0.23	0.39	0.03	0.08	0.34
MW 08_52	0.13	0.12	0.11	0.54	0.15	0.03	0.06	0.23	0.41	0.08	0.07	0.34
MW 01_42	0.12	0.12	0.11	0.29	0.13	0.01	0.05	0.21	0.41	0.02	0.09	0.36
MW 01_60	0.11	0.10	0.09	0.25	0.10	0.03	0.06	0.20	0.40	0.03	0.06	0.35
MW 06_53	0.11	0.11	0.10	12.41	0.14	0.02	0.06	0.20	0.40	0.05	0.08	0.33
MW 06_94	0.16	0.15	0.07	16.21	0.14	0.02	0.05	0.22	0.42	0.03	0.04	0.36
MW 07_20	0.11	0.11	0.09	0.97	0.07	0.01	0.05	0.20	0.41	0.04	0.09	0.29
MW 07_70	0.09	0.09	0.06	1.38	0.11	0.01	0.05	0.23	0.40	0.05	0.09	0.29
MW 04_80	0.10	0.10	-	10.01	-	-	-	-	-	-	-	-
MW 04_101	0.08	0.08	-	2.01	-	-	-	-	-	-	-	-
MW 05_58	0.10	0.10	0.06	0.66	0.10	0.01	0.06	0.20	0.42	1.07	0.06	0.28
MW 03_62	0.10	0.10	0.02	17.57	0.13	0.03	0.06	0.25	0.41	0.06	0.05	0.33
MW 03_72	0.06	0.06	-	14.40	-	-	-	-	-	-	-	-
Soil and perched groundwater												
SGW 01-3	0.13	0.12	0.23	0.27	16.15	-	-	-	-	1.62	0.65	-
SGW 06-2	0.09	0.09	0.43	0.20	147.56	-	-	-	-	2.95	9.08	-
SGW 06-3	0.07	0.07	0.28	36.73	6.47	-	-	-	-	2.20	1.38	-
SGW 06-4	0.07	0.07	0.00	26.47	0.58	-	-	-	-	0.80	0.60	-
SGW 03-3	0.07	0.07	0.14	92.07	6.44	-	-	-	-	2.62	3.97	-
PW 01	0.07	0.07	0.05	0.21	0.96	0.01	0.05	0.26	0.42	0.08	0.16	0.30
PW 02	0.16	0.15	0.11	0.43	2.89	0.02	0.06	0.46	0.41	0.41	0.39	0.31

Sample ID	Al (mM/L)	Rb mM/L	Pb (µM/L)	Fe (µM/L)	Zn (µM/L)	Ag (µM/L)	Cd (µM/L)	Co (µM/L)	Cr (µM/L)	Mn (µM/L)	Ni (µM/L)	V (µM/L)
2007												
Lakes												
Monsanto Lake	0.04	0.04	0.11	0.18	0.13	0.01	0.05	0.23	0.40	0.04	0.08	0.34
Pim Lake	0.05	0.04	0.11	0.18	0.14	0.01	0.06	0.22	0.43	0.03	0.07	0.31
Joe Lee Lake	0.04	0.04	0.08	0.88	0.12	0.01		0.19	0.40	0.03	0.04	0.32
Groundwater												
MW 08_11	0.11	0.10	0.08	13.43	0.13	0.02	0.06	0.25	0.40	0.04	0.04	0.35
MW 08_20	0.12	0.11	0.12	5.80	0.12	0.02	0.06	0.23	0.39	0.03	0.08	0.34
MW 08_52	0.13	0.12	0.11	0.54	0.15	0.03	0.06	0.23	0.41	0.08	0.07	0.34
MW 01_42	0.12	0.12	0.11	0.29	0.13	0.01	0.05	0.21	0.41	0.02	0.09	0.36
MW 01_60	0.11	0.10	0.09	0.25	0.10	0.03	0.06	0.20	0.40	0.03	0.06	0.35
MW 06_53	0.11	0.11	0.10	12.41	0.14	0.02	0.06	0.20	0.40	0.05	0.08	0.33
MW 06_94	0.16	0.15	0.07	16.21	0.14	0.02	0.05	0.22	0.42	0.03	0.04	0.36
MW 07_20	0.11	0.11	0.09	0.97	0.07	0.01	0.05	0.20	0.41	0.04	0.09	0.29
MW 07_70	0.09	0.09	0.06	1.38	0.11	0.01	0.05	0.23	0.40	0.05	0.09	0.29
MW 04_101	0.08	0.08	0.00	2.01	-	-	-	-	-	-	-	-
MW 04_80	0.10	0.10	0.00	10.01	-	-	-	-	-	-	-	-
MW 05_58	0.10	0.10	0.06	0.66	0.10	0.01	0.06	0.20	0.42	1.07	0.06	0.28
MW 03_62	0.10	0.10	0.02	17.57	0.13	0.03	0.06	0.25	0.41	0.06	0.05	0.33
MW 03_72	0.06	0.06	0.00	14.40	-	-	-	-	-	-	-	-
Soil and perched groundwater												
SGW 01-3	0.13	0.12	0.23	0.27	16.15	-	-	-	-	1.62	0.65	-
SGW 06-2	0.09	0.09	0.43	0.20	147.56	-	-	-	-	2.95	9.08	-
SGW 06-3	0.07	0.07	0.28	36.73	6.47	-	-	-	-	2.20	1.38	-
SGW 06-4	0.07	0.07	0.00	26.47	0.58	-	-	-	-	0.80	0.60	-
SGW 03-3	0.07	0.07	0.14	92.07	6.44	-	-	-	-	2.62	3.97	-
PW 01	0.07	0.07	0.05	0.21	0.96	0.01	0.05	0.26	0.42	0.08	0.16	0.30
PW 02	0.16	0.15	0.11	0.43	2.89	0.02	0.06	0.46	0.41	0.41	0.39	0.31

- = Not determined

Table A-5: Saturation indices of mineral phases modeled using the computer program PHREEQCI (Parkhurst and Appelo, 1999) for discharge water from the Elvin's Tailings Pile and Leadwood Tailings Pile, St. Francoise County, SE Missouri, USA

Sample ID	$Al(OH)_3$	Albite	Alunite	Anhydrite	Aragonite	Calcite	Chalcedony	Chlorite	Dolomite	Gibbsite	Gypsum	Illite	Kaolinite	K-feldspar	Sepiolite
2006															
ETP CreeK															
ETP 1	1.3	-1.2	8.2	-0.9	-0.6	-0.4	-0.4	-2.6	-1.1	4.1	-0.7	6.8	9.0	1.3	-5.9
ETP 2	0.3	-1.7	2.3	-0.9	0.3	0.4	-0.5	4.9	0.7	3.0	-0.7	4.9	6.6	0.7	-2.7
ETP 3	0.1	-1.8	1.2	-0.8	0.5	0.6	-0.5	6.1	1.1	2.7	-0.6	4.5	6.1	0.7	-2.1
ETP 4	0.1	-1.6	1.5	-0.8	0.5	0.6	-0.5	6.6	1.1	2.8	-0.6	4.8	6.2	0.8	-2.0
ETP 5	0.0	-1.7	0.8	-0.8	0.5	0.6	-0.5	7.0	1.1	2.7	-0.6	4.5	6.0	0.7	-1.7
ETP 6	0.1	-1.7	1.0	-0.8	0.5	0.6	-0.5	6.9	1.1	2.7	-0.6	4.6	6.1	0.7	-1.8
LTP Creek															
LTP 1	-0.2	-0.9	-0.8	-1.2	0.9	1.0	-0.1	6.7	1.8	2.5	-1.0	5.2	6.5	1.3	-0.7
LTP 2	0.1	-0.7	1.2	-1.2	0.6	0.7	-0.1	4.3	1.3	2.8	-1.0	5.7	7.2	1.4	-1.8
LTP 3	0.2	-1.0	1.8	-1.2	0.4	0.6	-0.2	3.2	1.0	2.9	-1.0	5.6	7.2	1.2	-2.4
LTP 4	-0.1	-0.8	0.1	-1.2	0.8	0.9	-0.1	5.8	1.6	2.6	-1.0	5.4	6.7	1.4	-1.1
LTP 5	0.3	-0.7	2.4	-1.2	0.4	0.5	-0.1	2.6	0.9	3.0	-1.0	5.9	7.4	1.4	-2.7
2007															
ETP CreeK															
ETP 1	1.4	-1.1	9.0	-0.9	-0.6	-0.4	-0.4	-4.1	-1.1	4.2	-0.7	6.9	9.2	1.3	-6.4
ETP 2	1.3	-1.1	8.1	-0.8	-0.3	-0.2	-0.4	-1.3	-0.5	4.0	-0.5	6.8	8.9	1.4	-5.4
ETP 3	0.7	-1.4	4.8	-0.8	0.1	0.3	-0.5	2.0	0.4	3.4	-0.5	5.6	7.5	1.0	-3.8
ETP 4	0.5	-1.5	4.0	-0.8	0.2	0.4	-0.5	3.1	0.6	3.2	-0.5	5.4	7.1	0.9	-3.4
ETP 5	0.6	-1.3	4.1	-0.8	0.2	0.4	-0.5	3.4	0.6	3.3	-0.5	5.6	7.3	1.1	-3.2
ETP 6	0.4	-1.5	3.3	-0.8	0.3	0.5	-0.5	3.9	0.8	3.1	-0.5	5.3	6.9	1.0	-2.9
LTP Creek															
LTP 1	-0.1	-1.0	0.0	-1.3	0.8	1.0	-0.2	5.3	1.7	2.7	-1.0	5.1	6.6	1.1	-1.4
LTP 2	0.0	-1.1	0.8	-1.1	0.8	0.9	-0.3	5.0	1.6	2.7	-0.9	5.2	6.6	1.2	-1.8
LTP 3	0.0	-1.2	0.7	-1.1	0.7	0.9	-0.3	5.1	1.6	2.7	-0.9	5.0	6.5	1.1	-1.8
LTP 4	-0.3	-1.3	-1.1	-1.1	1.0	1.1	-0.3	6.9	2.0	2.3	-0.9	4.5	5.8	0.9	-0.9
LTP 5	0.1	-1.0	1.3	-1.2	0.6	0.8	-0.3	4.5	1.4	2.8	-0.9	5.3	6.8	1.1	-2.1

VITA

HENDRATTA N. ALI

Candidate for the Degree of

Doctor of Philosophy

Dissertation: **CARBON CYCLING AND STABLE ISOTOPE EVOLUTION IN NEUTRAL MINE DRAINAGE**

Major Field: GEOLOGY

Biographical:

EDUCATION:
Completed the requirements for the Doctor of Philosophy in Geology at Oklahoma State University, Stillwater, Oklahoma in May 2010.

Completed the requirements for the Diplome D'Etude Approfondie ((Post Graduate of Science) in Earth Sciences; Specialty Environmental Soil Science at the University of Yaounde I, Yaounde, Cameroon in September 2003

Completed the requirements for the Master of Science in Earth Sciences, Specialty Soil Microbiology at the University of Yaounde I, Yaounde, Cameroon in January 2005

Completed the requirements for the Bachelor of Science in Earth Science at the University of Yaounde I, Yaounde Cameroon September 1998.

EXPERIENCE:
Instructor : GEOL 1014, Geology and Human Affairs, Oklahoma State University, Spring - Fall 2009

Geophysicists: CAMAC International-Allied Energy Corporation Summer Internship, June-August, 2009

Laboratory teaching assistant for Geology and Human Affairs, Aqueous Geochemistry in the School of Geology, Oklahoma State University, 2006-2008

Geologist / hydrologist / pedologist: Willbros Spie Capaq –Douala, Cameroon: Chad-Cameroon Pipeline Project, 2001- 2003

PROFESSIONAL MEMBERSHIPS:
American Association of Petroleum Geologists (AAPG); Society of Exploration Geophysicists (SEG); Association for Women in the Geosciences (AWG); Geological Society of America (GSA); National Association of Black Geologists and Geophysicists (NABGG)**.**

Name: HENDRATTA ALI Date of Degree: May, 2010

Institution: Oklahoma State University Location: Stillwater, Oklahoma

Title of Study: **CARBON CYCLING AND STABLE ISOTOPE EVOLUTION IN NEUTRAL MINE DRAINAGE**

Pages in Study: 130 Candidate for the Degree of Doctor of Philosophy

Major Field: GEOLOGY

Scope and Method of Study:

Dissolved inorganic carbon and stable carbon isotopes evolution in contaminated surface and groundwater was investigated by laboratory and field experiments.

The laboratory experiment was conducted by progressively acidifying natural and artificial water samples to determine shifts in $\delta^{13}C_{DIC}$ and carbon isotope fractionation during DIC transformation and to model carbon isotope evolution during progressive acidification.

The field experiments were conducted in three carbonate rich tailings piles found in the St Francois County, SE Missouri, where lead mining resulting in the disposal of tailings material in several tailings piles, to investigate how acid production and neutralization affects DIC generation and $CO_{2(g)}$ production in the vadose zone and how these reactions affect the carbonate evolution of groundwater and surface discharge from the tailings pile.

Findings and Conclusions:

The results of this study show that:

Carbon isotope values in conjunction with concentrations of DIC species ($CO_{2(aq)}$, HCO_3^-, and CO_3^{2-}) can be used to provide evidence for the effects of acidification on DIC in surface waters.

In natural and anthropogenic settings where sulfuric acid production by metal sulfides and neutralization by carbonates occur, the carbonate evolution of shallow groundwater is not described by the classical model ascribed to soil zone $CO_{2(g)}$

Groundwater discharged from carbonate rich mine tailings excess $CO_{2(aq)}$ that is loss to atmosphere. The $CO_{2(g)}$ that is loss is initially high and decreases with downstream. The $CO_{2(g)}$ loss results in kinetic isotopic enrichment of DIC and the magnitude of $\delta^{13}C_{DIC}$ shifts depends on the initial concentration of excess $CO_{2(aq)}$ in the water discharged to the surface and the amount of $CO_{2(g)}$ that is lost from the water.

ADVISER'S APPROVAL: Dr Atekwana Eliot